2038-5625

Italian Journal of Agrometeorology

Rivista Italiana di Agrometeorologia

n. 3 – 2019

Poste Italiane spa - Tassa pagata - Piego di libro
Aut. n. 072/DCB/FI1/VF del 31.03.2005

FIRENZE UNIVERSITY PRESS

Italian Journal of Agrometeorology

n. 3 - 2019

Firenze University Press

The ***Italian Journal of Agrometeorology*** (***IJAm - Rivista Italiana di Agrometeorologia***) is the official periodical of the Italian Association of Agrometeorology (AIAM) and aims to publish original scientific contributions in English on agrometerology, as a science that studies the interactions of hydrological and meteorological factors with the agricultural and forest ecosystems, and with agriculture in its broadest sense (including livestock and fisheries).

SUBSCRIPTION INFORMATION
IJAm articles are freely available online, but print editions are available to paying subscribers. Subscription rates are in Eur and are applicable worldwide.
Annual Subscription: € 50,00 Single Issue: € 25,00

CONTACT INFORMATION
Please contact ordini@fupress.com, if you have any questions about your subscription or if you would like to place an order for the print edition. Information on payment methods will be provided after your initial correspondence.

Published by
Firenze University Press – University of Florence, Italy
Via Cittadella, 7 - 50144 Florence - Italy
http://www.fupress.com/ijam

Italian Journal of Agrometeorology
Rivista Italiana di Agrometeorologia

Firenze University Press
www.fupress.com/ijam

OPEN ACCESS

Citation: G. Dal Monte, T. Labagnara, P. Cirigliano (2019) Agroclimatic evaluation of Val d'Agri (Basilicata, Italy) suitability for grapevine quality: the example of PDO "Terre dell'Alta Val d'Agri" area in a climate change scenario. *Italian Journal of Agrometeorology* (3): 3-12. doi: 10.13128/ijam-797

Received: December 18, 2017

Accepted: September 12, 2019

Published: December 28, 2019

Data Availability Statement: All relevant data are within the paper and its Supporting Information files.

Competing Interests: The Author(s) declare(s) no conflict of interest.

Dal Monte G. and Labagnara T. contributed equally to this work.

Agroclimatic evaluation of Val d'Agri (Basilicata, Italy) suitability for grapevine quality: the example of PDO "Terre dell'Alta Val d'Agri" area in a climate change scenario

Studio agro-climatico della Val d'Agri (Basilicata, Italia) per la viticoltura di qualità: l'esempio della DOP "Terre dell'Alta Val d'Agri" nel contesto dei cambiamenti climatici

Giovanni Dal Monte[1], Tilde Labagnara[2,*], Pasquale Cirigliano[2]

[1] *CREA-AA Consiglio per la ricerca in agricoltura e l'analisi dell'economia agraria – Centro Agricoltura e Ambiente - Roma, Via della Navicella 4, 00184 Roma*
[2] *CREA-VE Consiglio per la ricerca in agricoltura e l'analisi dell'economia agraria - Viticoltura ed Enologia- Arezzo, Viale Santa Margherita 80, 52100 Arezzo*
*Corresponding author. E-mail: giovanni.dalmonte@crea.gov.it, tilde.labagnara@gmail.com; pasquale.cirigliano@crea.gov.it

Abstract. In a changing climate, the agro-climatic characteristics of a wine region could significantly vary. Therefore, grapevine physiology, ripening time and grape quality at harvest, could be modified by climate change. The aim of this work is to investigate if there is a shift in climate suitability for the PDO "Terre dell'Alta Val d'Agri" wine growing area. Firstly, the climatic traits were assessed for the reference period 1985-2010. Afterwards, according to a "two periods" approach, the 2010-2018 time period, that represents the current condition, was evaluated. The Multicriteria Climatic Classification (MCC) (Tonietto and Carbonneau, 2004), through the use of Heliotermal, Cold night and Dryness indexes, was performed and the classification of the two periods was compared in order to highlight the differences in the suitability for wine production in the PDO area. The results show the trend towards a warmer and drier climate, with an increase in mean temperature (+1°C) and intensification of dryness (+21 mm of potential deficit). The study also shows that, according to MCC, no relevant viticultural regions in the world are highlighted with the same classification as Villa d'Agri for the 1985-2010 period. Otherwise in the recent period (2011-2018) the study area has similar climatic traits with an important wine-producing area, the Rio Negro wine region in Argentina. This agro-climatic shift reveals a great potential in the suitability of the PDO area for high-quality red wine production. In addition, the "two periods approach" could be applied to other grape growing regions in order to assess the effect of climate change on vineyard suitability for wine production.

Keywords. Multicriteria climatic classification (MCC), bioclimatic index, grapevine suitability, PDO "Terre dell'Alta Val d'Agri", agro-climate change.

Riassunto. I cambiamenti climatici in atto possono influenzare in maniera significativa le caratteristiche di una regione viticola ed incidere, di conseguenza, sulla fisiologia della vite, sul periodo di maturazione e sulla qualità dell'uva alla raccolta. Scopo del presente lavoro è di evidenziare se nell'area della DOP "Terre dell'Alta Val d'Agri" si è verificato un cambiamento climatico che ha inciso sulla vocazione viticola del territorio. A questo fine sono state esaminate le caratteristiche del periodo climatico di riferimento 1985-2010; caratteristiche poi confrontate, secondo un approccio "a due periodi", con gli anni più recenti 2011-18. Successivamente l'area oggetto di studio è stata esaminata, separatamente per i due periodi, secondo il metodo della Classificazione Climatica Multicriterio (MCC) (Tonietto and Carbonneau, 2004), che utilizza gli indici Eliotermico, di Secchezza e di Freschezza notturna. I risultati mostrano una tendenza verso un clima più caldo e più secco, con un innalzamento della temperatura media di 1°C e con una riduzione dell'acqua disponibile. Quanto alla MCC, si evidenzia come i valori del periodo 1985-2010 non si riscontrino in altre zone viticole di rilievo a livello mondiale, mentre le caratteristiche riscontrate negli anni 2011-18 si ritrovano nella regione del Rio Negro, in Argentina. L'approccio "a due periodi" potrebbe essere applicato anche ad altre regioni viticole, per verificare gli effetti del cambiamento climatico sull'idoneità di un territorio alla produzione di uve per vini di qualità.

Parole chiave. Classificazione climatica multicriterio (MCC), indici Bioclimatici, adattamento della vite, DOP "Terre dell'Alta Val d'Agri", cambiamenti climatici.

INTRODUCTION

The influence of climate on grape and wine quality is well known (Montes *et al.*, 2012), through the effect of both regional and local-scale climatic conditions during the growing season, and by its inter-annual variability, which generates variations in grapevine growth and then in berry composition (Gladstones 1992, Jones and Davis 2000, Jones *et al.*, 2005, Soar *et al.*, 2008). Among climate variables, air temperature is recognized as having the greatest effect on grapevine and on biochemical changes in berries during their development and ripening (Jackson 2000, Carbonneau *et al.*, 2007), affecting plant vigor, ripening rate and harvest date (Jackson and Lombard, 1993). Temperature is also known to determine the concentration of aromatic and color compounds in berries under specific night time temperatures (Kliewer and Torres 1972, Kliewer 1973, Fregoni and Pezzutto 2000). Climate can also account for differences in wine quality and style (Matese *et al.*, 2014). The effects of climate on wine quality differences within a vine-growing region (at meso-climate scale) have been studied, *inter alia*, in Alsace (France) by Dumas *et al.* (1997), in Bordeaux (France) by Bois (2002), in Tuscany (Italy) by Bindi and Maselli (2001), in Veneto (Italy) by Tomasi *et al.* (2013) and in Oregon (USA) by Jones *et al.* (2004). So viticultural microclimatic and mesoclimatic characteristics, obviously joined with soil characteristics, are key factors in determining varietal suitability, wine types and wine quality of a wine region (Carbonneau, 2003; Jones 2006). Given the strong influence of climate factors on viticulture, it is also evident the importance to investigate climate change in progress and its impacts on grapevine growing areas. Furthermore, grapevine has a greater potential risk from climatic variations than other crops because, in general, optimum ripening conditions of a single variety occur only in a defined geographic zone (Jones *et al.*, 2005). Basilicata region includes four Protected Denomination of Origin (PDO) for a total red wine production more than 33.000 hL (Source: I numeri del vino su dati ISTAT-aggiornamento 2019.) In the area of Alta Val d'Agri that includes the territory of Viggiano, Moliterno and Grumento Nova municipalities (Fig. 1), in 2003 was established the PDO "Terre dell'Alta Val d'Agri" (Ministerial Decree, 2003). The official varieties cultivated in the PDO area are mainly red varieties such as Merlot, Cabernet Sauvignon and Malvasia di Basilicata, but it is allowed the utilization for a 20% of autochthonous minor or local red varieties. Concerning climate, there are no in-depth scientific studies about the peculiar characteristics of this territory. The area (about 25.000 hectares) is located at LAT 40° 21' 31" N, LON 15° 49' 30" E and consists of two landscape systems: the system of hill slopes, between 600 and 850 m a.s.l., and the valley system, between 550 and 650 m a.s.l. (Catizzone, 1980). Nevertheless, viticulture is widespread in a limited area, largely inside the environment of valley floor of Val d'Agri. The area of PDO, in which grapevine are cultivated, is about 215 hectare and spread around the valley of Agri river and its affluent. There are three main soil types in the PDO area: Inceptisol, that is the most widespread, Anfisol and Entisol (Cirigliano *et al.*, 2007). The climatic potentiality of the PDO "Terre dell'Alta Val d'Agri" was deeply investigated. With this fact in mind, the aims of the present study are: *i)* to describe the climate of the reference period (1985-2010) and characterize the recent one. (2010-2018); *ii)* to investigate consequences and perspectives of the climate change on thermal and hydric resources of the territory and *iii)* to evidence the possible effects of climate change on grapevine suitability.

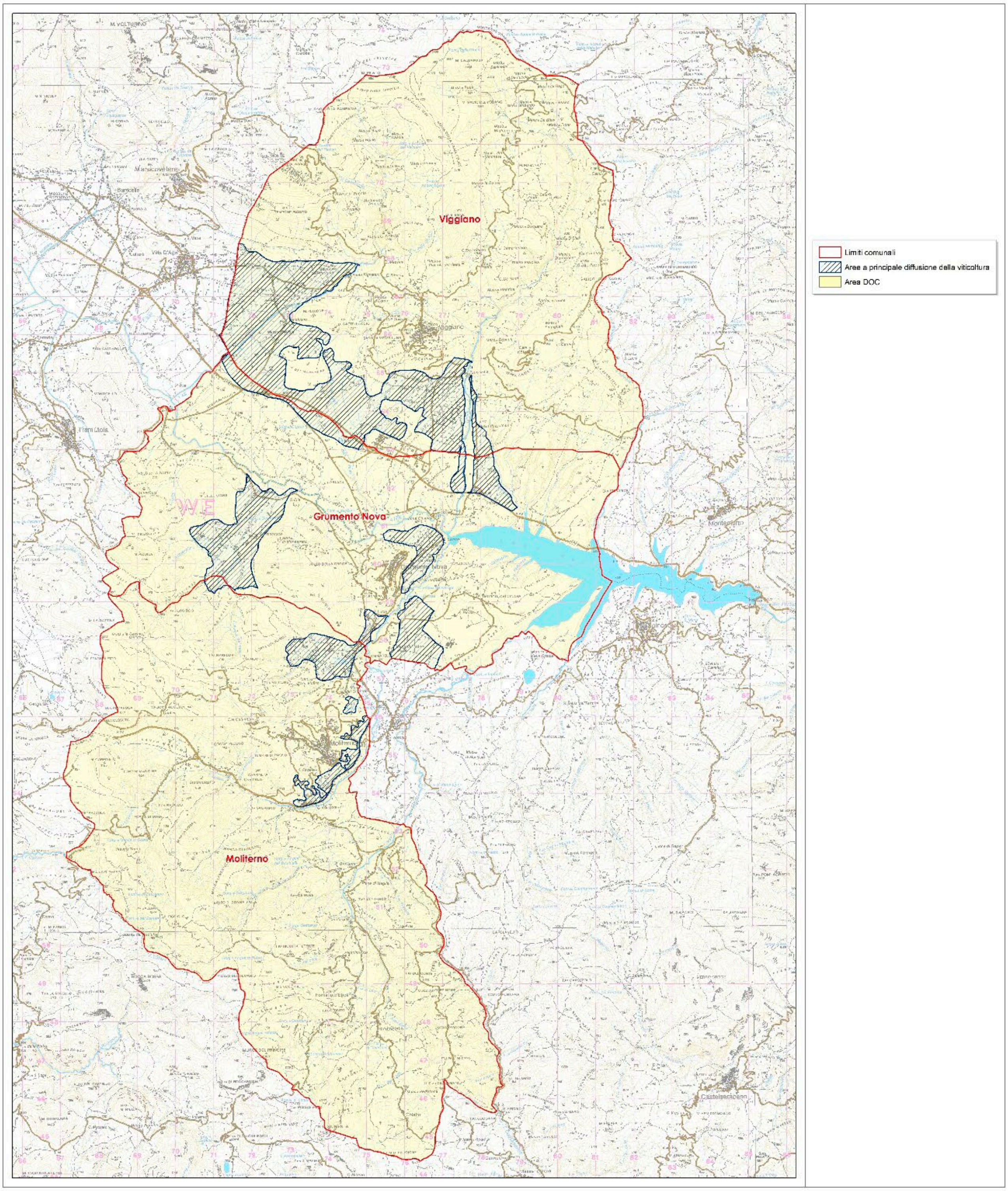

Fig. 1. The PDO "Terre dell'Alta Val d'Agri" area; it includes the territory of Viggiano, Moliterno and Grumento Nova municipalities.
Fig. 1. L'area della DOP "Terre dell'Alta Val d'Agri" che include i comuni di Viggiano, Moliterno e Grumento Nova.

MATERIALS AND METHODS

According to "OIV Guidelines for viticulture zoning methodologies on a climate level" (OIV, 2012), the best methodology to evaluate the agroclimatic features of a territory consists in three steps: the selection of appropriate climatic indicators, the evaluation of high qualitative climate data sources and the climatic identification of homogeneous zones. Since the purpose of this work is not to identify the homogeneous areas, but to better define the agro-climatic characteristics of the territory *a priori* defined as homogeneous, the research activity merely takes into account the first two steps and analyzes the achieved results.

Select climatic indicators

The multicriteria climatic classification (MCC system) proposed by Tonietto and Carbonneau (2004) was utilized in order to choose the most suitable climatic indicators. This system allows comparing the climate of the PDO area investigated with the main wine-growing areas in the world. According to the authors, the climate of a territory is strictly related to qualitative potential, grapes peculiarities or viticultural products (requirements of varieties, vintage quality, sugar, acidity, color, aroma) and the wine traits. Several studies evidenced the use of this climatic classification approach worldwide (e.g. Hormazabal *et al.*, 2002, Blanco-Ward *et al.*, 2007, Ferrer *et al.*, 2007, Jones *et al.*, 2009). Until now, no investigation was performed for the viticultural areas of Basilicata region, particularly for the PDO "Terre dell'Alta Val d'Agri". The present work, in addition to highlight the agroclimatic traits of the studied area and its suitability for grapevine cultivation, could also contribute to the validation of the classification system at the global scale. According to Tonietto and Carbonneau (2004), the best climatic indices (Tab. 1) to characterize the climate of grape-growing regions in terms of thermal and hydrological conditions are the Heliothermal index (HI), the Dryness index (DI) and the Cool night index (CI). The Heliothermal index allows assessing the thermal potential of a given region and links the thermal demands for variety ripening, reflecting the potential grape sugar content. The index estimates the suitability of a region to grow various grapevine varieties that depends on heat accumulations. Therefore, this index, using temperatures of the growing season (from April to September), give information about grapevine quality and varieties which can be cultivated in a certain area (Huglin, 1978). *Vitis vinifera* is highly sensitive to climate, temperature affect grape quality and production (Holland and Smit, 2014). Consequently, the amount of temperatures of growing seasons influences the entire grape and wine composition (Van Leeuwen and Destract-Irvine, 2017). HI represents

Tab. 1. List of bioclimatic indices used for climatic classification of PDO "Terre dell'Alta Val d' Agri", along with their corresponding definition and references.
Tab. 1. Lista degli indici bioclimatici per la classificazione della DOP "Terre dell'Alta Val d'Agri" e riferimenti bibliografici.

Bioclimatic index	Definition	Units	Reference
Heliotermal Index (HI)	$\sum_{April}^{September} \frac{[(T-10)+(Tx-10)]}{2} d$ *T* Mean Air Temperature (°C) *Tx* Maximum temperature (°C) *d* Length of day coefficient	°C	Huglin 1978
Dryness Index (DI)	$\sum_{April}^{September} (Wo\ + P - Tv - Es)$ *Wo* soil water reserve at the end of the growing season (mm) *P* Precipitation (mm) *Tv* = ETPk potential evapotranspiration in the vineyard (mm) (ETP = potential evapotranspiration, k = coefficient of radiation absorption by vineyard (in the Northern hemisphere: 0.1 for April 03 for May 0.5 from June to September)) *Es* effective evaporation from the soil (mm) (Es = ETP/N (1-k) JPm, where N = number of days in the month; JPm = number of days of effective evaporation from the soil per month, JPm = monthly rainfall in mm/5)	mm	Riou 1994
Cold night Index (CI)	Minimum air temperature of September	°C	Tonietto and Carbonneau 2004

a direct measurement of the impact of climate on viticulture and it is the most important index to evaluate the implications of global warming for viticulture worldwide (Marx *et al.*, 2017). The Dryness index (DI)[1] (Riou, 1994) evaluates soil water availability for vine growing cycle, by estimating soil water reserves, precipitation and potential evapotranspiration (potential water balance). This is also a good indicator for grapevine development, as water availability it can influence yield and quality (Edwards and Clingeleffer 2013; Van Leeuwen *et al.*, 2009; Roby *et al.*, 2004) especially polyphenol accumulation (Cirigliano *et al.*, 2017). The DI takes into account the vineyard potential evapotranspiration, the evaporation of bare soil and precipitation. The Cool Night Index (CI) accounts for minimum temperatures during the month before harvest (September, by convention, in the Northern emisphere) providing a gross estimate of the ripening stage, as large temperature ranges during ripening tend to be favorable to high-quality wines (Tonietto and Carbonneau, 2004). Furthermore, by combining these bioclimatic features of heat accumulation (HI), dryness (DI), and ripening conditions (CI), it is possible to determine the optimum viticulture suitability and direct comparison between different grapevine regions all over the world.

Select climate data source

The meteorological daily data (from 1985 to 2018) were collected in Villa d'Agri (PZ) station, located at LAT 40° 20' 58" N, LON 15° 49' 43" E, alt. 592 m a.s.l. This automatic station belongs to the agro-meteorological network of ALSIA (Agenzia Lucana per lo Sviluppo e l'Innovazione in Agricoltura). Reference evapotranspiration (ET_0) was estimated using the Hargreaves-Samani empirical equation (Hargreaves and Samani, 1982).

Climate change

In the last decades, several studies report techniques, methodologies and scenarios in order to evaluate trends and tendencies for future climate (Palliotti *et al.*, 2014; Hannah *et al.*, 2013; Fraga *et al.*, 2016). In order to investigate if climate change is taking place in the studied area and if there are climatic trends that can affect, positively or negatively, the cultivation of grapevine and the quality and typicality of wines, the available meteorological data series were divided in two different subsets and were analyzed separately, according to a "two periods" approach: the first subset of twenty-five years 1985-2010 is sufficient to calculate climatological standard normal of the area (WMO, 2011); the second one takes into account the recent period of eight years (2011-2018), which describes the current situation and can give predictive information about the near future: "in general, the most recent 5- to 10-year period of record has as much predictive value as a 30-year record" (WMO, 2011). In addition, the above-mentioned bioclimatic indexes were calculated separately for the two datasets. Results were compared and discussed in the following sections.

RESULTS

Climatic traits of 1985-2010 vs. 2011-2018 periods

In Tab. 2 the differences between the two periods were highlighted. The mean annual temperature of the reference period (1985-2010) was 12.8°C instead of 13.8°C of the years 2011-18. For the reference period (1985-2010), the coldest month was January, with a mean temperature of 4.8°C and the warmest month was July with a mean temperature of 22.1°C. During the growing season (from April 1st to September 30th), the average total amount of precipitation was 284 mm and the corresponding value of evapotranspiration ETo was 927 mm, with a potential deficit of 642 mm. In the recent period (2011-2018), the coldest month was January again, but with a mean temperature of 5.4°C; the warmest month was August with a mean temperature of 23.1°C (Tab. 2). In addition, the average total amount of precipitation was 275 mm during the growing season and the corresponding value of evapotranspiration ETo was 971 mm, with a potential deficit of 663 mm.

Bioclimatic indexes and climate suitability 1985-2010 vs. 2011-2018

The climatic changes highlighted in the previous paragraph, could implicate a change in bioclimatic indexes and in climate suitability for grapevine of the study area. Table 3 evidenced the main results of agroclimatic classification for Villa d'Agri area. The value of HI is 2239 for the reference period (1985-2010) and it falls in the HI +1 class. According to Tonietto and Carbonneau (2004), the climate could be defined as "temperate warm", where the heliothermal resources are sufficient for the growth of almost all cultivars, even the later ones. However, the value of HI for the last eight-years (recent period) is higher (2436°C) because it

[1] In this work the Drought Index was calculated adopting Wo = 200 mm (Tonietto and Carbonneau, 2004)

Tab. 2. Climatic values of Villa d'Agri area for the periods 1985-2010 and 2011-2018.
Tab. 2. Valori climatici di Villa d'Agri per i periodi 1985-2010 e 2011-2018.

Period	Annual T mean	Coldest Month	Coldest Month T mean	Warmest Month	Warmest Month T mean	Mean Temperature*	Rain*	ETo*	Potential deficit*
1985-2010	12.8°C	January	4.8°C	July	22.1°C	17.7°C	284 mm	927 mm in July	642 mm
2011-2018	13.8°C	January	5.4°C	August	23.1°C	18.7°C	275 mm	971 mm in July	663 mm

Tab. 3. Results for Multicriteria classification system (MCC) of PDO "Terre dell'Alta Val d'Agri": heliothermal index, cool night index, dryness index and Classes of viticultural climate for the two periods are highlighted.
Tab. 3. Risultati relativi alla classificazione climatica multicriterio (MCC) della DOP "Terre dell'Alta Val d'Agri" sono riportati i valori degli indici eliotermico, di freschezza notturna e secchezza, per i periodi 1985-2010 e 2011-2018.

Index	1985-2010				2011-2018			
	Value	Class of viticultural climate	Acronym	Class interval	Value	Class of viticultural climate	Acronym	Class interval
Heliotermal Index, HI	2239	Temperate warm	HI+1	>2100 ≤ 2400	2436	Warm	HI+2	>2400 ≤ 3000
Cold Night index, CI (°C)	10.2	Very cool night	CI+2	≤12	10.4	Very cool night	CI +2	≤12
Dryness index, DI (mm)	-70	Moderately dry	DI+1	≤50 > −100	-177	Very dry	DI+2	≤−100

Tab. 4. Day-night thermal excursions of Villa d'Agri: 1985-2010 and 2011-2018 val ues.
Tab. 4. Escursioni termiche giornaliere di Villa d'Agri: confronto tra i valori 1985-2010 e 2011-2018.

Period	Mean*	Maximum monthly*	Absolute maximum*	Monthly mean* (August-September)
1985-2010	13.4°C	18.2°C August	27.4°C 7/7/2000; 10/9/2008	16.7°C
2011-2018	15.7°C	20.4°C July	29.1°C 18/9/2015	18.8°C

*Day-night thermal excursion.

reflects the rise in temperature of the last years, so the HI class is +2 "warm", where there is "a potential which exceeds the heliothermal needs to ripen the varieties, even the late ones (with some associated risks of stress)" (Tonietto and Carbonneau, 2004). (See also Figure 2 (a)). Concerning the CI index, there is only few differences between the values of the two periods (10.2 vs. 10.4) and both of them fall in the same class CI +2 "very cool nights", characterized by very low night temperature (for details see Figure 2 (b)). This index reflects the main specific climatic characteristic of the studied area: the very high values of diurnal temperature variation (see Tab. 4), particularly during berries ripening. The last index analyzed was the dryness index DI. Results highlighted a change in the value of the last eight years. In fact, in the reference period, the value is -70 and the class is DI+1 "moderately dry", so the climate was characterized by the presence of dryness. However, the value of DI in the recent period is -177 (with a high variation of more than 250% over the first period) and the class is +2 "very dry" (Tab. 3 and Fig. 2 (c)). Generally, this class represents areas with more than 100 mm of annual water deficit, where there are frequently water stress effects and vineyards irrigation are currently applied.

DISCUSSION

Climate change has strongly reached the attention of the scientific community concerning natural, social and political sciences. Furthermore, climate is one of the main factors that influence more the agricultural sector. Concerning the viticulture, scientists have deeply investigated the global implication of climate change on grapevine. Rise temperature is advancing maturity and compressing the harvest. Thermal regimes, seasonal condition, vine water status and the exploration of adaptation options for grapevine growers are key factors in order to evaluate the climate impact on yield, enologically important berry traits and viticulture suitabil-

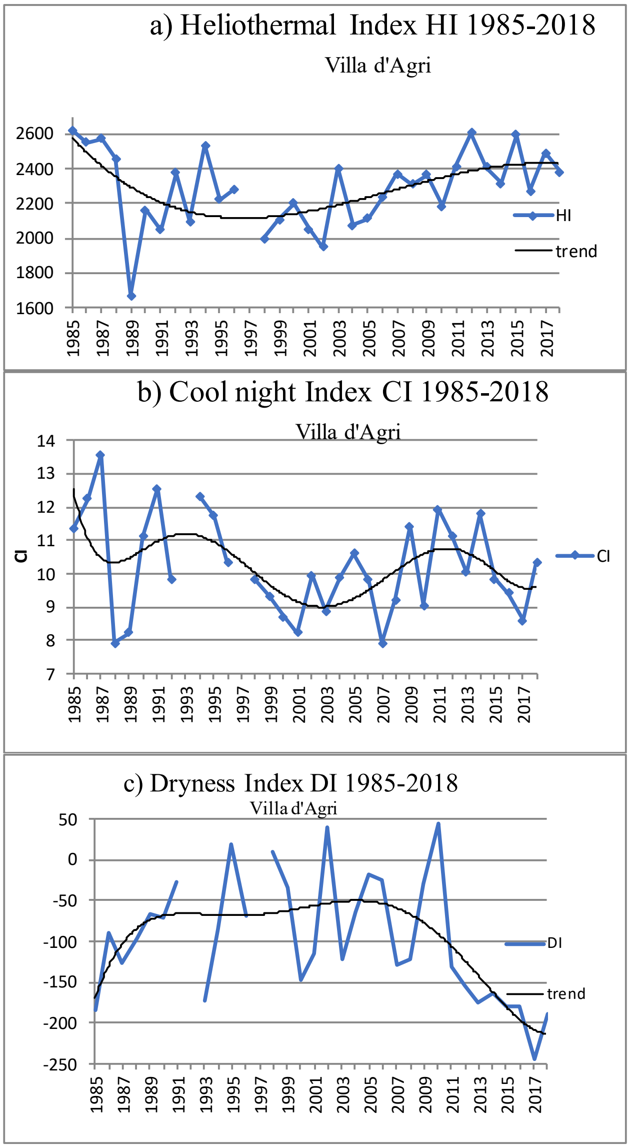

Fig. 2. Multicriteria climatic classification (MCC) of Villa d'Agri for the years 1985-2018; a) Heliotermal index (HI), b) Cold night index (CI) and c) Dryness index (D). The trend is shown by the continuous line.

Fig. 2. Classificazione climatica multicriterio (MCC) di Villa d'Agri per gli anni 1985-2018; a) Indice eliotermico (HI), b) Indice di Freschezza notturna (CI) e c) Indice di Secchezza. Il trend è evidenziato dalla linea continua.

ity. (Moran *et al.*, 2018; Marx *et al.*, 2017). However, few research groups have actually examined the implications and the consequences of the effect of climate change in small territories, mainly at regional scale (Zottele and Delay, 2017; Teslic *et al.*, 2017; Serpa *et al.*, 2017 and others). According to Multicriteria climatic classification system (MCC) (Tonietto and Carbonneau, 2004), the PDO "Terre dell'Alta Val d'Agri) was classified as "temperate warm", with "very cool nights" and "moderately dry" for the climatic period (1985-2010). Recently, according to climate change, the period between 2011-18 is classified, instead, as "warm", with "very cool nights" and "very dry", highlighting a clear trend towards rise temperatures and a less significant reduction in precipitation during the grapevine growing season. Therefore, some physiological problems could occur in zones with high heat accumulation, which could affect the aromatic potential of grapes not only in the earliest cultivars (Crespo *et al.*, 2017 and Pons *et al.*, 2017). However, in this area, rise in temperature is compensate for the very high day thermal excursions of the ripening period (Tab. 4) and the reduction of available water could be faced with rescue by irrigation. Nevertheless, both periods may fall into Gladstone's description of 'an ideal vineyard climate' (Gladstone's, 1992). The author reported that climate should be consistently warm, but not hot, days and cool nights throughout ripening, but particularly around the time of veraison to enhance maximal carbohydrate accumulation particularly for color formation. It is very interesting to note that in Tonietto and Carbonneau (2004), no important world viticultural regions were highlighted with the same classification as Villa d'Agri for the 1985-2010 period, indicating that no similar areas in the world corresponded to qualitative wine production. According to Jones *et al.*, (2005), the historical and estimated climate changes could move some regions into more optimal climatic conditions for the production of traditional grapevine varieties. Furthermore, climate change can enhance grape growing in some regions (Fraga *et al.*, 2012; Hannah *et al.*, 2013), this is the case for the small territory of Villa d'Agri in Basilicata, where climatic change could positively impact on grape growing. As a result of this study, in the recent period (2011-2018), the PDO "Terre dell'Alta Val d'Agri" wine-producing area highlights similar characteristics with another wine-producing region, according to the same Multicriteria classification categories (Tonietto and Carbonneau, 2004). In fact, in the 2011-2018 period (which has also a predictive value for the near future), Villa d'Agri falls in the same classification as Rio Negro wine region in Argentina, where (as in Villa d'Agri) night temperatures are very low. In the south area of Argentina (Patagonia), the Rio Negro province accounts for some 3% of total wine production of the country and the day-night temperature variations make a particular environment for the production of qualitative wine. In this contest, this desert climate produces arid growing conditions. Otherwise, the combination of warm, sunny days and very cold nights create an especially healthy environment for viticulture (Goldner and

Zamora, 2007). According to Kliewer and Torres (1972) night cooler temperatures increased anthocyanin concentration two to four times in comparison to grapevine grown under warmer conditions in Cardinal, Pinot noir and Tokay. Day-night thermal excursion has high positive effect on grape color and significantly affect the volatile content at grape maturity. (Alessandrini *et al.*, 2017). Consequently, the Rio Negro region is subject to a pronounced infra-day temperature variation, where warm days are followed by cold nights. This lengthens the growing season and leads to a balance of rich grape traits and acidity in the wines. Accordingly, Rio Negro is one of Argentina's up-and-coming wine regions and more grapevine producers are exploring its viticultural potential. The climate is cooler than in much of the rest of Argentina and "elegant, cool-climate styles of Pinot Noir, Sauvignon Blanc and Malbec are produced here" (Caballero, 2017). Due to these changes of temperatures and dryness conditions during 2011–2018, the PDO area become, from the agro-climatic point of view, more suitable for grapevine cultivation particularly for qualitative wines production. Basilicata region, from this perspective, is rich in term of grapevine biodiversity and it is part of the Third Centre of Domestication of *Vitis vinifera* (Del Lungo, 2016). Under this agro-climatic scenario, it could be suggested the selection of ancient autochthonous varieties that have been subjected to many natural selection cycles in thousands of years and have been crossed extreme climatic phases. For this reason, they have accumulated some genes, mainly still unexpressed, in their DNA, through the spontaneous intersection and mutation processes that allow them to give positive effect on yield and important grapevine properties in a climatic change condition (Labagnara *et al.*, 2018). Many authors investigated the potentialities of these ancient autochthonous varieties highlighting their peculiar traits (Labagnara *et al.*, 2018 and Alba *et al.*, 2016). In the PDO "Terre dell'Alta Val d'Agri", according to findings highlighted in this work, it could be suggested a future use of ancient varieties that could be suitable under these climate conditions. The ancient autochthonous varieties Aglianico B., Giosana B. and Santa Sofia (Alba *et al.*, 2016) are mainly proposed for their historical and cultural heritage of the PDO "Terre dell'Alta Val d'Agri".

CONCLUSIONS

The present study aimed to analyze the climatic potentiality and suitability of the area of the PDO "Terre dell'Alta Val d'Agri" according a "two periods" approach. The results confirm that the current climatic characteristics of the studied area are favorable for grapevine growth. In particular the day-night thermal excursion increased in the 2011-2018; consequently, it allows the increase of grape properties in terms of preserving a good level of sugar, freshness and aromatic complexity in berries. The global climate change is affecting the PDO "Terre dell'Alta Val d'Agri" with an increase in temperature and a small decrease in precipitation during the growing season. These changes evidence the agro-climatic similarity of PDO with the Rio Negro (Argentina) wine-growing region, highlighting new potentialities. These finding, in addition to the possibility to introduce the cultivation of ancient autochthonous late varieties or with greater thermal needs, could turn climate change into a threat to opportunities for the enhancement of Basilicata viticulture. The "two periods" approach can be applied to other grape growing regions in order to verify if climate change is modifying the suitability of the area for wine production.

ACKNOWLEDGMENTS

The authors thank dr. Emanuele Scalcione, of ALSIA, for supplying the weather data

REFERENCES

Alba V., Bergamini C., Gasparro C., Mazzone F., Roccotelli S., Antonacci D., Caputo A. R., Del Lungo S., Dal Monte G., Cirigliano P., Labagnara T., Pisani F., Cerbino D. 2016. Basivin-Sud la ricerca del germoplasma viticolo in Basilicata. In: Adda Editore II edition (Eds.). ISBN 9788867172351.

Alessandrini M., Gaiotti F., Belfiore N., Matarese F., D'Onofrio C. and Tomasi D., 2017. Influence of vineyard altitude on Glera grape ripening (Vitis vinifera L.): effects on aroma evolution and wine sensory profile. J. Sci. Food Agric., **97**, 2695-2705. doi: 10.1002/jsfa.8093

Baccaglio M. 2019. I numeri del vino su dati ISTAT 2019. Source: www.inumeridelvino.it

Bindi M., and Maselli F., 2001. Extension of crop model outputs over the land surface by the application of statistical and neural network techniques to topographical and satellite data. Clim. Res. **16**, 237-246.

Blanco-Ward D., Garcia-Queijeiro J.M. and Jones G.V., 2007. Spatial climate variability and viticulture in the Mino River Valley of Spain. Vitis **46**, 63-70.

Bois B., 2002. Variabilité mésoclimatique à l'intérieur du département de la Girondeet ses conséquences sur la culture de la vigne en Bordelais. École Nationaled'Ingénieurs des Travaux Agricoles, Bordeaux, 66 pp.

Caballero A., 2017. Vitivinicultura y enología afectadas por el cambio climático. Comahue, **2**- Marzo p. 37-41

Carbonneau A., 2003. Ecophysiologie de la vigne et terroir. Terroir, zonazione, viticoltura Trattato internazionale: Phytoline. pp. 61-102.

Catizzone M., 1980. La carta dei "Land System della Val d'Agri. Nota alla carta in scala 1:100.000. In: Ricerche pedologiche in Val d'Agri, C.N.R.-Centro di studio della Genesi, Classificazione e Cartografia del suolo, Firenze, 1-36.

Cirigliano P., Chiriacò M.V., Nunez A., Dal Monte G. and Labagnara T., 2017. Combined effect of irrigation and compost application on Montepulciano berry composition in a volcanic environment of Latium region (central Italy). Ciencia e Investigacion Agraria, **44**, (2), 195-206.

Cirigliano P., Zaccardi O., Caputo A., Castillo C., Murgia J., 2007. I quaderni dell'Alsia. (Eds) SUPEMA, 43-57 Rome, Italy.

Crespo J., Rigou P., Romero V., Garcia M., Arroyo T., Cabellos J.M., 2017. Effect of seasonal climate fluctuations on the evolution of glycoconjugates along the ripening period of grapevine cv. Muscat a petits grains blancs berries. J. Sci. Food Agric DOI: 10.1002/jsfa.8656

Del Lungo S., Caputo A. R., Gasparro M., Alba V., Bergamini C., Roccotelli S., Mazzone F., Pisani F., 2016. Lucania as the heart of III vine domestication center: The rediscovery of autochthonous vines. In: Proc: XXXIX the World Congress of Vine and Wine,

VII BIO Web of Conferences DOI:10.1051/bioconf/20160701021

Dumas V.; Lebon E., Morlat R., 1997. Differentiation of local climate in the Alsatian vineyards. J. Int. Sci. Vigne Vin. **31** (1), 1-9.

Edwards E.J. and Clingeleffer P.R., 2013. Interseasonal effects of regulated deficit irrigation on growth, yield, water use, berry composition and wine attributes of Cabernet Sauvignon grapevines. Australian Journal of Grape and Wine Research **19**, 261-276.

Ferrer M., Pedocchi R., Michelazzo M., Gonzalez Neves G., CarbonneauA., 2007. Delimitación y descripción de regiones vitícolas del Uruguay en base al método de clasificación climática multicriterio utilizando índices bioclimáticos adaptados a las condiciones del cultivo. Agrociencia (2007) Vol **XI** N° 1 pág. 47-56

Fraga H., Atauri A.R., Malheiro AC., Santos J.A., 2016. Modelling climate change impacts on viticultural yield, phenology and stress conditions in Europe. Global Change Biology **22**, 3774-3788.

Fraga H., Malheiro A.C., Moutinho-Pereira J., Santos J.A., 2012. An overview of climate change impacts on European viticulture. *Food Energy Secur.* **1**, 94-110. doi:10.1002/fes3.14

Fregoni C. and Pezzuto S., 2000. Principes et premières approches de l'indice bioclimatique de qualité de Fregoni. Progrès Agricole et Viticole, **117** (18), 390-396.

Gladstones J.S., 1992. Viticulture and environment: a study of the effects of environment on grapegrowing and wine qualities, with emphasis on present and future areas for growing winegrapes in Australia. Adelaide: Winetitles.

Goldner M.C. and Zamora M.C., 2007. Sensory characterization of *Vitis vinifera* cv. Malbec wines from seven viticulture regions of Argentina. Journal of Sensory Studies, **22**, 520-532. doi:10.1111/j.1745-459X.2007.00123.x

Hannah L., Roehrdanz P.R., Ikegami M., Shepard A.V., Shaw M.R., Tabor G., Zhi L., Marquet P.A., Hijmans R.J., 2013. Climate change, wine, and conservation. Proc. Natl. Acad. Sci. U. S. A. **110**, 6907-6912. doi:10.1073/pnas.1210127110

Hargreaves G. H., Samani Z.A., 1985. Estimating potential evapotranspiration. Journal of Irrigation and Drainage Engineering, 108 (3): 225-230.

Holland T., Smit B., 2014. Recent climate change in the Prince Edward County winegrowing region, Ontario, Canada: Implications for adaptation in a fledgling wine industry. Regional Environmental Change **14**, 1109-1121

Hormazabal S., Lyon G. and Carbonneau A., 2002. Variabilité et limite du macroclimat viticole méditerranéen des Départements de l'Aude, del'Hérault et du Gard, dans le Midi de la France. Progrès Agricole et Viticole **119**, 102-110

Huglin P., 1978. Nouveau Mode d'Évaluation des Possibilités Héliothermiques d'un Milieu Viticole. C R Seances Acad. Agric. France **64**, 1117-1126

Jackson, R.S.; 2000: Wine Science: Principles, Practice, Perception. 2nd edn. Academic Press, San Diego, CA.

Jackson D.I. and Lombard P.B., 1993. Environmental and management practices affecting grape composition and wine quality-A review. Amer. J. Enol. Viticult. **44**, 409-430.

Jones G.V. and Davis R.E., 2000. Climate Influences on Grapevine Phenology, Grape Composition, and Wine Production and Quality for Bordeaux, France, Am. J. Viti. Enol. **51**, 249-261.

Jones G.V., White M.A., Cooper O.R. and Storchmann K., 2005. Climate Change and Global Wine Quality. Climatic Change, **73** (3): 319-343.

Jones G.V., Snead N., Nelson P., 2004. Modeling viticultural landscapes: A GIS analysis of the terroir potential in the Umpqua Valley of Oregon. Geoscience Canada Volume **31**, Issue 4, Pages 167-178.

Jones G.V., 2006. Climate and Terroir: Impacts of Climate Variability and Change on Wine. In Fine Wine and Terroir - The Geoscience Perspective. Macqueen, R.W., and Meinert, L.D., (eds.). Newfoundland, Canada: Geoscience Canada, Geological Association of Canada.

Jones G., Moriondo M., Bois B., Hall A. and Duff A., 2009. Analysis of the spatial climate structure in viticulture regions worldwide. Le Bulletin de l'Organisation Internationale de la Vigne et du Vin **82**, 507-518.

Kliewer W.M., Torres R.E., 1972. Effect of controlled day and night temperatures on grape coloration. American Journal of Enology and Viticulture. **23**, 71–77.

Kliewer W.M., 1973. Berry composition of Vitis vinifera cultivars as influenced by photo- and nycto-temperatures during maturation. J. Am. Soc. Hort. Sci. **98**: 153-159.7

Labagnara T., Bergamini C., Caputo A.R., Cirigliano P., 2018. *Vitis vinifera* L. germoplasm diversity: a genetic and ampelometric study in ancient vineyards in the South of Basilicata region (Italy), (Article in press in Vitis)

Marx W., Haunschild R., Bornmann L., 2017. Global Warming and Tea Production-The Bibliometric View on a Newly Emerging Research Topic. Climate, **5**, 3-46.

Matese A., Crisci A., Di Gennaro S.F., Primicerio J., Tomasi D., Marcuzzo P., GuidoniS., 2014. Spatial variability of meteorological conditions at different scales in viticulture. Agricultural and Forest Meteorology 189-190 159-167.

Montes C., Pèrez-Quezada J.F., Pena-Neira A., TonietttoJ., 2012. Climatic potential for viticulture in Central Chile. Australian Journal of Grape and Wine Research **18**, 20-28.

Moran M., Petrie P., and Sadras V., 2018. Late Pruning and Elevated Temperature Impact On Phenology, Yield Components and Berry Traits in Shiraz. American Journal of Enology and Viticulture. doi: 10.5344/ajev.2018.18031

OIV, 2012: OIV guidelines for vitiviniculture zoning methodologies on a soil and climate level. Resolution OIV-VITI 423-2012 rev. **1**, 19 pp.

Palliotti A., Tombesi S., Silvestroni O., Lanari V., Gatti M., Poni S., 2014. Changes in vineyard establishment and canopy management urged by earlier climate-related grape ripening. Scjenta Horticolture **178**, 43-54.

Pons A., Allamy L., Schuttler A., Rauhut D., Thibon C. and Darriet P., 2017. What is the expected impact of climate change on wine aroma compounds and their precursors in grape?. OENO One, **51**(2), 141-146. doi:http://dx.doi.org/10.20870/oeno-one.2016.0.0.1868

Riou C., 1994. The effect of climate on grape ripening: application to the zoning of sugar content in the European Community Centre, Commun de Recherché Commission Europeenne, Luxembourg Office for Official Publications of the European Communities.

Roby G., Harbertson J. F., Adams D. A. and Matthews M. A., 2004. Berry size and vine water deficits as factors in winegrape composition: Anthocyanins and tannins. Australian Journal of Grape and Wine Research **10**, 100-107, 2004.

Serpa D., Nunes J.P., Keizer J.J., Abrantes N., 2017. Impacts of climate and land use changes on the water quality of a small Mediterranean catchment with intensive viticulture. Environ. Pollut. **224**, 454-465.

Soar C.J., Sadras V.O., Petrie P.R., 2008: Climate drivers of red wine quality in four contrasting Australian wine regions. Aust. J. Grape Wine Res. **14** (2): 78-90. doi: 10.1111/j.1755-0238.2008.00011.x

Teslic N., Vujadinovic M., Ruml M., Antolini G. and Others, 2017. Climatic shifts in high quality wine production areas, Emilia Romagna, Italy, 1961-2015. Clim Res **73**:195-206. https://doi.org/10.3354/cr01468

Tomasi D., Gaiotti F., Jones G.V., 2013. The Power of the Terroir. Springer Verlag, ISBN-13: 9783034806275.

Tonietto J. and Carbonneau A., 2004. A multicriteria climatic classification system for grape-growing regions worldwide. Agricultural and Forest Meteorology, **124**, 81-97.

Van Leeuwen C., Tregoat O., Chone X., Bois B., Pernet D. and Gaudillere J.P., 2009. Vine water status is a key factor in grape ripening and vintage quality for red Bordeaux wine. How can it be assessed for vineyard management purposes? J. Int. Sci. Vigne Vin, 2009, **43**, n° 3, 121-134.

Van Leeuwen C., Destract-Irvine A., 2017. Modified grape composition under climate change conditions requires adaptation in the vineyard. *OENO One*, 2017, **51**, 2 147-154

WMO, 2011. Guide to Climatological Practices. WMO-No. 100

Zottele F. and Delay E., 2017. How much can a virtual territory help us to understand the resilience of the heroic viticulture? A case study in Trentino (IT). 5th international congress on mountain and steep slope viticulture. Conegliano, Italy. Extreme viticulture: values, beauties, alliances, vulnerabilities. http://vit.entecra.it/sito_cong2, halshs-01472179

Italian Journal of Agrometeorology
Rivista Italiana di Agrometeorologia

Firenze University Press
www.fupress.com/ijam

Citation: S. Falzoi, F. Acquaotta, M.A. Pulina, S. Fratianni (2019) Hydrological drought analysis in Continental Temperate and Mediterranean environment during the period 1981-2017. *Italian Journal of Agrometeorology* (3): 13-23. doi: 10.13128/ijam-798

Received: January 14, 2019

Accepted: September 18, 2019

Published: December 28, 2019

Data Availability Statement: All relevant data are within the paper and its Supporting Information files.

Competing Interests: The Author(s) declare(s) no conflict of interest.

Hydrological drought analysis in Continental Temperate and Mediterranean environment during the period 1981-2017

Analisi della siccità idrologica in ambiente Temperato Continentale e ambiente Mediterraneo, nel periodo 1981-2017

Simone Falzoi[1,*], Fiorella Acquaotta[1,2], Maria Antonia Pulina[3], Simona Fratianni[1,2]

[1] *Earth Science Department, University of Torino, via Valperga Caluso 35 - 10125, Torino, Italy*

[2] *Research Centre on Natural Risks in Mountain and Hilly Environments - NatRisk, Largo Braccini, 2 – 10095, Grugliasco (TO), Italy*

[3] *Agriculture Department, University of Sassari, Viale Italia 39 – 07100, Sassari, Italy*

*Corresponding author. E-mail: simone.falzoi@unito.it; fiorella.acquaotta@unito.it; pulina@uniss.it; simona.fratianni@unito.it

Abstract. A 37 year (1981-2017) study of the hydrological drought trend was conducted in two Italian regions, Piedmont and Sardinia, with different climatic features (Temperate Continental climate and Mediterranean climate, respectively). For this purpose, we have examined the daily data of 13 meteorological stations uniformly installed in the two areas, and the trends of the Standardised Precipitation Index (SPI) and Standardised Precipitation Evapotranspiration Index (SPEI) have been also evaluated. The similarities and differences between the indices of the two regions were then considered. In most stations of both zones, there is a statistically significant trend of increase in the SPI and decrease in the SPEI. Nevertheless, the trend of indices averaged over stations of the two indices is not significant in either of the two climatic zones considered.

Keywords. Hydrological drought, SPI, SPEI, climate indices.

Riassunto. Uno studio di 37 anni (1981-2017) sull'andamento della siccità idrologica è stato realizzato in Piemonte e in Sardegna, due regioni italiane che presentano diverse caratteristiche climatiche (rispettivamente clima Temperato Continentale e clima Mediterraneo). A tal fine, sono stati esaminati i dati giornalieri di 13 stazioni meteorologiche installate uniformemente nelle due aree, e sono stati altresì valutati gli andamenti dell'Indice di Precipitazione Standardizzata (SPI) e dell'Indice di Evapotraspirazione e Precipitazione Standardizzati (SPEI). Sono state quindi considerate le somiglianze e le differenze tra gli indici delle due regioni. Nella maggior parte delle stazioni di entrambe le zone, vi è una tendenza statisticamente significativa di aumento dello SPI e di diminuzione dello SPEI. Tuttavia, l'andamento dei valori medi sulle stazioni dei due indici non è significativo in nessuna delle due zone climatiche considerate.

Parole chiave. Siccità idrologica, SPI, SPEI, indici climatici.

INTRODUCTION

Drought is a natural hazard caused by a lower-than-average reduction of precipitation. When the phenomenon occurs for the duration of a season or for extended periods of time, it creates insufficient conditions to supply human and environmental demands (WMO, 2006). In contrast to aridity, which is defined as a permanent condition, drought is a temporary climate phenomenon that typically begins as a dry spell or a period of abnormally dry weather.

A drought can alternatively be broadly defined as a temporary, recurring reduction in the precipitation in an area, and is considered as one of the most important climate change impacts on natural and socio-economic systems. Few extreme events are as economically and ecologically disruptive as drought, which affects millions of people in the world each year (Dai, 2011). Its effects occur after long periods without precipitation, therefore it is difficult to objectively quantify its characteristics in terms of intensity, amplitude, duration and spatial extent (Bordi *et al*., 2009; Vicente-Serrano *et al*., 2010; Bevan *et al*., 2014). In recent years, drought has become more intense and frequent, which has a negative impact on the socio-economic balance of the countries concerned. For example, in recent years the Californian government had to limit water use for irrigation and domestic use (Dettinger and Cayan, 2014); in 2012 an increase in food price was caused by a simultaneous drought in USA and Russia (Van Loon, 2015); in 2011, a mass migration in the Horn of Africa was caused by drought (Viste *et al*., 2012); and in 2010, drought affected food production in large parts of China (Lu *et al*., 2011).

Mountain regions and the Mediterranean basin, considered "hot spots" of climate change, are susceptible to drought situations and are heavily impacted by extreme events (Ronchi *et al*., 2007; Capra and Scicolone, 2012). Over the past 30 years, the temperature in Piedmont increased by 0.7 °C (Fratianni *et al*., 2015), and July of 2015 was the hottest month on record, while the period from July to October of 2017 was one of the driest in the last 60 years, with the main Piedmontese river Po always below the average flow. While no significant variation was recorded in the annual amount of precipitation, the seasonal distribution has changed with a decrease during the winter season of -1.5 mm year^{-1} in the north of Italy, and -7.7 mm year^{-1} in the central part (Fratianni and Acquaotta, 2017). Extreme drought years have been reported in Sardinia since 1981, with a greater frequency in the last decade, especially in the springtime, at the beginning of the vegetative season, and in the South of the island (Pulina, 2012). Temperature and extreme events are expected to increase at the end of the century, according to future climate projections. For example, for the near future (next 15-20 years), Perini *et al.* (2011) predicted a strong decrease in winter and spring precipitation in Northern and Southern Italy, and a reduction of summer rainfall in Southern Italy and in the Islands. While, by the 2100s, a general temperature increase of about 3 °C is expected in all seasons across the whole of Italy, peaks of 4 °C are projected for the Po Valley in winter and over the whole north-west region in summer (Bucchignani *et al*., 2016), according to the RCP4.5 scenario, with increasingly frequent and long-lasting heat waves, which will extend to more than thirty days over the entire summer season (Collins *et al*., 2013; Drumond *et al*., 2017; González-Hidalgo *et al*., 2018). On the contrary, the RCP8.5 scenario predicts a strongly significant precipitation reduction in spring and summer in the Alpine area with a negative anomaly from 0.1 to 0.4 mm day^{-1} (Bucchignani *et al.* 2016). In these future climate scenarios, drought events will become increasingly common, more intense and less predictable, especially in vulnerable environments such as Alps and Mediterranean.

Although numerous climatic and biological classifications have been proposed for aridity and drought conditions (e.g. De Martonne, 1926; Thornthwaite, 1948; Palmer, 1965; Agnew and Anderson, 1992; Pashiardis and Michaelides, 2008; Hannaford *et al*., 2011; Nastos *et al*., 2013; Beguéria *et al*., 2014; Beguéria *et al*., 2018), it is still difficult to define wetness limits precisely and delineate the boundary between different degrees or levels of aridity/drought or the opposite, humidity. In 2009, the World Meteorological Organization, recommended that the Standardised Precipitation Index, SPI (McKee *et al*., 1993) be used around the world to characterize meteorological droughts. Cheval *et al.* (2014), analysed the spatial and temporal variability of meteorological drought in Romania by using SPI and distinguished winter and summer driving factors of the drought spells. SPI was also investigated in six regions of southern South America in order to observe the duration of dry sequences (Minetti *et al*., 2010). Furthermore, SPI is a useful index to analyse and compare time series of monthly precipitation in the past with the ongoing time series (Rana *et al.,* 2016). Temperature, wind and relative humidity are also important factors to include in characterizing drought, and most recently, Vicente-Serrano *et al.* (2010) proposed a further index which combines precipitation, temperature and evapotranspiration, called Standardised Precipitation Evapotranspiration Index (SPEI). SPI and SPEI were both used to characterize the summer 2015, which ranks as the hottest and climatologically driest summer since 1950 over extended regions in eastern Europe (Ionita *et al.*, 2017).

The aims of this work are *i*) to analyse the hydrological drought conditions, which are related to the effect of the absence of precipitation on water resources, in two different Italian climatic regions: Temperate Continental climate in Piedmont region and Mediterranean climate in Sardinia region; *ii*) to compare the two above-mentioned standardised indices (SPI and SPEI) to delineate drought conditions between two different environments, and *iii*) to verify potential drought trends during a period of 37 years (1981-2017), in an ongoing climate change scenario.

MATERIALS AND METHODS

Study area

The study was conducted in two Italian regions, Piedmont and Sardinia (Fig. 1), with a marked climatic difference (Fig. 2).

Piedmont region is located in the continental area at the base of the Western Alps, between 44°02'N and 46°26'N and between 06°49'E and 08°32'E. Although the region is relatively small, it is characterised by a varied topography with a predominance of mountains. The Alps, where most peaks are over 2,500 m, mark the border with France to the West and Switzerland to the North. The hilly areas which border the western part of the Po Valley complete the physical boundaries of the region. The altitudinal gradient (from about 100 m to 4,000 m a.s.l.) strongly influences the regional climate, which experiences great variation in temperature and precipitation over a short distance (Nigrelli *et al.*, 2018). The climate is Continental Temperate, "*Cf*", according to Köppen's classification (Fratianni and Acquaotta, 2017). The average annual temperature varies between 11-12 °C in the lowlands area and it does not exceed 1 °C in mountainous areas above 2,400 m a.s.l. Annual precipitation rate varies from 500-700 mm in the plains to 2,000 mm in the interior Alpine valleys. The rainfall pattern is characterized by a classic bimodal trend, with two peaks in spring and autumn, and a minimum in winter (Bandini, 1931; Baronetti *et al.*, 2018).

Sardinia region is the second largest island in the Mediterranean Sea and is located between 38°53'N and

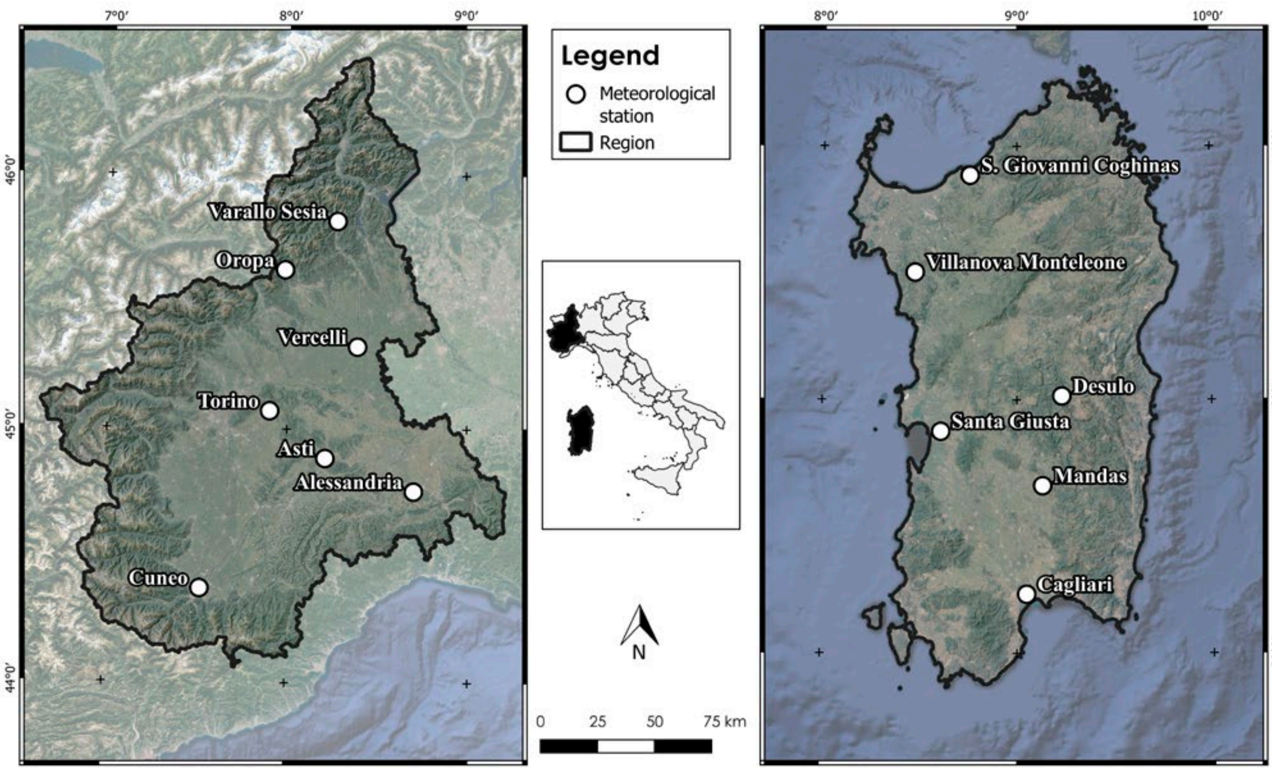

Fig. 1. Study area: Piedmont region on the left, Sardinia region on the right; white dots indicate positions of meteorological stations.

Fig. 1. Area di studio: Regione Piemonte a sinistra, Regione Sardegna a destra; i punti bianchi indicano le posizioni delle stazioni meteorologiche.

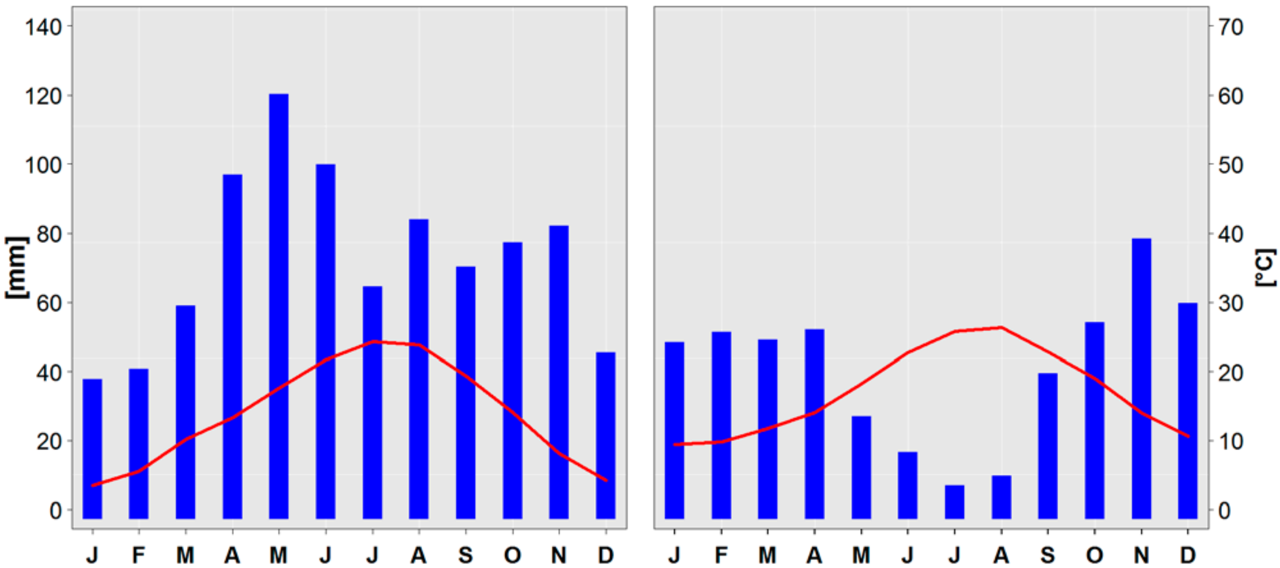

Fig. 2. Thermo-pluviometric diagram for Torino data series (on the left) and Cagliari/Elmas (on the right) during the period 1981-2017. Blue bars: precipitation amount; red lines: temperature.

Fig. 2. Diagramma termopluviometrico per le serie di Torino (a sinistra) e di Cagliari/Elmas (a destra), nel periodo 1981-2017. Barre azzurre: precipitazioni; linee rosse: temperatura

41°15'N and between 8°08'E and 9°48'E. The topography is mainly characterized by hills and plateaus, but also by flat areas in the West and mountainous areas in the East, with peaks higher than 1,300 m a.s.l. The average altitude is 334 m a.s.l. The climate is typically Mediterranean, "*Csa*", according to Köppen's classification, with mild and relatively rainy winters and hot, dry summers. Mean annual temperatures are strongly influenced by the distance from the sea and by the orography; the values range from 16-17 °C in the western plains (Campidano and Nurra) to 10-12 °C in the eastern highlands (Gennargentu, Limbara). The average annual precipitation is less than 500 mm in the lowlands area, while it exceeds 1,300 mm on the highest peaks. The maximum rainfall is normally recorded in December, with average values exceeding 200 mm in the mountainous areas (Pulina, 2015).

Meteorological data

Daily weather data in Piedmont region were collected from thermo-pluviometric stations of the Italian Hydrographic Mareographic Service (SIMN). Alessandria, Asti, Cuneo, Oropa, Torino, Varallo Sesia and Vercelli were the stations considered (Tab. 2). These are uniformly distributed in the region (Fig. 1) with an altitude range between 90 m and 1,180 m a.s.l. Meteorological stations above the limit of 1,200 m a.s.l. were excluded from the analysis in order to standardise the measurements with the Sardinian stations.

In the Sardinia region, daily temperature and precipitation data were obtained from the Hydrographic Sector of Sardinia Region (RAS) and Desulo, Mandas, San Giovanni Coghinas, Santa Giusta and Villanova Monteleone were the weather stations considered. These were supplemented by the addition of Cagliari/Elmas station from the Italian Air Force meteorological station network (Tab. 2). The altitude range of the stations (Fig. 1 and Tab. 2) is between 10 and 920 m a.s.l.. Their location is representative of the different geographical and topographical conditions of the island.

Daily precipitation (P) and maximum (T_x) and minimum (T_n) daily temperature data were considered for all stations during the period 1981-2010, which is the current climatological standard 30-year period (WMO, 2017).

An additional seven years (2011-2017) were collected for the stations of Torino and Cagliari/Elmas, in Piedmont and Sardinia region respectively, resulting in a total of 37 years of data. The two additional series of data (1981-2017), in the most representative stations of the two territories, were analysed in order to compare the most recent trends in two different areas. Fig. 2 shows the thermo-pluviometric diagrams of the two stations.

Method

A Quality Control (QC) analysis was conducted on the daily data series by using the R software *ClimPACT2* package (Alexander and Herold, 2016) to identify gaps, outliers and erroneous values (Acquaotta *et al.*, 2019). This algorithm detects incorrect values, such as P < 0 mm or $T_x < T_n$ and provides a series of graphical representations in the form of box diagrams in a monthly and annual scale, to evaluate discontinuities present in the series (Acquaotta *et al.*, 2016).

Outlier values are identified through the calculation of the estimated thresholds on the statistical characteristics of the series (Fortin *et al.*, 2016).

After the QC, on the T_x and T_n series, we carried out two homogenization tests, HOMER (Mestre *et al.*, 2013) and SLIDHOM (Mestre *et al.*, 2011) to identify and to correct the breaks or discontinuities (Acquaotta and Fratianni, 2014). HOMER was applied on monthly scale to identify the breaks, while the SPLIDHOM was carried out on the daily series to correct the inhomogeneities.

In order to characterize the hydrological drought in both regions, we used two derived indices: Standardised Precipitation Index - SPI (McKee *et al.*, 1993) and Standardised Precipitation Evapotranspiration Index - SPEI (Vicente-Serrano *et al.*, 2010). The two drought indices have been calculated for every meteorological station and subsequently represented as a single average value for each region.

SPI is an index based on monthly cumulative precipitation and classifies the accumulated precipitation of the month under consideration with respect to the long-term average monthly accumulated precipitation for the same month (or other time scales). SPI quantifies a deficit or surplus of rain over mean values, using a probabilistic approach for the precipitation event. The rainfall series is adapted to a gamma distribution, then transformed into a normal distribution having a null mean and a standard deviation equal to 1. SPI indicates the number of standard deviations by which a particular event exceeds from mean conditions.

SPEI is a multiscalar drought index designed to take into account both precipitation and potential evapotranspiration (PET). SPEI looks at long-term rainfall at different timescales and compares it with expected demand as indicated by potential evapotranspiration. The PET has been estimated with the Thornthwaite equations (Thornthwaite, 1948), a temperature-based method that uses only mean monthly temperature and latitude of the site to estimate potential evapotranspiration. The monthly average temperature and cumulative precipitation values were used to calculate SPEI.

Tab. 1. Classification of the wet and drought periods of SPI and SPEI, according to McKee et al. (1993) and Vicente-Serrano et al. (2010), respectively. SPI and SPEI indices are dimensionless.
Tab. 1. Categorizzazione dei periodi umido e di siccità di SPI e SPEI, rispettivamente secondo McKee et al. (1993) e Vicente-Serrano et al. (2010). Gli indici SPI e SPEI sono adimensionali.

Category	SPI and SPEI values (dimensionless)
Extremely wet	≥ 2.00
Severely wet	1.5 – 1.99
Moderately wet	1.00 – 1.49
Close to normal	-0.99 – 0.99
Moderately dry	-1.49 – -1.00
Severely dry	-1.99 – -1.50
Extremely dry	≤ -2.00

Classification of wet and dry periods based on SPI and SPEI indices as shown in Tab. 1.

On the annual scale (12-months) we calculated the trends of SPI and SPEI and then we compared the results with the annual trend of four climate indices, total annual P (prectot) for days with P ≥ 1.0 mm, total annual P from heavy rain days (r95p) with annual sum of daily P > 95th percentile, amount of hot days (T_X90p) percentage of days when T_X > 90th percentile, and amount of hot nights (T_N90p) percentage of days when T_N > 90th percentile (Tab. 2). The trend was computed by a linear least square and statistical significance was calculated at 95 % confidence level using F test, for both indices, in each station (Tab. 2) of the two regions (Fig. 3 and Fig. 4). A negative trend value means an increase of drought spells, and the statistical significance of the trend was verified by using the non-parametric test of Mann-Kendall (p value < 0.05) (Giaccone *et al.*, 2015).

Furthermore, the SPI and SPEI trends were calculated for the Torino and Cagliari/Elmas meteorological data on a timescale of 12 and 24 months, based on the period from 1981 to 2017.

RESULTS AND DISCUSSION

The Standardised Precipitation Index for the seven stations of Piedmont region showed no homogeneous trend (Tab. 2). The series of Cuneo, Torino and Vercelli stations showed a statistically significant upward trend. At these locations, increasing trends were observed in two climate indices of precipitation, prectot and r95p. Neither of the two indices were statistically significant according to the Mann-Kendall test. The trend was downward and statistically significant for Oropa site where the precipitation indices show decreasing trends and statistically significant for r95p. The series of Alessandria, Asti and Varallo Sesia stations, as well as the average SPI for those three stations showed no trend. Also, the trends of precipitation indices are not statistically significant, and the coefficients do not identify important variations. They range between 1.83 mm year^{-1} to 4.17 mm year^{-1} for prectot and between -4.87 mm year^{-1} to 0.94 mm year^{-1} for r95p (Tab. 2).

The period with the greatest number of consecutive wet months (SPI > 0) (Fig. 3) ranged from July 1992 to April 1997, a total of 58 months, while the period with the greatest number of consecutive dry months (SPI < 0) ranged from December 2004 to June 2008, 43 months. On average, wet periods alternated with dry periods of six months in this region.

On the other hand, the trend of SPEI is decreasing and is statistically significant in all the Piedmontese stations considered (Tab. 2). The maximum decrease (-0.004), is calculated for the Oropa station, followed by Asti and Cuneo (-0.003). The behaviour of this index is well correlated with the behaviour of temperature index, T_X90p. The trend of T_X90p is increasing and is statistically significant in most of the stations. The trends range between 0.67 % year^{-1}, calculated in Oropa, to 0.33 % year^{-1}, calculated in Alessandria (Tab. 2).

The average SPEI among stations shows a downward trend (-0.002), but not statistically significant. The longest wet period observed was between July 1992 and April 1997, 58 months, while the longest dry period lasted from November 2004 to November 2008, 49 months (Fig. 3).

Regarding Sardinia region, the SPI (Tab. 2) showed an increasing and statistically significant (0.002) trend only in 2 of the 6 stations considered (Santa Giusta and Desulo). The SPI calculated for the other stations and the average SPI for those stations showed no significant trend during the considered period. The trends on precipitation indices are not statistically significant in Santa Giusta e Desulo, with an increasing trend as for prectot while is decreasing for r95p. Also, in the other stations the trends are not statistically significant but for prectot the slopes are negative and near to zero, ranging between -0.99 mm year^{-1} to -0.47 mm year^{-1} (Tab. 2). The average SPI value over stations (Fig. 4) remained consistently above 0 for a maximum of 34 months, from April 1984 to January 1987 and for 30 consecutive months, from October 2003 to March 2006. Values were less

Tab. 2. Weather stations list analysed in Piedmont and Sardinia regions for the reference period 1981-2010, with their values of Elevation (Alt. m a.s.l.), coordinates (Lat N; Lon E), the calculated SPI and SPEI annual trends (year^{-1}) at 12 months, annual total wet-day (prectot), total annual P from heavy rain days (r95p), amount of hot days (T_X90p), and amount of hot nights (T_N90p) at 12- month time scale. Statistically significant trends with a *p value* ≤ 0.05 are indicated in bold.

Tab. 2. Elenco delle stazioni meteorologiche analizzate nelle regioni piemontesi e sarde per il periodo di riferimento 1981-2010, con i loro valori di quota (m s.l.m.), coordinate (Lat N; Lon E), i valori dei trend annuali di SPI e SPEI (anno^{-1}), precipitazioni totali (prectot) ed intense (r95p), numero di giorni di caldo (T_X90p), e numero di notti di caldo (T_N90p) su scale temporale di 12 mesi. I valori statisticamente significativi (p ≤ 0,05) sono evidenziati in grassetto.

	Station	Alt. m a.s.l.	Lat N	Lon E	SPI	SPEI	prectot	r95p	T_x90p	T_n90p
Piedmont Region	Alessandria	90	4955808	476651	0	**-0.002**	1.83	1.47	**0.33**	0.16
	Asti	117	4970569	437876	0	**-0.003**	3.41	0.94	**0.40**	**-0.32**
	Cuneo	575	4914085	382681	**0.002**	**-0.003**	3.98	4.05	0.62	0.10
	Oropa	1180	5053196	420664	**-0.003**	**-0.004**	-18.77	**-17.17**	**0.67**	0.14
	Torino	239	4991497	413680	**0.003**	**-0.001**	7.00	3.42	0.43	-0.11
	Varallo Sesia	453	5074366	443680	0	**-0.001**	1.40	-4.87	**0.55**	-0.04
	Vercelli	135	5019297	452240	**0.002**	**-0.002**	4.17	3.12	**0.58**	0.09
Sardinia Region	Cagliari	21	4342672	504315	0	0	-0.47	0.87	**0.20**	**0.24**
	Desulo	920	4429509	519699	**0.002**	**0.002**	4.71	-0.09	**-0.37**	-0.17
	Mandas	491	4390215	511294	0	0	-0.99	0.39	**0.22**	**0.26**
	S. Giovanni Coghinas	210	4526143	479570	0	**-0.003**	-0.95	-0.20	**0.36**	0.08
	Santa Giusta	10	4414049	466626	**0.002**	0	1.30	-0.16	**0.21**	0.01
	Villanova Monteleone	567	4483757	455470	0	**-0.002**	-0.88	-2.39	0.06	-0.05

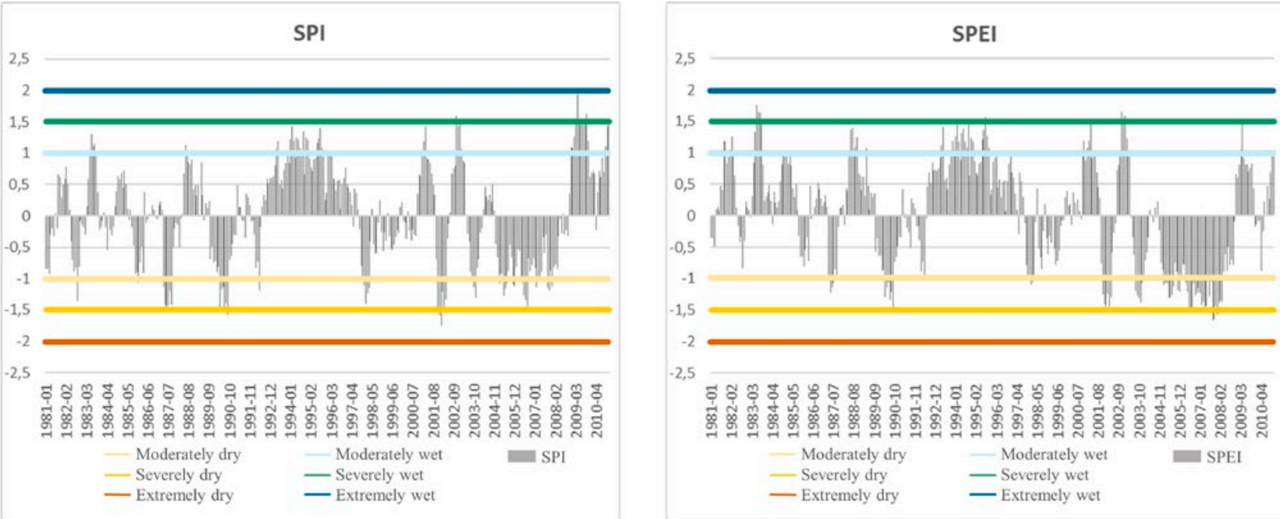

Fig. 3. Average of SPI (on the left) and SPEI (on the right) values for the stations of Piedmont region. The yellow/brown and blue/green coloured lines indicate the critical values of the indices in dry and wet conditions, respectively.
Fig. 3. Valori medi di SPI (a sinistra) e SPEI (a destra) per le stazioni della Regione Piemonte. Le linee colorate giallo/marrone e blu/verde indicano i valori critici degli indici in condizioni rispettivamente secche e umide.

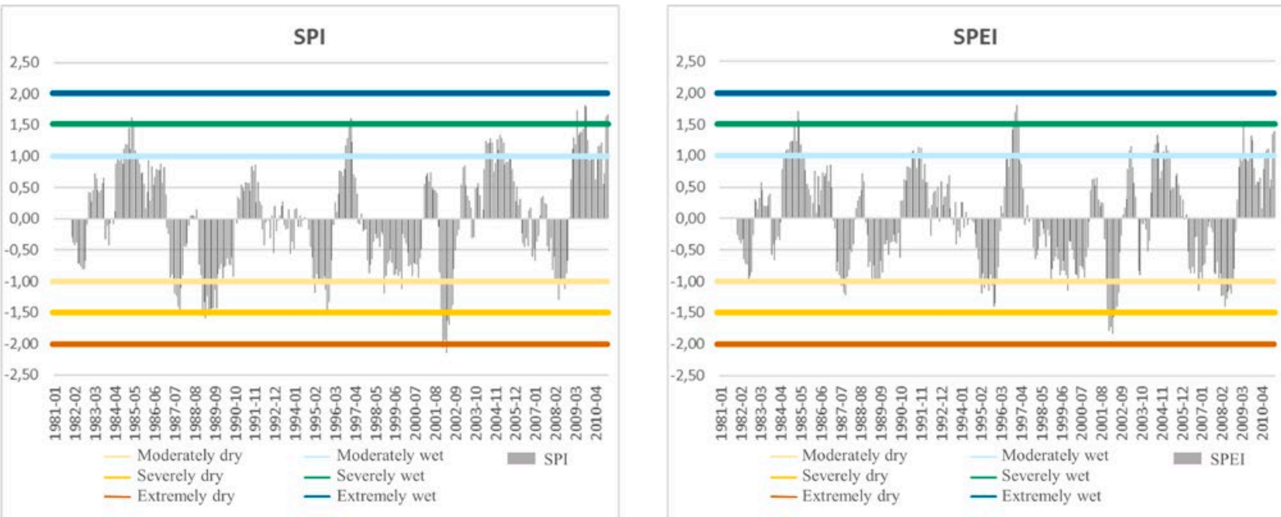

Fig. 4. Average of SPI (on the left) and SPEI (on the right) values for the stations in Sardinia region. The yellow/brown and blue/green coloured lines indicate the critical values of the indices in dry and wet conditions, respectively.
Fig. 4. Valori medi di SPI (a sinistra) e SPEI (a destra) per le stazioni della Regione Sardegna. Le linee colorate giallo/marrone e blu/verde indicano i valori critici degli indici in condizioni rispettivamente secche e umide.

than zero for a total of 40 months from September 1997 to December 2000, and for 25 consecutive months from November 1988 to November 1990. According to the classification of McKee *et al.* (1993), which evaluates the severity of drought, there were nine months considered "*Severely dry*", and two months "*Extremely dry*" (from January to March 2002), during the period 1981-2010.

The trend of SPEI (Tab. 2) is statistically significant in three of the six Sardinian stations considered. A positive trend was observed for Desulo station (0.002), and negative trend for the stations of Villanova Monteleone (-0.002) and San Giovanni Coghinas (-0.003). These behaviours are well correlated with the behaviour of temperature indices, in particular with maximum tem-

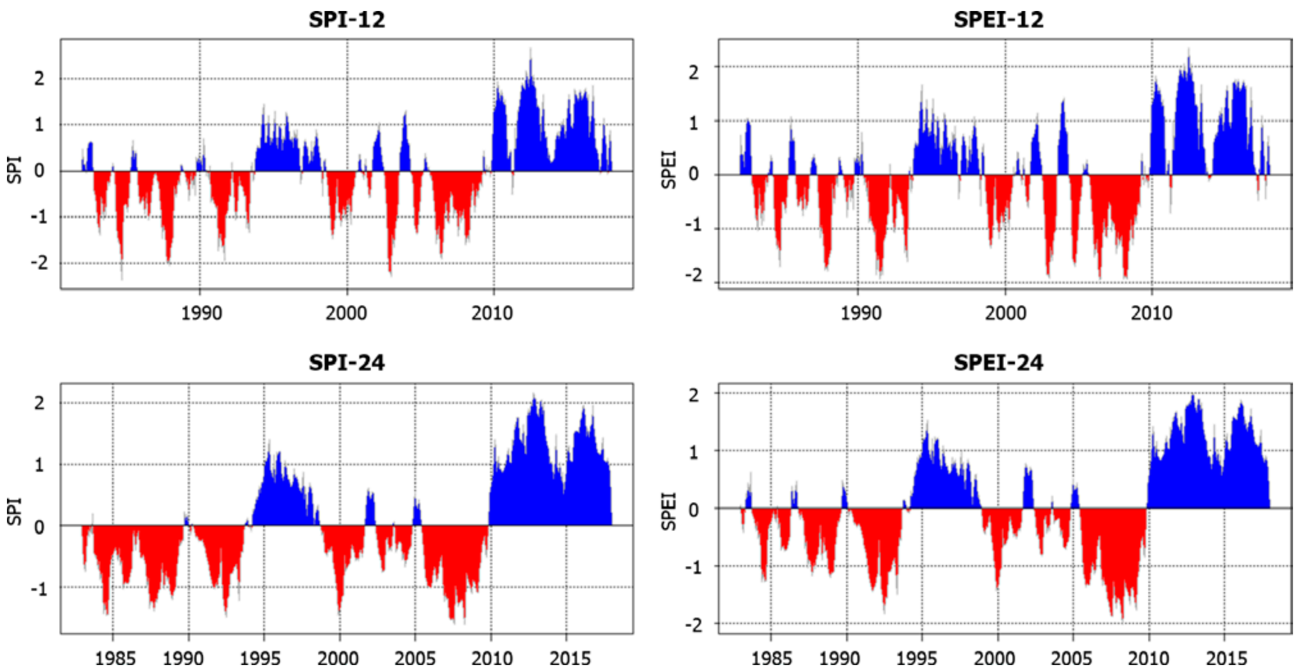

Fig. 5. SPI (on the left) and SPEI (on the right) values for the Torino station in Piedmont region, calculated on the period of 12, 24 months.
Fig. 5. Valori SPI (a sinistra) e SPEI (a destra) per la stazione di Torino in Piemonte, calcolati nel periodo di 12, 24 mesi.

perature, T_X90p. The T_X90p trend in Desulo is decreasing and statistically significant, -0.37 % year^{-1}, while in San Giovanni Coghinas and Villanova Monteleone the trends increase, but only in San Giovanni Coghinas the slope is statistically significant, 0.36 % year^{-1} (Tab. 2).

The average of SPEI shows a downward trend (< -0.001), but this is not statistically significant. The analysis of the trend of the average SPEI values (Fig. 4) showed the longest wet period was from May 1984 to January 1987 (33 months), and the longest dry period was from December 1997 to December 2000 (37 months in total).

Fig. 5 and Fig. 6 show the trend of the SPI and SPEI values calculated in the station of Torino and Cagliari/Elmas respectively, during the period 12 and 24 months.

In the last seven years in Torino, the SPI-24 and SPEI-24, as much as in the 12 months time scale, show a more humid trend with a remarkable increase of precipitation, which contrasts with the period 1981-2010 in the same region, in which dry events were prevalent. From 1993 to 1998 the second longest wet period was recorded, clearly highlighted by the 24 month graph (Fig. 5).

From a general point of view, the SPEI exhibits the difference between the dry and wet months better than the SPI. This is evident in the comparison between SPI-12 and SPEI-12. The wet episodes before 1990 are clearly shown in the SPEI-12 but are absent on the SPI-12 (Fig. 5).

In contrast to the trend experienced by Torino, the trend in Cagliari/Elmas is more regular with a clear alternation between drought and humid periods, as shown in the 24 month graphs (Fig. 6), with an exception during the period 2000-2006, during which the dry period lasted longer and no wet episodes were recorded. SPI-12 and SPI-24 recorded "*Moderately wet*" periods in the years between 2012 and 2015. SPI shows values greater than zero in the last two years in contrast to the SPEI, which shows smaller values for the same periods.

As described by Vicente-Serrano *et al.* (2010), the influence of PET on drought conditions is difficult to estimate. In this analysis it is possible to compare the extent of drought indicated by both SPI, which is a precipitation-based index in which PET is not included, and SPEI, in which PET is included, for the same time period. This comparison illustrates the different and sometimes contrasting outcomes regarding the evaluation of drought when PET is included in the analysis. For example, at the end of the time series in Cagliari/Elmas, SPI-12 and SPI-24 indicate a wet period while SPEI-12 and SPEI-24 indicate a continuation of drought condition (Fig. 6).

CONCLUSIONS

The trend analysis of hydrological drought in two different environments, Temperate Continental climate

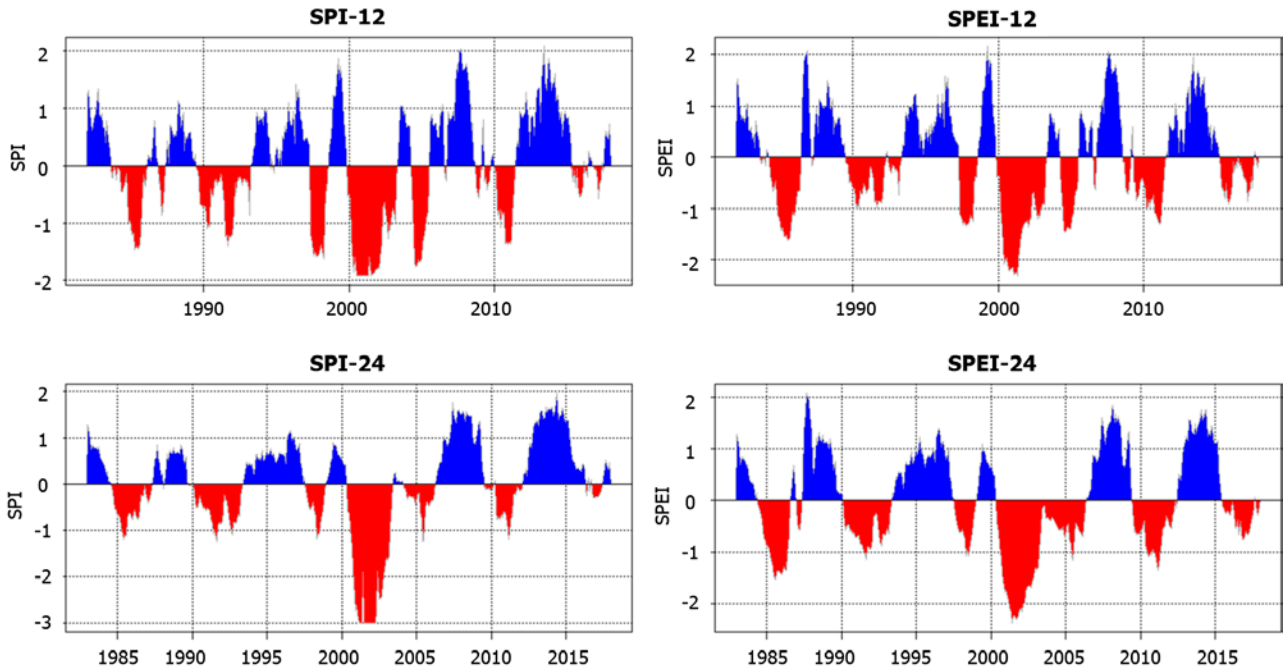

Fig. 6. SPI (on the left) and SPEI (on the right) values for the Cagliari/Elmas station in Sardinia region, calculated on the period of 12, 24 months.
Fig. 6. Valori SPI (a sinistra) e SPEI (a destra) per la stazione di Cagliari/Elmas in Sardegna, calcolati nel periodo di 12, 24 mesi.

and Mediterranean climate, was conducted using the thermo-rainfall series of seven stations in Piedmont region and six stations in Sardinia region, during the period 1981-2017. The Standardised Precipitation Index, SPI, and the Standardised Evapotranspiration Precipitation Index, SPEI, were calculated for each station, and average indices were also calculated for both regions.

Similarities and differences were detected between the two environments. Index trends were more defined in Piedmont region. In particular, the SPEI trend is significantly negative in all the stations considered, while the SPI trend is statistically significant with a positive correlation in three of the seven stations. Meanwhile, indices in Sardinia region showed a clear trend in only half of the stations considered. However, the trends of the average index values for all stations are not significant in either of the two climatic environments considered. Probably because of uncertainties in the SPEI drying trends might be overestimated due to the use of Thornthwaite PET estimation in this analysis. The use of this method is a limitation of the SPEI, as Thornthwaite PET is less physically realistic than other estimation techniques such as Hargreaves or Penman-Monteith equation.

On an annual level, no significant variations in precipitation quantity are recorded in either region, as confirmed by the Fratianni and Acquaotta (2017), and other studies did not show significant changes in annual precipitation in the Mediterranean basin (Coll *et al.*, 2017). On the contrary, in recent years the distribution of rainfall has changed due to the increase in extreme events.

According to Vicente-Serrano *et al.* (2010), both drought indices respond mainly to variability in precipitation, which is the main explanatory variable for drought. Nevertheless, trends of the drought indices in both regions are well correlated with the trends shown by the climate indices, in particular the temperature indices, such as the amount of hot days (T_X90p) and the amount of hot nights (T_N90p). A greater variation is calculated in Piedmont for both the precipitation pattern (prectot) and its manifestation as short but intense events (r95p). Meanwhile, the climate indices calculated in Sardinia for the rain series do not show significant change. However, there is a significant increase in temperatures classified as hot (T_X90p), in both regions. This trend impacts the performance of the SPEI, for which decreasing, and statistically significant trends were calculated in most cases.

The average duration of the wet period was longer in Piedmont region, where we calculated 58 consecutive months with SPI values greater than zero (from July 1992 to April 1997), compared to 34 consecutive months in Sardinia (from April 1984 to January 1987). The duration of dry periods was almost the same in both regions, 43 months with SPI values less than zero in Piedmont (from December 2004 to June 2008) and 40 consecutive months in Sardinia (from September 1997 to December 2000).

An increase in drought for most of the twenty-first century is predicted by future climate projections. Ecosystems and human activities could be profoundly impacted by the projected drying trends, while observed drying trends are having an effect on social-ecological systems, e.g. reduction in vineyard yield in Piedmont in 2017, accompanied by an increase in alpine wildfire. Concerted political and practical action to conserve water is necessary to minimize the impact of future drought, such as appropriate water management policies, and climate-smart agriculture practices.

REFERENCES

Acquaotta F., Baronetti A., Bentivenga M., Fratianni S., Piccarreta M., 2019. Estimation of rainfall erosivity in Piedmont (North West Italy) by using 10-minute fixed-interval rainfall. *Időjárás*, 123(1), DOI:10.28974/idojaras.2019.1.

Acquaotta F., Fratianni S., 2014. The importance of the quality and reliability of the historical time series for the study of climate change. *Revista Brasileira de Climatologia*, 14, 20-38, ISSN: 1980-055X.

Acquaotta F., Fratianni S., Venema V., 2016. Assessment of parallel precipitation measurements networks in Piedmont, Italy. *Int. J. Climatol.*, 36, 3963-3974.

Agnew C., Anderson W., 1992. Water in the arid realm. Routledge, London.

Alexander L., Herold N., 2016. ClimPACT2 Indices and software. User manual available online.

Bandini A., 1931. Tipi pluviometrici dominanti sulle regioni italiane. *Tech. report*, Roma: Ministero dei Lavori Pubblici.

Baronetti A., Acquaotta F., Fratianni S., 2018. Rainfall variability from a dense rain gauge network in North -West Italy. *Climate Research*, 75(3), 201-213.

Beguería S., Serrano-Notivoli R., Tomas-Burguera M., 2018. Computation of rainfall erosivity from daily precipitation amounts. *Science of The Total Environment*, 637, 359-373.

Beguería S., Vicente-Serrano S.M., Reig F., Latorre B., 2014. Standardized precipitation evapotranspiration index (SPEI) revisited: parameter fitting, evapotranspiration models, tools, datasets and drought monitoring. *Int. J. Climatol.*, 34 (10), 3001-3023.

Bevan S.L., Los S.O., North P.R.J., 2014. Response of vegetation to the 2003 European drought was mitigated by height. *Biogeosciences*, 11(11), 2897-2908.

Bordi I., Fraedrich K., Sutera A., 2009. Observed drought and wetness trends in Europe: an update. *Hydrol. Earth Syst. Sci.*, 13, 1519-1530.

Bucchignani E., Montesarchio M., Zollo A.L., Mercogliano P., 2016. High-resolution climate simulations with COSMO-CLM over Italy: performance evaluation and climate projections for the 21st century. *Int. J. Climatol.*, 36, 735-756.

Capra A., Scicolone B., 2012. Spatiotemporal variability of drought on a short-medium timescale in the Calabria region (Southern Italy). *Theor. Appl. Climatol.*, 116, 371-384.

Cheval S., Busuioc A., Dumitrescu A., Birsan M.V., 2014. Spatiotemporal variability of meteorological drought in Romania using the standardized precipitation index (SPI). *Climate Research*, 60(3), 235-248.

Coll J.R., Aguilar E., Ashcroft L., 2017. Drought variability and change across the Iberian Peninsula. *Theor. Appl. Climatol*, 130, 901-916. DOI 10.1007/s00704-016-1926-3.

Collins M., Knutti R., Arblaster J., Dufresne J.L., Fichefet T., Friedlingstein P., Gao X., Gutowski W.J., Johns T., Krinner G., Shongwe M., Tebaldi C., Weaver A.J., Wehner M., 2013. Long-term Climate Change: Projections, Commitments and Irreversibility. In: Climate Change 2013: The Physical Science Basis. Contribution of Working Group I to the Fifth Assessment Report of the Intergovernmental Panel on Climate Change [Stocker T.F., Qin D., Plattner G.-K., Tignor M., Allen S.K., Boschung J., Nauels A., Xia Y., Bex V., Midgley P.M. (eds.)]. Cambridge University Press, Cambridge, United Kingdom and New York, NY, USA.

Dai A., 2011. Drought under global warming: a review. *Climate Change*, 2(1), 45-65.

De Martonne E., 1926. Aréisme et indice aridité. Comptes Rendus de L'Acad. Sci., Paris, 182, 1395-1398.

Dettinger M., Cayan D.R., 2014. Drought and the California Delta - a matter of extremes. San Francisco Estuary and Watershed Sci., 12(2).

Drumond A., Gimeno L., Nieto R., Trigo R.M., Vicente-Serrano S.M., 2017. Drought episodes in the climatological sinks of the Mediterranean moisture source: The role of moisture transport. *Global and Planetary Change*, 151, 4-14.

Fortin G., Acquaotta F., Fratianni S., 2016. The evolution of temperature extremes in the Gaspé Peninsula, Quebec, Canada (1974–2013). *Theor. Appl. Climatol.*, 1-10.

Fratianni S., Acquaotta F., 2017. The climate of Italy. In Landscapes and Landforms of Italy. Springer International Publishing, pp 539. DOI: 10.1007/978-3-319-26194-2_4.

Fratianni S., Terzago S., Acquaotta F., Faletto M., Garzena D., Prola M.C., Barbero S., 2015. How Snow and its Physical Properties Change in a Changing Climate Alpine Context? *Engineering Geology for Society and Territory*, 1, 57-60.

Giaccone E., Colombo N., Acquaotta F., Paro L., Fratianni S., 2015. Climate variations in a high altitude Alpine basin and their effects on a glacial environment (Italian Western Alps). *Atmosfera*, 28, 117-128, ISSN: 0187-6236.

González-Hidalgo J.C., Vicente-Serrano S.M., Peña-Angulo D., Salinas C., Tomas-Burguera M., Beguería S., 2018. High-resolution spatio-temporal analysis of drought episodes in the western Mediterranean basin (Spanish mainland, Iberian Peninsula). *Acta Geophysica*, 1-12.

Hannaford J., Lloyd-Hughes B., Keef C., Parry S., Prudhomme C., 2011. Examining the large-scale spatial coherence of European drought using regional indicators of precipitation and streamflow deficit. *Hydrol Process*, 25, 1146-1162.

Ionita M, Tallaksen L.M., Kingston D.G., Stagge J.H., Laaha G., Van Lanen H.A.J., Scholz P., Chelcea S.M., Haslinger K., 2017. The European 2015 drought from climatological perspective. *Hydrol. Earth. Syst. Sci*., 21, 1397-1419.

Lu E., Luo Y., Zhang R., Wu Q., Liu L., 2011. Regional atmospheric anomalies responsible for the 2009-2010 severe drought in China. *J. Geophys. Res*., 116(D2114).

McKee T.B., Doesken N.J., Kleist J., 1993. The relationship of drought frequency and duration to time scales. *American Meteorological Society*, 8th Conference on Applied Climatology, 17-22 Janvier, Anaheim, 179-184.

Mestre O., Domonkos P., Picard F., Auer I., Robin S., Lebarbier E., Böhm R., Aguilar E., Guijarro J., Vertacnik G., Klancar M., Dubuisson B., Stepanek P., 2013. HOMER: a homogenization software – methods and applications. *Időjárás*, 117(1), 1-158.

Mestre O., Gruber C., Prieur C., Caussinus H., Jourdain S., 2011. SPLIDHOM: A method for homogenization of daily temperature observations. *J. Appl. Meteorol. Climatol*., 50, 2343-2358. DOI: 10.1175/2011JAMC2641.1

Minetti J.L., Vargas W.M., Poblete A.G., de la Zerda L.R., Acuña, L.R., 2010. Regional droughts in southern South America. *Theor. Appl. Climatol*., 102(3-4), 403-415.

Nastos P.T., Politi N., Kapsomenakis J., 2013. Spatial and temporal variability of the aridity index in Greece. *Atmos. Res*., 119(140-152).

Nigrelli G., Fratianni S., Zampollo A., Turconi L., Chiarle M., 2018. The altitudinal temperature lapse rates applied to high elevation rockfalls studies in the Western European Alps. *Theor. Appl. Climatol*., 131(3-4), 1479-1491.

Palmer W.C., 1965. Meteorological drought. US Research Paper No. 45. US Department of Commerce Weather Bureau, Washington DC.

Pashiardis S., Michaelides S., 2008. Implementation of the Standardized Precipitation Index (SPI) and the Reconnaissance Drought Index (RDI) for Regional Drought Assessment: A case study for Cyprus. *European Water*, 23/24: 57-65.

Perini L., Salvati L., Zitti M., Bajocco S., 2011. A proposal for a meteorological index of climate change impact. *Italian Journal of Agrometeorology*, 1, 17-24.

Pulina M.A., 2012. Sécheresses et déficience hydrique des sol dans des zones agricoles de la Sardaigne durant la période 1951-2010. *Actes du colloque*, XXVème AIC, Septembre, Grenoble.

Pulina M.A., 2015. Extreme temperatures in Sardinia during the period 1951-2012. *Geomorphology for Society*, 5th AIGEO National Conference, September, Cagliari.

Rana G., Muschitiello C., Ferrara R.M., 2016. Analysis of a precipitation time series at monthly scale recorded in Molfetta (south Italy) in the XVIII century (1784-1803) and comparisons with present pluviometric regime. *Italian Journal of Agrometeorology*, 3, 23-30.

Ronchi C., Rabuffetti D., Salandin A., Vargiu A., Barbero S., Pelosini R., 2007. Development of the Piedmont Region Hydrological Bulletin as a Support to Water Resources Monitoring and Management. In: Rossi G., Vega T., Bonaccorso B. (eds) Methods and Tools for Drought Analysis and Management. Water Science and Technology Library, vol 62.

Thornthwaite C.W., 1948. An approach toward a rational classification of climate. *Geogr. Rev*., 38, 55-94.

Van Loon A.F., 2015. Hydrological drought explained. *WIREs Water*, 2(4), 359-392.

Vicente-Serrano S.M., Beguería S., López-Moreno J.I., 2010. A multi-scalar drought index sensitive to global warming: The Standardized Precipitation Evapotranspiration Index-SPEI. *J. Clim*., 23, 1696-1718.

Viste E., Korecha D., Sorteberg A., 2012. Recent drought and precipitation tendencies in Ethiopia. *Theor. Appl. Climatol*., 112, 535-551.

World Meteorological Organization, 2006. Drought monitoring and early worming: concepts, progress and future challenges. N° 1006.

World Meteorological Organization, 2017. Guidelines on the calculation of climate normals. N° 1203.

Italian Journal of
Agrometeorology
Rivista Italiana di Agrometeorologia

Firenze University Press
www.fupress.com/ijam

OPEN ACCESS

Citation: A. Mascitelli, P. Bombi, V. Coletta, B. De Cinti, S. Federico, G. Matteucci, A. Mazzoni, V.G. Muzzini, I. Petenko, S. Dietrich (2019) Tree Motion: following the wind-induced swaying of arboreous individual using a GNSS receiver. *Italian Journal of Agrometeorology* (3): 25-36. doi: 10.13128/ijam-512

Received: July 11, 2019

Accepted: October 29, 2019

Published: December 28, 2019

Data Availability Statement: All relevant data are within the paper and its Supporting Information files.

Competing Interests: The Author(s) declare(s) no conflict of interest.

Tree Motion: following the wind-induced swaying of arboreous individual using a GNSS receiver

Movimento dell'albero: analisi dell'oscillazione indotta dal vento di un individuo arboreo utilizzando un ricevitore GNSS

Alessandra Mascitelli[1,5,*], Pierluigi Bombi[3], Virginia Coletta[2], Bruno De Cinti[3], Stefano Federico[2], Giorgio Matteucci[4], Augusto Mazzoni[1], Valerio G. Muzzini[3], Igor Petenko[2], Stefano Dietrich[2]

[1] *Geodesy and Geomatics Division, Sapienza University of Rome, Rome, Italy*
[2] *Institute of Atmospheric Sciences and Climate, National Research Council of Italy, Rome, Italy*
[3] *Institute of Research on Terrestrial Ecosystems, National Research Council of Italy, Montelibretti, Rome, Italy*
[4] *Institute for Agricultural and Forest Systems in the Mediterranean, National Research Council of Italy, Ercolano, Naples, Italy*
[5] *Department of Civil and Environmental Engineering, Politecnico di Milano, Milan, Italy*
*Corresponding author. E-mail: alessandra.mascitelli@uniroma1.it

Abstract. Climate-induced stresses, more than in the past, expose trees to hazards possibly compromising their stability, with serious risk for people, objects, structures and infrastructures. In order to prevent trees falling phenomena, a constant improvement of the knowledge of relations between trees and meteorological events (trees-wind in particular) is crucial. Any new technology able to support research and monitoring in this direction must therefore be studied, tested, and finally adopted in order to create an infrastructure that would bring indisputable advantages from a social, economic and environmental point of view. The aim of this study is to test the applicability of GNSS receivers for monitoring wind-associated tree movements. The case study reported here refers to an experimental analysis carried out on an Italian stone pine (Pinus pinea L.). The analysis was carried out by applying a single-frequency GNSS receiver (an u-blox M6 evaluation kit available on the market at 300$) at the top of the tree and evaluating the results obtained in term of velocities and positions. Then, values obtained were correlated with wind characteristics by a sonic anemometer installed very close to the pine tree (within 15 meters), in order to independently record the impacting wind fields (velocity, direction). This allowed us to study the correlation between the wind velocity (cause) and tree movements (effect). Statistic outputs evaluation provides very promising results, showing the capability of this instrumental solution in the analysis of movement patterns. The study, indeed evidenced that accuracy of measurements and their relative errors are enough for the research purposes.

Keywords. Tree movement, GNSS, Positioning, Wind, Risk prevention.

Riassunto. Le sollecitazioni indotte dal clima, oggi più che in passato, espongono gli alberi a rischi che possono comprometterne la stabilità, comportando gravi rischi per persone, cose, strutture e infrastrutture. Al fine di prevenire i fenomeni di caduta degli alberi, è fondamentale un costante miglioramento della conoscenza delle relazioni tra alberi ed eventi meteorologici (alberi-vento in particolare). Ogni nuova tecnologia in grado di supportare la ricerca e il monitoraggio in questa direzione deve quindi essere studiata, testata e adottata a livello nazionale al fine di creare un'infrastruttura che apporterebbe indiscutibili vantaggi dal punto di vista sociale, economico e ambientale. Lo scopo di questo studio è quello di testare l'applicabilità dei ricevitori GNSS per il monitoraggio dei movimenti degli alberi associati al vento. Il caso studio qui riportato si riferisce ad un'analisi sperimentale effettuata su un pino cembro italiano (Pinus pinea L.). L'analisi è stata effettuata applicando un GNSS a singola frequenza (un kit di valutazione u-blox M6 disponibile sul mercato a 300$) in cima all'albero e valutando i risultati ottenuti in termini di velocità e posizioni.
Successivamente, i valori ottenuti sono stati correlati con le caratteristiche del vento attraverso i dati ottenuti da un anemometro sonico installato molto vicino al pino (circa 15 metri), al fine di registrare indipendentemente i campi di vento (velocità, direzione). Questo ci ha permesso di studiare la correlazione tra la velocità del vento (causa) e i movimenti degli alberi (effetto). La valutazione statistica delle uscite ha fornito risultati molto promettenti, dimostrando la potenzialità del metodo proposto nell'analisi dei modelli di movimento. Lo studio, infatti, ha evidenziato che l'accuratezza delle misure è sufficiente ai fini della ricerca.

Parole chiave. Movimento dell'albero, GNSS, Posizionamento, Vento, Prevenzione del rischio.

INTRODUCTION

Weather and climate variations exhibit vegetated environment to risks that could jeopardize tree stability causing serious hazards and severe economic losses both in an urban and forest context. (Alexander, 1964; Alexander, 1967; Neustein, 1965; Persson, 1975; Lohmander and Helles, 1987; Chirici et al., 2017; Motta et al., 2018). To prevent the falling of trees, close monitoring is the key to the early detection of problems and hence finding the best management options. The roots strength, the crown shape and dimension, the stem and stump elasticity and resistance, are the most important parameters affecting trees' stability. The interaction of these parameters affects the tree motion patterns under wind action, making these a reliable proxy of the overall tree's stability.

Several studies have been produced to investigate the tree-wind relationship using fundamental physics, empirical experiments, and mechanistic model-based approaches in interaction (Baker, 1995; Baker, 1997; Brüchert et al., 2003; Achim et al., 2003; Achim et al., 2005; Cucchi et al., 2005). As reported in James, 2010, the instruments and technology used by researchers to study the trees-wind relationship, has developed over many years a large range of methods. These include stopwatches (Sugden, 1962; Mayhead, 1973b) accelerometers (Blackburn et al., 1988; Peltola, 1996b), displacement transducers, (Gardiner, 1995; Kerzenmacher and Gardiner, 1998; Milne, 1991; Roodbaraky et al., 1994), prism based systems (Hassinen et al., 1998), lasers (Baker, 1997), tilt sensors (Flesch and Wilson, 1999b; Sellier et al., 2003; Sellier et al., 2006; Gilman et al., 2008; Rudnicki et al., 2001) and video based techniques (Peltola, 1996a). More recent technology and electronic instruments such as strain gauges, displacement sensors and portable data loggers have been used to obtain more accurate information on tree response under static and dynamic loading (Brüchert et al., 2000; Milne, 1991; Baker and Bell, 1992; Gardiner, 1995; Rodbaraky et al., 1994; Flesch and Wilson, 1999b; Hassinen et al., 1998; Holbo et al., 1980; Sellier and Fourcaud, 2005). The instruments used depend of course on what the researcher is going to demonstrate and each one presents advantages and disadvantages depending on circumstance. Stopwatches, for instance, are very cheap and simple to set up but it presents, on the other hand, low accuracy and reliability. Accelerometers on the other hand offer a convenient method for measuring the motion and frequency response of trees in two coordinate directions. As evidenced by Hassinen et al., (Hassinen et al., 1998) anyway, with an accelerometer, a guess has to be made of the initial position of the tree and any error is compounded when double integrating to obtain displacement. This leads to an accumulating error in calculated displacement and an exaggeration of the low frequency response of the tree (White et al., 1976; Blackburn et al., 1988; Peltola et al., 1993; Peltola, 1996; Gardiner, 1992; Gardiner, 1995). This is why displacement transducers and video-based techniques are considered more reliable and accurate for measuring stem displacement. In addition, video techniques easily allow the definition of the initial position of the tree, which is difficult to do with accelerometers or displacement transducers (Peltola, 1996). The limit of image interpretation is that the procedure is complicated and cumbersome.

Global Navigation Satellite Systems (GNSS), indicate the set of all the constellations of artificial terrestrial satellites for user navigation. GNSS technology was always

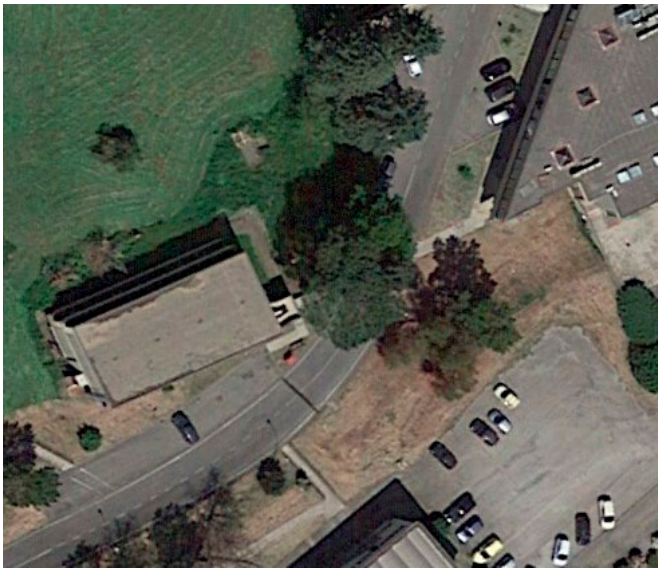

Fig. 1. Tree location.
Fig. 1. Localizzazione dell'albero.

Fig. 2. Receiver position on the tree.
Fig. 2. Posizione del ricevitore sull'albero.

used in many different applications: navigation (Branzanti et al., 2017), monitoring (Sampietro et al., 2017), seismology (Fratarcangeli et al., 2018), meteorology (Mascitelli et al., 2019; Campanelli et al., 2018), gravimetry (Capponi et al., 2018) and in each context GNSS signals are processed in order to obtain data able to integrate the information content in terms of positions, velocities and accelerations. We applied for the first time this technology to the tree motion monitoring, with the aim to investigate the applicability of GNSS receivers for detecting wind-associated tree movements.

In this study, we monitored the sway motion of the trunk of an Italian stone pine (*Pinus pinea* L.) under the wind action using, as a motion sensor, a GNSS receiver able to trace only the single frequency (Mascitelli et al., 2018). The use of the GNSS for tree monitoring could have several advantages principally because the spread application of this technology in several other monitoring contexts can assure it many improvement opportunities, but also because of competitive cost and good performances (Caldera et al., 2016).

CASE STUDY

For almost 2 months, from November 16th, 2017 to January 4th, 2018, a single-frequency GNSS receiver was used to observe the tree movements and patterns in relation to wind characteristics. These data include windy events of varying intensity and type that allow a sufficiently complete study of the impact of the wind on stone pine (*Pinus pinea L.*).

The location hosting the instrumented stone pine is the CNR-RM 1 Research Area of Montelibretti (Italy) (Figure 1). The tree is located near a building that covers part of its trunk and that could interact with its growth and consequently with its behaviour, anyway this interaction has been assessed as acceptable in view of the usefulness of this position in terms of simplifying the system's logistics. In front of the building and the tree there is a road that crosses the entire area. The other sides of the tree are substantially free and characterized by an expanse of uncultivated land Figure 1 b. The tree is about 13 meters high and has a diameter at breast height (DBH) of about 60 centimetres, the sensor is placed on trunk at a height of 11.30 m.

The period analysed (51 days) was, in general, characterized by low wind intensities. In particular, 36 days had hourly averaged wind speed less than 3 m/s for the whole day. These days were characterized by local diurnal circulation. Nine of the remaining days had hourly averaged wind speed greater than 4 m/s at least for an hour of the day. The remaining days had hourly averaged wind speed between 3 and 4 m/s for at least one hour. During the days of high wind speed (> 4 m/s, two prevalent directions were observed: Scirocco (winds coming from SE over the area) and Mistral (winds coming from NW over the area). For these days the intensity of mechanical turbulence increased.

INSTRUMENTS

Sonic Anemometer

High-frequency measurements of the three wind components were made with an ultrasonic anemometer/thermometer uSonic-3 by Metek Scientific (https://metek.de/product/usonic-3-scientific) installed at a height of ≈ 8 m, ≈ 1 m above the roof of the building, and at a distance of ≈ 15 m from the GNSS receiver. From these measurements, we computed the averaged wind speed and direction as well as the standard deviations of all wind components.

GNSS receiver

In this study we used a single frequency receiver (LOW4), an u-blox M8T Leica Geosystems, able to track multi constellation. For this study, only GPS observations were used. The antenna was located on the top of tree, connected to a receiver positioned in the adjacent building. With the collected data an analysis of tree displacements in terms of coordinates and velocities was carried out. In order to process position data, we resorted to a differential positioning method (Leick, 2004) using a geodetic receiver located about 8 kilometres from the tree (FIAN provided by Netgeo).

DATA PROCESSING

Wind Measurements

To obtain accurate information on 3-axis wind speed and direction with high temporal resolution, the ultrasonic anemometer was used at a sample frequency of 40 Hz. After averaging over every 4 points, time series of three wind components *x*, *y*, and *z* with frequency 10 Hz were archived in a data-logger CR3000 by Campbell. The spatial resolution is determined by a distance between pairs transducer/receivers of 0.20 m.

Spikes were determined and eliminated in the data processing and the percentage of spike data were recorded for later quality control. Each [*x, y, z*] vector block was indexed to find points with abnormal deviation from the mean; that is, *current value - mean value* outside the expected range. These ranges were +/- 10 ms^{-1} for wind data. The spike elimination was made by interpolating the neighbouring data. The planar fit method (Lee et al. 2004) was used to correct the data for possible errors due to the tilt of the support and a 2D-rotation in the mean wind coordinates was applied. For analysis of correlation between wind velocity and tree motion, wind components *x* (East direction) and *y* (North direction) were averaged over one second.

Another parameter, which has been considered in these analyses, is the turbulence kinetic energy (TKE). Generally, the TKE can be quantified by the mean of the turbulence normal stresses:

$$TKE = (1/2)\,(\langle u'^2\rangle + \langle v'^2\rangle + \langle w'^2\rangle),$$

where *u', v'* and *w'* are fluctuations of the longitudinal, lateral and vertical wind components.

Tree Measurements

Velocity

The analysis in term of components of tree velocity was conducted through the use of VADASE (Variometric Approach for Displacements Analysis Stand-alone Engine). The approach is based on time single-differences of carrier phase observations collected at a high-rate (1 Hz or more) using a stand-alone receiver, and on standard GPS broadcast products (orbits and clocks), which are ancillary information routinely available (Colosimo et al., 2011).

The data stream obtained by our single frequency receiver (LOW4) was managed by RTKLIB, an open source GNSS toolkit for performing standard and precise positioning (Takasu et al., 2009), to convert the observation data from UBX protocol (specific u-blox format) to RINEX (Receiver Independent Exchange Format) format. Data were processed for days in different wind conditions.

Position

Regarding the determination of the position, also in this case we used the software RTKLIB. We have processed RINEX files via RTKPOST, an RTKLIB executable. We used the differential method and set the positioning mode both static and kinematics (Leick, 2004): the first serves to obtain a reference position, whereas the second one is finalized to the study of movement. To conduct this analysis, we also needed observation data referring to a reference station that, in this case, was a receiver located about 8 kilometres from the tree, in Fiano Romano (Rome). The receiver is the FIAN station, belonging to the Netgeo network and the ancillary data needed for the processing has been

Tab. 1. Medians geocentric coordinates.
Tab. 1. Mediane delle coordinate geocentriche.

Doy	X [m]	Y [m]	Z [m]
322	4624594.959	1036919.530	4254167.129
323	4624594.963	1036919.523	4254167.137
324	4624594.962	1036919.541	4254167.148
326	4624594.967	1036919.540	4254167.154
328	4624594.971	1036919.539	4254167.159

Tab. 2. Statics value - positioning.
Tab. 2. Valutazioni statistiche sul posizionamento.

Doy	$\bar{E}$ [m]	σ_E [m]	$RMSE_E$ [m]	$\bar{N}$ [m]	σ_N [m]	$RMSE_N$ [m]
322	0.032	0.052	0.061	0.022	0.053	0.058
323	0.011	0.071	0.071	0.016	0.066	0.068
324	-0.003	0.059	0.059	0.006	0.047	0.047
326	-0.001	0.068	0.068	0.004	0.049	0.049
328	-0.005	0.059	0.059	-0.005	0.043	0.043

Tab. 3. Statics value – velocity.
Tab. 3. Valutazioni statistiche sulle velocità.

Doy	$\bar{E}$ [m/s]	σ_E [m/s]	$RMSE_E$ [m/s]	$\bar{N}$ [m/s]	σ_N [m/s]	$RMSE_N$ [m/s]
322	0.0006	0.0020	0.0020	-0.0001	0.0030	0.0030
323	0.0011	0.0020	0.0020	-0.0002	0.0030	0.0030
324	0.0005	0.0010	0.0020	0.0000	0.0020	0.0020
326	0.0007	0.0010	0.0020	0.0000	0.0020	0.0020
328	0.0005	0.0010	0.0010	0.0000	0.0020	0.0020

provided by CODE (Center for Orbit Determination in Europe). Data were processed for days in different wind conditions and the results of this processing were cut with a CE90 test (Circular Error with 90% probability) (Eq. 1)

$$CE90 = \frac{2.146}{\sqrt{2}}\sqrt{\sigma_E^2 + \sigma_N^2} \quad (1)$$

Where σ_E^2 is the squared standard deviation related to East coordinate and σ_N^2 is the squared standard deviation related to North coordinate. CE90 test was used to evaluate a threshold for removal of outliers. These data were compared with the velocity output and with data obtained from the sonic anemometer.

RESULTS

Non-Windy days

The first step concerned the analysis of some days characterized by absence of wind; the aim was to evaluate the behaviour of the system in quiet conditions. To perform the data analysis python language was applied. The days considered are all in the same week of November 2017, which goes from 18^{th} to 24^{th}, 322-328 day of year (doy). In these days, tree positions were obtained by static positioning for each epoch, and daily medians of the geocentric coordinates (X, Y and Z) were computed as well. The result is a set of coordinates for each day, which can be used as daily barycentric reference of the GNSS sensor on tree (Table 1).

It can be noted that there is a repeatability of the solution. In fact, the variation between the medians of all components in different days is very low, below the decimetres. It can be said that the solution is stable. Statistical analyses were carried out for all data relating to the tree, i.e. speed and positions, split in the two direction components (East and North); mean, mean squared deviation (σ) and RMSE (Root mean square error) were computed (Table 2 and 3).

As can be seen, the measurements have a good accuracy. As regards positions, there are differences to the order of some cm, as regards the velocities, the variations are relative to third decimal place (mm/s).

Windy days

To study the response of the tree to wind stresses we analysed days characterized by specific weather phenomena. First, we defined a wind speed limit above which a given day can be defined as windy, i.e. the hourly average wind speed must be greater than 4 m/s for at least one hour. The wind was recorded at a frequency of 10 Hz, whereas GPS works with a frequency of 1 Hz. In order to have comparable data, we averaged every 10 sonic values to obtain one record per second. In the months of the study campaign, we selected three days when the hourly average wind speed was > 4 m/s: 26^{th} November (Day of year 330), 12^{th} December (Day of year 346), 17^{th} December (Day of year 351).

November 26th, from this point of view, is very interesting because there is a change in the wind direction around mid-day, so the wind in the morning blows to North-West and in the afternoon to South-East (as can be seen in the upper left panel in Fig. 3). The other two days instead are characterized by winds having a prevailing direction that characterizes the entire

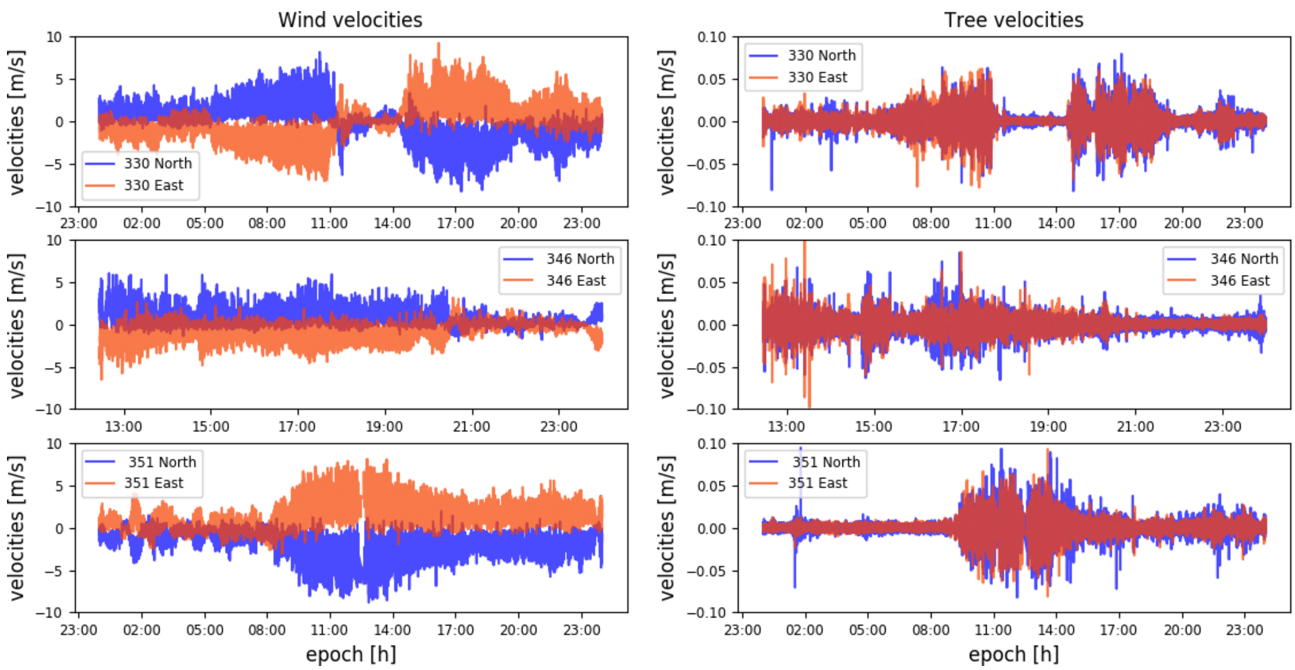

Fig. 3. Comparison between sonic anemometer data and GPS device data for 26th November (upper panels), 12th December (middle panels) and 17th December (lower panels).
Fig. 3. Confronto tra i dati da anemometro sonico e i dati da GPS per i giorni 26 Novembre (pannello in alto), 12 Dicembre (pannello centrale) e 17 Dicembre (pannello in basso).

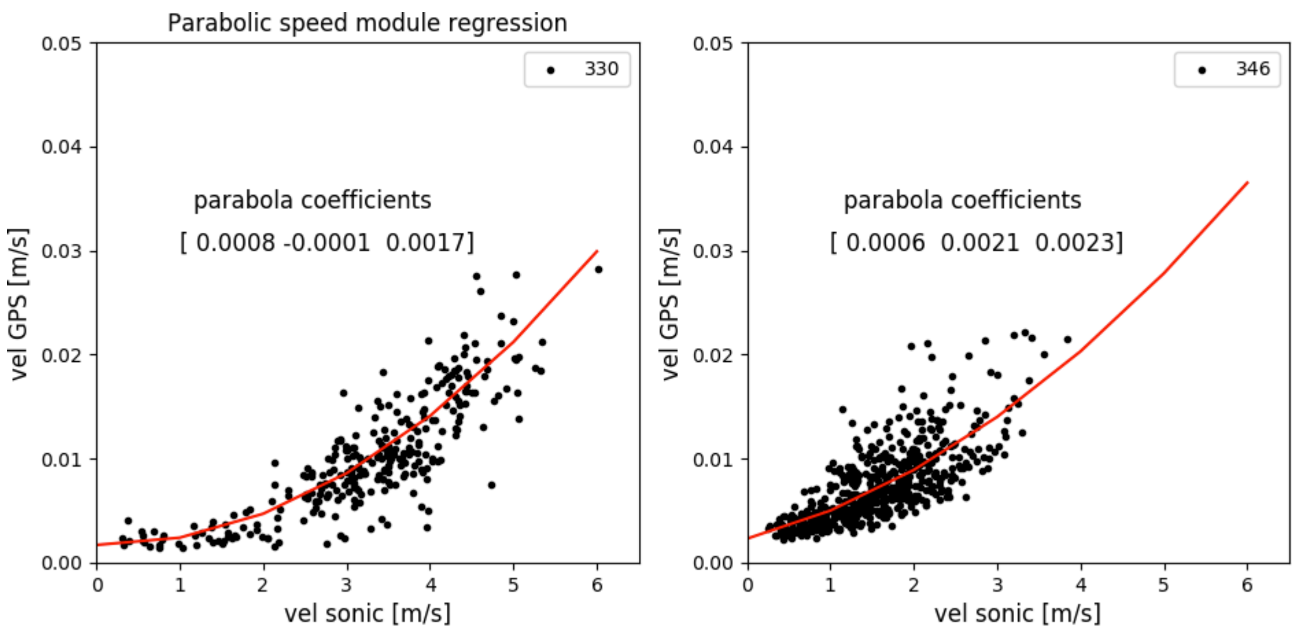

Fig. 4. Parabolic correlation between velocities averaged every 60 seconds – 26th November morning (doy: 330) and 12th December (doy: 346).
Fig. 4. Correlazione parabolica tra velocità mediate ogni 60 secondi - 26 Novembre mattina (doy: 330) e 12 Dicembre (doy: 346).

day. Particularly on December 12th, the wind blows to North-West (Scirocco, as in the morning of the 26th), instead, during the 17th goes to South-East (Mistral, as in the afternoon of the 26th).

Trends of velocities registered by sonic anemometer and by GPS device are coherent (Fig. 3), confirming that the receiver located on the trunk is effectively able to register the tree response to the wind. Sonic anemom-

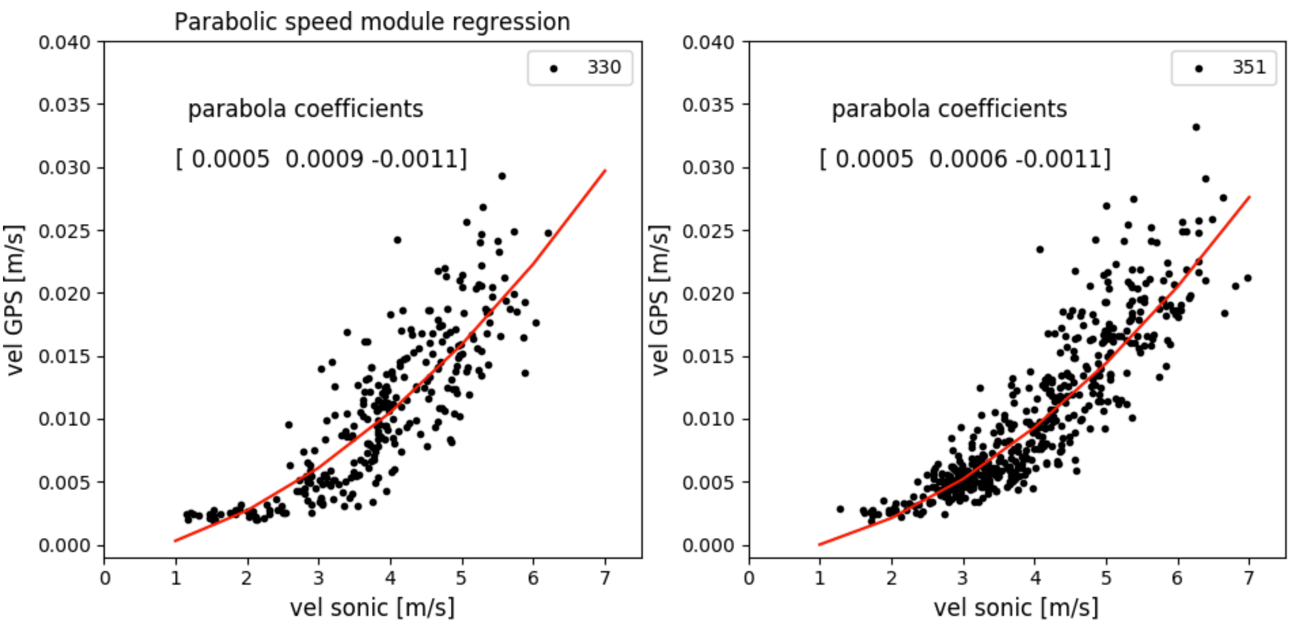

Fig. 5. Parabolic correlation between velocities averaged every 60 seconds – 26th November afternoon (doy: 330) and 17th December (doy: 351).
Fig. 5. Correlazione parabolica tra velocità mediate ogni 60 secondi - 26 Novembre pomeriggio (doy: 330) e 17 Dicembre (doy: 351).

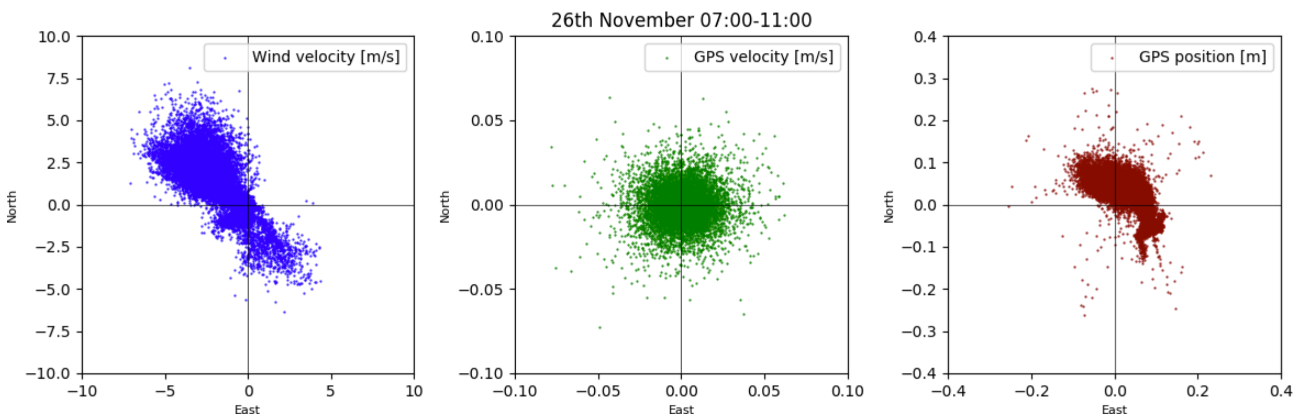

Fig. 6 Example of components comparison for days characterized by north-west wind.
Fig. 6. Esempio di confronto tra componenti per i giorni caratterizzati da vento di nord-ovest.

eter clearly discerns the two directional components, whereas the GPS located on the tree reveals an oscillating motion (Gardiner et al., 2016; De Langre, 2008) that causes the almost completely overlapping of the two components.

As can be deduced from the previous graphs, it is possible to analyse separately the windy event characterising the morning of 26th November and the one characterising the afternoon. It is also evident the similarity in directional terms of the two events, belonging to the same day, with those highlighted in the following dates, respectively 12th and 17th December.

To analyse the relation between the two velocities (the wind speed registered by the anemometer and the tree swaying speed registered by the GPS), a scatterplot of the speed modules, averaged every 60 seconds, was made obtaining a parabolic correlation. The comparison carried out between different events highlights the similarity of system response to similar stresses, i.e. parabola coefficients (Figure 4 and Figure 5).

Figure 6 shows plans of components (wind velocity, tree velocity and tree positions) for the wind event on the morning of 26th November. There is an excellent coherence as regards the response recorded by the sen-

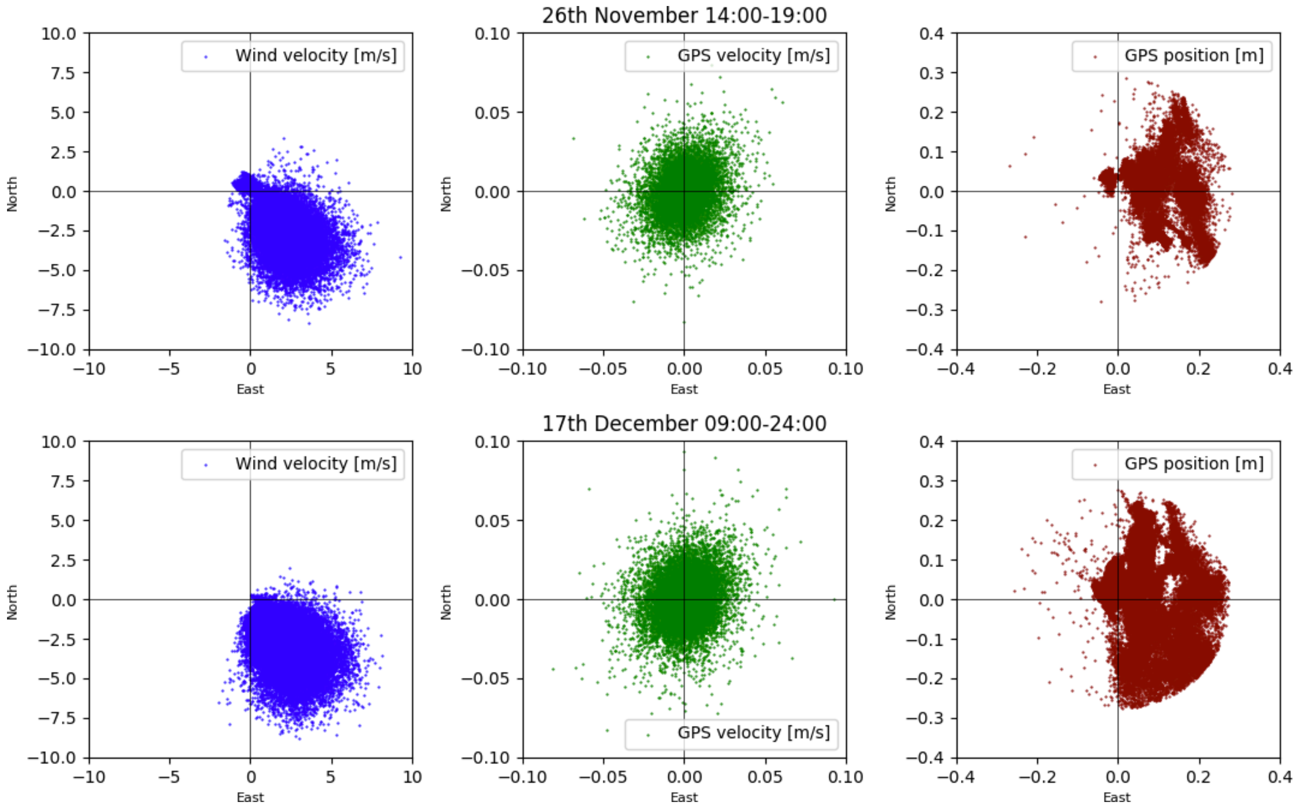

Fig. 7. Example of components comparison for days characterized with south-east wind.
Fig. 7. Esempio di confronto tra componenti per i giorni caratterizzati da vento di sud-est.

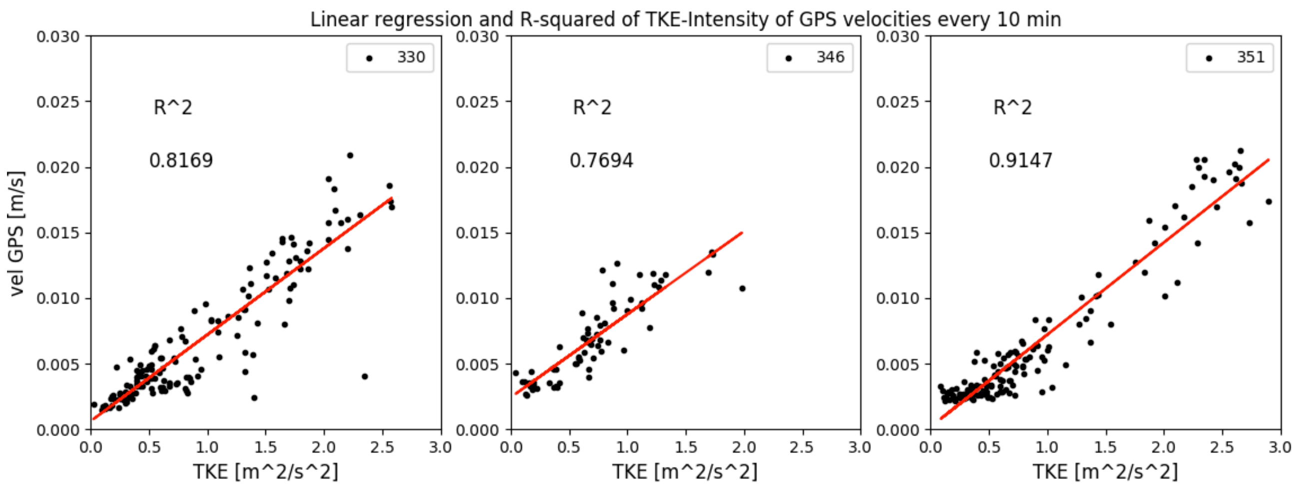

Fig. 8. Scatterplot of TKE and velocity registered by GPS receiver.
Fig. 8. Scatterplot di TKE e velocità registrate dal ricevitore GPS.

sor on the tree also on positions, in fact, it moves in the direction in accordance with the wind (third graph on the right, Fig. 6).

To evaluate constant reaction of tree to similar stresses we performed a comparison analysis, in velocities and positions, between wind events having the same direction. Planimetric graphs in Figure 7 were made to better understand the relation between quantities and depict the results.

In Figure 7 two events characterized by Mistral wind, respectively 26th November afternoon and 17th December, were considered. In the left panels of Figure 7 are reported the wind speeds related to the wind intense events; as shown these two cases are similar in terms of direction and they have also the same intensity. In the middle panels of Figure 7 are reported the tree velocities registered by the GPS device, which clearly illustrate the range of the speed values of the system when we refer to comparable events; whereas in the right panels of figure 7, the positions are shown.

By this picture it is possible to notice that tree reacts univocally to similar wind stresses both in terms of velocity and position. It is also interesting to note that, in both the above figures (Fig. 6 and Fig. 7), the positions taken by the sensor have a shifted barycentre with respect to the rest position of the tree. This behaviour is in line with what can be observed in relation to the oscillations of tree individuals.

The turbulence kinetic energy (TKE) is strictly correlated, in a linear way, with GPS velocity in all the three days (i.e. 26th November, 12th December and 17th December) (Fig. 8).

DISCUSSION

The study was conducted on days that were not windy and on days that were characterized by winds with speeds greater than 4 m/s (value based on Beaufort wind force scale). As far as non-windy days are concerned, statistical analyses have been carried out to understand the accuracy of measurements and their relative errors, which are some cm for positions and some mm/s for speeds. So from these analyses, it can be said that accuracy is good and error is acceptable. This condition has been achieved also because of an accurate positioning of the sensor on the upper part of the tree, which has minimised the impact of multipath and cycle slip (Leick, 2004). The solution robustness was confirmed by the repeatability of daily medians of geocentric coordinates (Table 1). During windy days absolute values of tree and wind speeds, averaged every 60 seconds, have been put in relation and a parabolic correlation has been observed, therefore as wind speed increases tree starts to move increasing its speed. Another interesting point to consider is the scale factor between the two measures; this is caused by the fact that the forcing wind is setting in motion a body that is far from the concept of ideal rigid body.

Observing the positions recorded by GNSS sensor it can be seen that tree moves coherently with wind direction and that the tree has chartered patterns of movement coherent with those observed by trees studied by other technologies (Hassinen et al., 1998; Mayer, 1985; Mayer, 1987; Mayer, 1989; Amtmann, 1986). In addition, it has been noted, through comparisons between different days, that tree has a constant response to events of similar wind (Fig. 7); a confirmation in this way is provided by parabolic coefficients, indeed for days with comparable winds they are very close to each other. Different comparisons have also been made with turbulent kinetic energy (TKE) which, coherently with results previously obtained, has an excellent linear correlation with tree speed (Fig. 8).

CONCLUSION AND FUTURE RESEARCH

Increasing the intensity and frequency of extreme weather events exposes trees more than ever to conditions that could compromise their stability. This leads to serious risk for people, objects, structures and infrastructures, especially in urban settings where the fall of a tree is more likely to have serious consequences. However, by studying the effects of wind on arboreal individuals, it is possible to understand, and then eventually monitor the extent of the risk of falling in order to provide reliable alerts.

The preliminary study shown in this paper focuses on a tree belonging to the species Pinus Pinea L., located in the CNR-RM1 research area of Montelibretti (Italy). It was decided to study this specific species because it is very common in cities, where the instability of trees can cause more damage. The aim of this study is to test the applicability of GNSS receivers for monitoring wind-associated tree movements, so in order to study the movements of the tree, a single-frequency GNSS sensor has been placed at the top of the trunk and wind speed was recorded by a sonic anemometer located about 20 m from the tree. This study evidenced that accuracy of measurements and their relative errors are enough for the purposes of the measurements made. Statistic outputs evaluation provided very promising results, showing the capability of this instrumental solution in the analysis of movement patterns.

Future investigations will focus on automating the system and further tests will be carried out on different tree species (monocormic and polycormic trees) to assess their behaviour in response to intense weather events. This instrument will be very useful in order to evaluate the criteria that have been applied up to this point and to attempt an implementation in view of an early warning system.

REFERENCES

Achim A., Nicoll B., Mochan S., Gardiner B., 2003. Wind stability of trees on slopes. In Proc. Int. Conf. Wind Effects on Trees, September (Vol. 16718, No. 2003, pp. 231-237).

Achim A., Ruel J.-C., Gardiner B.A., Laflamme G., Meunier S., 2005. Modelling the vulnerability of balsam fir forests to wind damage. Forest Ecology and Management, 204: 35-50.

Alexander R.R., 1964. Minimizing windfall around clear cuttings in spruce–fir forests. Forest Sci. 10, 130–142.

Alexander R.R., 1967. Windfall After Clearcutting on Fool Creek: Fraser Experimental Forest, Colorado (Vol. 92). Rocky Mountain Forest and Range Experiment Station, Forest Service, US Dept. of Agriculture.

Amtmann R., 1986. Dynamische Windbelastung von Nadelbaumen. Forstliche Forschungsberichte Munchen. No. 74, 218 pp.

Baker C.J., 1995. The development of a theoretical model for the windthrow of plants. Journal of Theoretical Biology, 175: 355-372.

Baker C.J., 1997. Measurements of the natural frequencies of trees. Journal of Experimental Botany, 48(310): 1125-1132.

Baker C.J., Bell H.J., 1992. Aerodynamics of urban trees. Journal of Wind Engineering and Industrial Aerodynamics., 44: 2655-2666.

Blackburn P., Petty J.A., Miller, K.F., 1988. An assessment of the static and dynamic factors involved in windthrow. Forestry, 61(1): 29-43.

Branzanti M., Colosimo G., Mazzoni A., 2017. Variometric approach for real-time GNSS navigation: First demonstration of Kin-VADASE capabilities. Advances in Space Research 59.11: 2750-2763.

Brüchert F., Speck O., Spatz H.-C.H., 2003. Oscillations of plants' stems and their damping: theory and experimentation. Philosophical Transactions of the Royal Society of London Series B-Biological Sciences, 358(1437): 1487-1492.

Brüchert F., Gardiner B.A., 2000. Wind Exposure Effects on the Mechanical Properties of Sitka Spruce (Picea sitchensis), Proceedings of 3rd Plant Biomechanics Conference., Freiberg, pp. 403-412.

Caldera S., Realini E., Barzaghi R., Reguzzoni M., Sansò, F., 2016. Experimental study on low-cost satellite-based geodetic monitoring over short baselines. Journal of Surveying Engineering, 142(3), 04015016.

Campanelli M., Mascitelli A., Sanò P., Diémoz H., Estellés V., Federico S., Iannarelli A.M., Fratarcangeli F., Mazzoni A., Realini E., Crespi M., Bock O., Martínez-Lozano J. A., Dietrich, S., 2018. Precipitable water vapour content from ESR/SKYNET sun–sky radiometers: validation against GNSS/GPS and AERONET over three different sites in Europe. Atmospheric Measurement Techniques, 11.1: 81-94.

Capponi M., Sampietro D., Sansò F., 2018. Very Improved KINematic Gravimetry: a new approach to aerogravimetry.

Chirici G., Giannetti F., Travaglini D., Nocentini S., Francini S., D'Amico G., Calvo E., Fasolini D., Broll M., Maistrelli F., Tonner J., Pietrogiovanna M., Oberlechner K., Andriolo A., Comino R., Faidiga A., Pasutto I., Carraro G., Zen S., Contarin F., Alfonsi L., Wolynski A., Zanin M., Gagliano C., Tonolli S., Zoanetti R., Tonetti R., Cavalli R., Lingua E., Pirotti F., Grigolato S., Bellingeri D., Zini E., Gianelle D., Dalponte M., Pompei E., Stefani A., Motta R., Morresi D., Garbarino M., Alberti G., Valdevit F., Tomelleri E., Torresani M., Tonon G., Marchi M., Corona P., Marchetti M., Tonner J., 2019. Stima dei danni della tempesta "Vaia" alle foreste in Italia. Forest@-Journal of Silviculture and Forest Ecology, 16(1), 3.

Colosimo G., Crespi M., Mazzoni A., 2011. Real-time GPS seismology with a stand-alone receiver: A preliminary feasibility demonstration. Journal of Geophysical Research: Solid Earth, 116(B11).

Cucchi V., Stokes A., Meredieu C., Berthier S., Najar M., Bert D., 2003. Root anchorage of Maritime pine (Pinus pinaster Ait.) growing in different soil conditions. Wind Effects on Trees. Karlsruhe, University of Karlsruhe, 307-314.

De Langre E., 2008. Effects of wind on plants. Annu. Rev. Fluid Mech., 40: 141-168.

Flesch T.K., Wilson J.D., 1999b. Wind and remnant tree sway in forest cutblocks. II. Relating measured tree sway to wind statistics. Agricultural and Forest Meteorology, 93: 243-258.

Fratarcangeli F., Savastano G., D'Achille M.C., Mazzoni A., Crespi M., Riguzzi F., Devoti R., Pietrantonio G., 2018. VADASE reliability and accuracy of real-time displacement estimation: application to the Central Italy 2016 earthquakes. Remote Sensing 10.8: 1201.

Gardiner B.A., 1992. Mathematical modelling of the static and dynamic characteristics of plantation trees. In: Franke, J., Roeder, A. Eds.., Mathematical Modelling of Forest Ecosystems. Sauerlanders Verlag, Frankfurt am Main, pp. 40–61.

Gardiner B.A., 1995. The interactions of wind and tree movement in forest canopies. In: M.P. Coutts and J. Grace (Editors), Wind and Trees. Cambridge University Press., pp. 41-59.

Gardiner B., Berry P., Moulia B, 2016. Wind impacts on plant growth, mechanics and damage. *Plant Science*, 245: 94-118.

Gilman E.F., Grabosky J.C., Jones S., Harchick C., 2008a. Effects of Pruning Dose and Type on Trunk Movement in Tropical Storm Winds. Arboriculture and Urban Forestry, 34(1), 13-19.

Hassinen A., Lemettinen M., Peltola H., Kellomaki D., Gardiner B.A., 1998. A prism-based system for monitoring the swaying of trees under wind loading. Agric. For. Meteorol. 90, 187–194.

Holbo H.R., Colbett T.C., Horton P.J., 1980. Aeromechanical behaviour of selected Douglas-fir. Agricultural. Meteorology, 21: 81-91.

James K.R., 2010. A dynamic structural analysis of trees subject to wind loading (Doctoral dissertation).

Kerzenmacher T., Gardiner B.A., 1998. A mathematical model to describe the dynamic response of a spruce tree to the wind. Trees, 12: 385-394

Lee X., Massman W., Law B., 2004. *Handbook of Micrometeorology*, Kluwer Academic Publishers, Dordrecht, 250 pp.

Leick A., Rapoport L., Tatarnikov D., 2015. GPS satellite surveying. John Wiley & Sons.

Lohmander P., Helles F., 1987. Windthrow probability as a function of stand characteristics and shelter. Scand. J. Forest Res. 2 2., 227–238.

Mayer H., 1985. Baumschwingungen und Sturmgef¨ahrdung des Waldes. Wissenschaftliche Mitteilung. Universit¨at Mu¨nchen. Meteorologisches Institut. No. 51, 247 pp.

Mayer H., 1987. Wind-induced tree sways. Trees 1, 195–206.

Mayer H., 1989. Windthrow. Phil. Trans. R. Soc. London, Ser. B 324, 267–281.

Mascitelli A., Federico S., Fortunato M., Avolio E., Torcasio R.C., Realini E., Mazzoni A., Transerici C., Crespi M., Dietrich S., 2019. Data assimilation of GPS-ZTD into the RAMS model through 3D-Var: preliminary results at the regional scale. Measurement Science and Technology, 30(5), 055801.

Mascitelli A., De Cinti B., Petenko I., Mazzoni A., Federico S., Bombi P., Muzzini V.G., Dietrich S., 2018. Monitoring of mechanical stability of arboreal individuals by GNSS low-cost sensors. In EGU General Assembly Conference Abstracts (Vol. 20, p. 19639).

Milne R., 1991. Dynamics of swaying of Picea sitchensis. Tree-Physiology, 9(3): 383-399.

Motta R., Ascoli D., Corona P., Marchetti M., Vacchiano G., 2018. Selvicoltura e schianti da vento. Il caso della "tempesta Vaia". Forest@-Journal of Silviculture and Forest Ecology, 15(1), 94.

Neustein S.A., 1965. Windthrow on the margins of various sizes of felling area. In: Report on forest research for the year ended March 1964. Forestry Commission, pp. 166–171.

Peltola H., Kellomaki S., Hassinen A., Lemettinen M., Aho J., 1993. Swaying of trees as caused by wind: analysis of field measurements. Silva Fennica 27 2., 113–126.

Peltola H., 1996a. Model computations on wind flow and turning moment by wind for Scots pines along the margins of clear-cut areas. Forest Ecology and Management, 83(3): 203-215.

Peltola H., 1996b. Swaying of trees in response to wind and thinning in a stand of Scots pine. Boundary-Layer Meteorology. 77: 285-304.

Persson P., 1975. Stormskador paskog—uppkomstbetingelser och inverkan av skogliga atgarder. Skogshogskolan, Institutionen for skogsproduktion. Summary: Windthrow in forests—its causes and the effect of forestry measures. Swedish University for Agricultural Science, Department of Forest Management, Sweden, No. 36, 294 pp.

Roodbaraky H.J., Baker C.J., Dawson A.R., Wright C.J., 1994. Experimental Observations of the Aerodynamic Characteristics of Urban Trees. Journal of Wind Engineering and Industrial Aerodynamics, 52: 171-184.

Rudnicki M., Silins U., Liefferd V.J., Josi G., 2001. Measure of simultaneous tree sways and estimation of crown interactions among a group of trees. Trees, 15: 83-90.

Sampietro D., Caldera S., Capponi M., Realini E., 2017. Geoguard-An Innovative Technology Based on Low-cost GNSS Receivers to Monitor Surface Deformations. In First EAGE Workshop on Practical Reservoir Monitoring.

Sellier D., Soulier D., Fourcaud T., Brunet Y., 2003. The Venfor Project: Influence of the aerial architecture on tree swaying - An experimental approach. In Wind effects in trees. (B. Ruck, ed, University of Karlsruhe, Germany.

Sellier D., Fourcaud T., 2005. A mechanical analysis of the relationship between free oscillations of Pinus pinaster Ait. saplings and their aerial architecture. Journal of Experimental Botany, 56(416): 1563-1573.

Sellier D., Fourcaud T., Lac P., 2006. A finite element model for investigating effects of aerial architecture on tree oscillations. Tree Physiology, 26, 799-806.

Sugden M.J., 1962. Tree sway period - a possible new parameter for crown classification and stand competition. Forestry Chronicle, 38: 336-344.

Takasu T., Yasuda A., 2009. Development of the low-cost RTK-GPS receiver with an open source program

package RTKLIB. In: International symposium on GPS/GNSS. International Convention Center Jeju Korea. p. 4-6.
White R.G., White M.F., Mayhead G.J., 1976. Measurement of the motion of trees in two dimensions. Tech. Report No. 86. Institute of Sound and Vibration Research, University of Southampton, 22 pp.

Italian Journal of Agrometeorology
Rivista Italiana di Agrometeorologia

Firenze University Press
www.fupress.com/ijam

OPEN ACCESS

Citation: L. Şaylan, R. Kimura, N.Altinbaş, B. Çaldağ, F. Bakanoğullari (2019) Modeling of Surface Conductance over Sunn Hemp by Artificial Neural Network. *Italian Journal of Agrometeorology* (3): 37-48. doi: 10.13128/ijam-589

Received: August 8, 2019

Accepted: November 30, 2019

Published: December 28, 2019

Data Availability Statement: All relevant data are within the paper and its Supporting Information files.

Competing Interests: The Author(s) declare(s) no conflict of interest.

Modeling of Surface Conductance over Sunn Hemp by Artificial Neural Network

Modellazione della conduttanza di superficie su canapa mediante rete neurale artificiale

Levent Şaylan[1,*], Reiji Kimura[2], Nilcan Altinbaş[1], Bariş Çaldağ[1], Fatih Bakanoğullari[3]

[1] *Department of Meteorological Engineering, Faculty of Aeronautics and Astronautics, Istanbul Technical University, 34469, Maslak, Istanbul, Turkey*
[2] *Arid Land Research Center, Tottori University, 1390, 680-0001, Hamasaka, Tottori, Japan*
[3] *Atatürk Soil Water and Agricultural Meteorology Research Institute Directorate, 39000 Kırklareli, Turkey*
*Corresponding author. E-mail: saylan@itu.edu.tr

Abstract. Performances of an Artificial Neural Network (ANN), a multiple linear regression (MLR) and the Jarvis type model were compared to estimate the surface conductance which is a driving factor affecting evapotranspiration. It was modeled by ANN and MLR using various parameters including global solar radiation, temperature, soil water content, relative humidity, precipitation and irrigation, vapor pressure deficit, wind speed and leaf area index. The measurements were carried out during the growing season of sunn hemp in 2004. The best relationship (r^2=0.73) between the surface conductance and all variables was estimated by the ANN when r^2 was 0.91 in the training period. The average absolute relative error was 26.54% for the ANN (r^2=0.80), 51.07% for the MLR (r^2=0.53) and 58.30% for Jarvis model (r^2=0.26) when vapor pressure deficit, temperature, soil water content, global solar radiation and leaf area index were considered to model. The results showed that the ANN approach had a better modeling potential of the surface conductance compared to the MLR and Jarvis model.

Keywords. Agriculture, Air-water interaction, Evapotranspiration, Neural Networks.

Riassunto. Le prestazioni di una rete neurale artificiale (ANN), una regressione lineare multipla (MLR) e il modello di tipo Jarvis sono state confrontate per stimare la conduttanza di superficie, che è un fattore trainante che influenza l'evapotraspirazione. È stato modellato con ANN e MLR utilizzando vari parametri tra cui radiazione solare globale, temperatura, contenuto di acqua del suolo, umidità relativa, precipitazioni e irrigazione, deficit di pressione di vapore, velocità del vento e LAI. Le misurazioni sono state eseguite durante la stagione di crescita della canapa nel 2004. La migliore relazione (r^2 = 0,73) tra la conduttanza superficiale e tutte le variabili è stata stimata dalla RNA quando r^2 era 0,91 nel periodo di training della rete. L'errore relativo assoluto medio è stato del 26,54% per l'ANN (r2 = 0,80), del 51,07% per l'MLR (r^2 = 0,53) e del 58,30% per il modello Jarvis (r^2 = 0,26) quando il deficit di pressione di vapore, temperatura, contenuto di acqua del suolo, radiazione solare globale e il LAI. I risultati hanno mostrato che l'approccio ANN aveva un potenziale di modellazione migliore della conduttanza superficiale rispetto al modello MLR e Jarvis.

Parole chiave. Agricoltura, interazione aria-acqua, evapotraspirazione, reti neurali.

1. INTRODUCTION

As a dynamic system, the crop growth is influenced by many factors. Surface conductance is one of them and controls evapotranspiration which is strongly related to the stomatal activity and photosynthesis process of vegetation. As a component of hydrological cycle, evapotranspiration plays a crucial role for planning irrigation schedule. It is also affected by many factors such as surface conductance, energy partitioning, water use efficiency and carbon exchange over vegetation surfaces (Woodward and Smith 1994; Sellers *et al*., 1996; Zhang *et al*., 2007). As well known, energy fluxes above canopy such as latent heat flux are mainly controlled by closure of stomata. Unfortunately, surface conductance isn't a routinely and easily measured variable. In general, it is calculated by using some improved equations under consideration of interactions between meteorological and plant factors. Many studies were focused on the estimation of surface conductance by assuming it as a function of driving environmental and biological factors (Şaylan and Bernhofer, 1993). In earlier studies, the surface conductance was modeled by linear and nonlinear techniques. As stated by Huntingford and Cox (1997), the response of surface conductance is highly nonlinear for local environmental conditions. Nonlinearity of surface conductance can also be seen in the Jarvis-Stewart model (Jarvis, 1976; Stewart, 1988).

Neural networks are widely used nonlinear approaches in order to find an alternative way to solve complex problems. From past to present, many studies such as Kohonen (1984) and Hammerstrom (1993) showed the power of neural networks in modeling complicated systems. Bolte (1989), Zhuang and Engel (1990), Thai and Shewfelt (1991), and Kaul *et al.* (2005) successfully applied the neural networks in the agriculture and engineering field. Huntingford and Cox (1997) applied ANN for modeling the surface conductance of plants. Additionally, van Wijk and Bouten (1999) modeled water and CO_2 fluxes in the forest by ANN. Pachepsky *et al.* (1996) indicated that ANN gave better results for the soil water content according to soil physical properties than other regression techniques. Sahoo *et al.* (2005) also applied this approach for the estimation of pesticides in groundwater. Additionally, the same technique was applied by Terzi and Keskin (2005) for modeling evaporation; by Kumar *et al.* (2002), Lin *et al.* (2007) and Kişi (2007) for the determination of evapotranspiration; by Mohandes *et al.* (1998) for the modeling of global solar radiation. Öztopal (2006) used ANN to model wind data. Doğan (2008) modeled reference evapotranspiration by adaptive neuro-fuzzy inference system. Alves and Pereira (2000) applied the Jarvis model to obtain the surface resistance by using Penman-Monteith equation. Şen *et al.* (2009) used a fuzzy logic model for the prediction of surface ozone. Şaylan *et al.* (2017) applied ANN and ANFIS approaches to model the soil water content. Ribeiro *et al.* (2018) used MLR and ANN techniques to build cross validation in estimating the yield response to drought. Yang *et al.* (2018) used a back-propagation ANN to model above-ground biomass which is an important factor for agricultural management. Niedbala (2019) built an ANN to predict winter rapeseed yield in Poland. Benali *et al.* (2019) used ANN to model solar radiation in three components: beam, diffuse and global. Another recent study on the projection of harvestable water from air humidity data using the ANN approach was conducted by Khaledi (2019).

ANN techniques are capable to show high rates of success when applied in complex applications. Especially in meteorological applications, neural network models can be used to model radiation variables indicating crucial improvements against traditional models used in statistics (Lopez *et al*., 2001).

Estimation of surface conductance is useful for agriculture and highly related with evapotranspiration. Knowledge about the characteristics of surface conductance of sunn hemp related to evapotranspiration status can be used to investigate the effects of particular factors on crop. It is also important for the planning of irrigation and therefore for the management of water. Yet, surface conductance modeling over the growing period is a complex problem.

The characteristics of sunn hemp were investigated by Takagi *et al.* (2009). There is however still a clear need to better understand the relationship between surface conductance and environmental factors. There are only few studies on the application of ANNs for the estimation of surface conductance such as Shen *et al.* (2002).

The main objective of this study was to model and compare the surface conductance of sunn hemp as a function of plant and meteorological variables by using nonlinear ANN, linear MLR and Jarvis type approaches. Related conductance data were collected from the high infiltrated sandy soil in the experiment field at the Arid Land Research Center of Tottori University located in Tottori, Japan. It was assumed that the surface conductance is affected by air temperature (T), global solar radiation (R_g), vapor pressure deficit (VPD), soil water content (SWC), relative humidity (RH), precipitation and irrigation (P+I), wind speed (u) and leaf area index (LAI).

2. MATERIALS AND METHODS

2.1. Site description

This study was conducted on a research area (Fig. 1) located at the Arid Land Research Center (ALRC), Tottori University, city of Tottori, Japan (35° 32' N, 134° 13' E, 15 m above sea level). From climatological point of view, this field is characterized by humid temperate climate. The long term annual mean temperature and total precipitation are 14.6 °C and 1900 mm, respectively. The field was about 1 ha. In addition, the experiment field was tilled on July 29 and harvested on October 18, 2004 (Takagi 2005; Takagi *et al*., 2009). The contents of sand, silt and clay in the soil were 96.1%, 0.4% and 3.5% respectively. The field capacity and permanent wilting point of the soil were 0.074 m^3 m^{-3} and 0.022 m^3 m^{-3}, respectively (Dehghanisanij *et al*., 2004). Although, the study area is one of the comparatively humid areas of Japan, the field was irrigated to protect the crops against water shortage because of high infiltration of the sandy soil, so water stress did not occur during growing period. Additionally, heavy rain was experienced due to a typhoon during the last two weeks of the sunn hemp growing season (Takagi *et al*., 2009).

2.2. Methods

2.2.1. Artificial neural networks (ANN)

As stated in Lopez *et al*. (2001), ANN approach bases on finding out the input and output variables' relationship by studying previously recorded data. An ANN model consists of two phases which are training and testing phases. Input, hidden and output layers are required in an ANN. The input and output layers cover the nodes corresponding to input and output variables, respectively (Fig. 2). Every layer consists of a certain number of neurons. They are interconnected each of these by some weights. In the hidden layer, every neuron receives its input from the input layers according to Eq. (1):

$$y_j = \sum_{i=1}^{m} w_{ij} x_i \tag{1}$$

where y_j is the input value of the j^{th} neuron in the hidden layer, m is the number of neurons in the input layer, w_{ij} is established weight and x_i is the input value (Kaul *et al*., 2005).

Every neuron in the hidden layer gives output (O_j) through an activation function. O_j is the sigmoidal function in the form of:

$$O_j = f\left(y_j\right) = \frac{1}{1+e^{\frac{-\left(y_j+b_j\right)}{\theta}}} \tag{2}$$

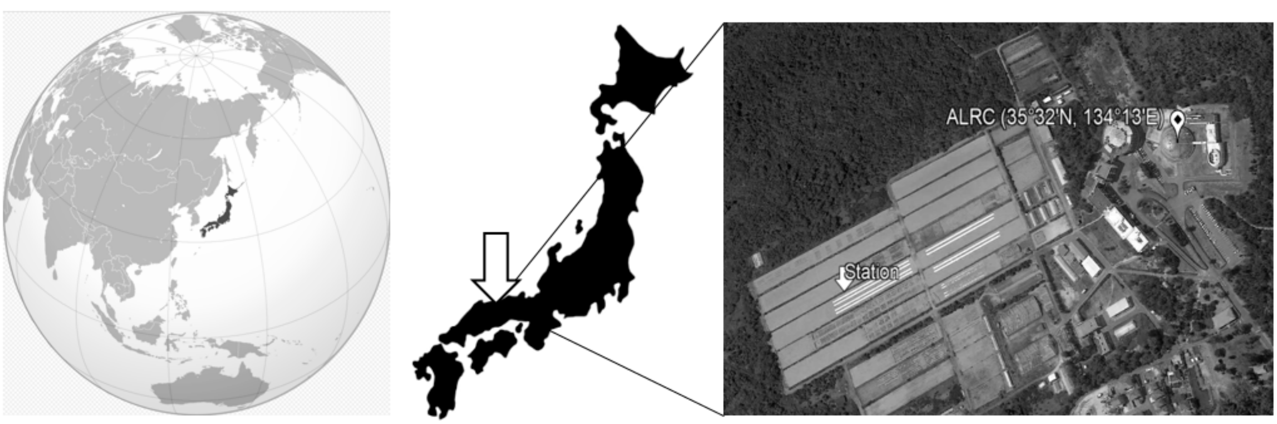

Fig. 1. Research area located at the ALRC, Tottori, Japan.
Fig. 1. Area di studio situata presso l'ALRC, Tottori, Giappone.

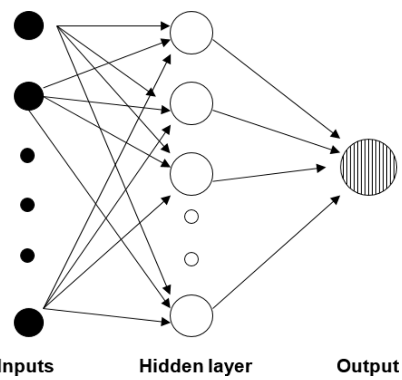

Fig. 2. A typical neuron with layers.
Fig. 2. Un neurone tipico con strati.

where $f(y_j)$ is the output of the neuron, b_j is the initial value and θ represents the bias (Hamidi and Kayaalp, 2008). Detailed theoretical description of the neural networks can be found in Haykin (1994).

In this study, back propagation neural network approach was used. The total sum of squared errors between measured and modeled values was minimized by tuning ANN parameters as used by van Wijk and Bouten (1999). The transfer function used for the hidden layer was the sigmoidal function.

2.2.2. Surface conductance

In this study, the surface conductance was determined by rearranged Penman-Monteith equation (Monteith and Unsworth, 1990).

$$g_s = \frac{\gamma LE}{\rho C_p VPD} + \frac{g_a}{\left(\frac{\beta s}{\gamma} - 1\right)} \tag{3}$$

where g_s is the surface conductance (m s^{-1}), g_a is the aerodynamic conductance (m s^{-1}), ρ is the density of the air (kg m^{-3}), β is Bowen ratio, γ is psychrometric constant (kPa $^{\circ}C^{-1}$), C_p is the specific heat at constant pressure (J kg^{-1} $^{\circ}C^{-1}$), VPD is the vapor pressure deficit (kPa), s is the rate of change of saturation vapor pressure with temperature (kPa $^{\circ}C^{-1}$).

The aerodynamic conductance is calculated by using following Eq. (4) based on wind speed (Jensen *et al.*, 1990):

$$g_a = \frac{k^2 u}{\ln\left(\frac{(z_m - d)}{z_o}\right) \ln\left(\frac{(z_m - d)}{z_{oh}}\right)} \tag{4}$$

where k is von Karman`s constant (0.41), u is wind speed (m s^{-1}) at height z (m), z_m (m) is the height of wind speed, z_o (m) is the roughness parameter for momentum, z_{oh} (m) is the roughness parameter for heat and water and d (m) is the zero plane of displacement. d, z_o and z_{oh} are calculated by the equations given below (Allen *et al.*, 1998):

$$d = h\frac{2}{3} \tag{5}$$

$$z_o = 0.123h \tag{6}$$

$$z_{oh} = 0.1 z_o \tag{7}$$

The latent heat flux (LE) was calculated by using Bowen Ratio Energy Balance (BREB) method as follows (Bowen, 1926):

$$\beta = \gamma\left(\frac{\Delta T}{\Delta e}\right) = \frac{H}{LE} \tag{8}$$

$$R_n - G - LE - H = 0 \tag{9}$$

$$LE = \frac{R_n - G}{(1+\beta)} \tag{10}$$

where R_n is net radiation (Wm^{-2}); G is soil heat flux (Wm^{-2}); LE is latent heat flux (Wm^{-2}); H is sensible heat flux (Wm^{-2}); ΔT is the temperature gradient (^{o}C) and Δe is the vapor pressure gradient (kPa) over the height interval above canopy surface.

2.2.3. Jarvis type model

The surface conductance model was built by Jarvis (1976) and developed by Noilhan and Planton (1989). In this study, the surface conductance was calculated by following equation (Dickonson, 1984; Niyogi and Roman, 1997):

$$\frac{1}{g_s} = r_s = r_{smin} LAI^{-1} F_1 F_2^{-1} F_3^{-1} F_4^{-1} \tag{11}$$

where r_s is surface resistance (s m^{-1}), r_{smin} is the minimum surface resistance. Detailed information about the calculation of F_1, F_2, F_3 and F_4 as functions related to global solar radiation, soil water content, vapor pressure deficit and temperature, can be found in Niyogi and Roman (1997), Dickinson (1984) and Kimura *et al.* (2006).

3. MEASUREMENTS

Vertical gradients of T and RH were measured at fixed levels of 0.5, 1 and 1.5 m above the ground surface to apply BREB approach for the determination of actual evapotranspiration. For this aim, ventilated psychrometers were used to measure the variations of T and RH. The wind speed at 2 m was measured by a cup anemometer (3101-5, Young), though the wind direction was measured at a height of 3 m. In addition, a four component net radiometer sensor (MR40, EKO Inc.) was installed at 2 m high above the surface to measure short and longwave radiations. Soil heat flux was measured by two soil heat flux plates (PHF-01, REBS Inc.) installed at 2 cm depth. Moreover, the soil water content was measured at 0-30 cm depth at three different points in the field by using soil water content reflectometers (CS615, Campbell Sci.). Furthermore, precipitation was collected by a tipping bucket rain gauge (34-T, Ota Keiki). Whole data were collected at 10 and 30 min. intervals using a datalogger (CR23x, Campbell Sci.). Necessary information about components of the measurement system can be found in Takagi (2005) and Takagi *et al.* (2009).

4. RESULTS AND DISCUSSION

4.1. Observations

During the growing season of sunn hemp, the leaf area index (LAI) was periodically measured. The maximum LAI at the end of the period was 3.52. All meteorological variables were measured from 1st of August (DOY 214) to 8th of October 2004 (DOY 282). It has been observed that the mean temperatures were in a decreasing trend within this period, as expected. With the beginning of the rainy season, an expected decrease also occurred in VPD. SWC values generally followed the variations in P+I. Time series of the daily averaged meteorological factors (input variables) and daytime (R_n>0) energy balance components which were determined from 10-min data during the growing period were given in Fig. 3. Meteorological data could not be measured for four days because of some unexpected technical problems. At the early stages of the period, in August, the VPD was high, but it showed a decreasing trend until the end of the period (Fig. 3). As a result of heavy rain, the VPD decreased. This situation caused raise in soil water content on many days in September and October.

During the period, daily mean T at 2 m was about 25 ˚C and ranged from 18 to 30 ˚C. Because the last days of the period encountered the typhoon season, the lowest T was measured. T was decreasing gradually toward the end of the period. Daily average RH was about 81% ranged from 64 to 95%. As a consequence of heavy rain, RH showed a tendency for increase in September and October, when T dropped during the same period. The

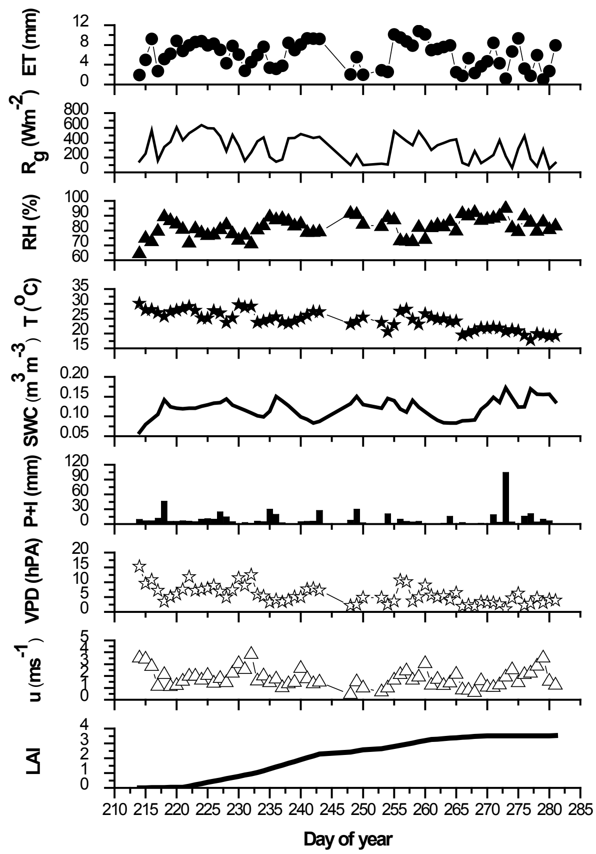

Fig. 3. Time series of daily averaged meteorological factors and daytime energy balance components.

Fig. 3. Serie temporali di dati meteorologici medi giornalieri e componenti del bilancio energetico diurno.

total irrigation and precipitation amounts were 172 and 408.5 mm during the period. Totally, 187 mm rainwater fell in the last 11 days (during the typhoon season) of this experiment period. Missing meteorological data were filled by using data recorded at the fixed meteorological station of ALRC located about 300 m away from the experiment field. Daily mean wind speed (u) at 2 m height was 1.8 m s^{-1} and reached up to the maximum value of 3.8 m s^{-1}. After beginning of the measurements, daily mean SWC increased due to the irrigation and precipitation. SWC at 0-30 cm depth was 0.12 m^3 m^{-3} and showed an increasing trend. At the end of the period, SWC reached up to 0.17 m^3 m^{-3}. The amount and distribution of the P and I resulted in temporary increases in SWC during this growing period. Because of irrigation, precipitation, increasing temperature and radiation, daily total evapotranspiration of sunn hemp was about 6 mm. Furthermore, daily mean VPD ranged from 1 hPa to 15.3 hPa with an average value of 5.7 hPa (Takagi *et al.*, 2009).

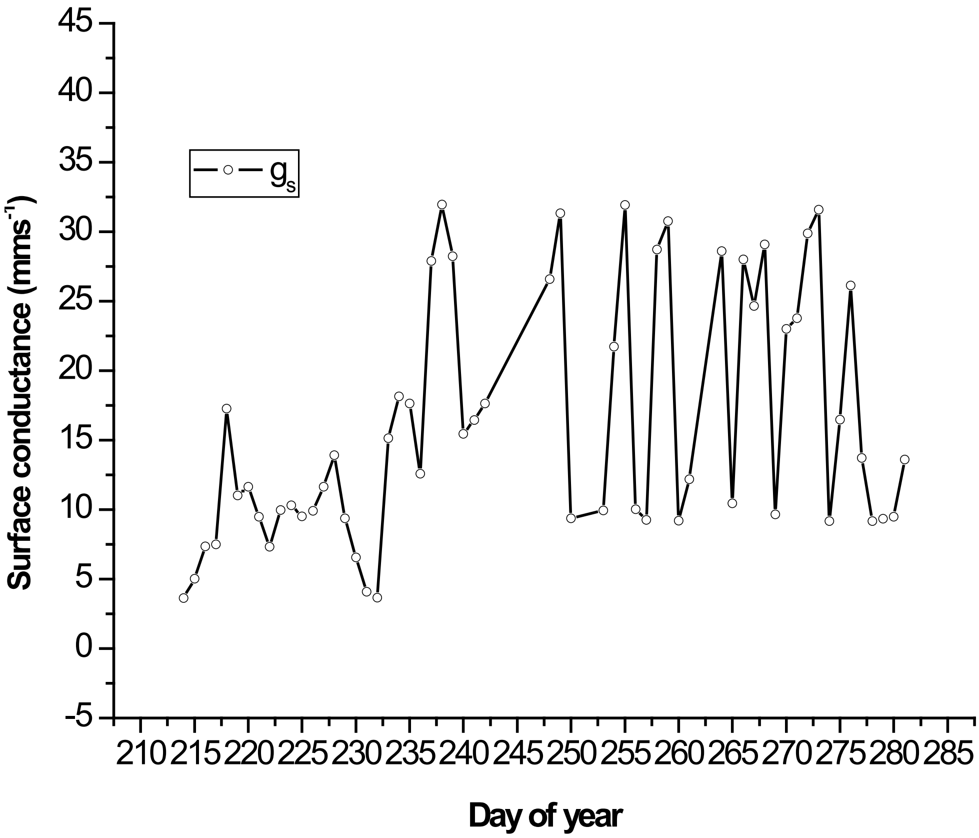

Fig. 4. Time series of surface conductance.
Fig. 4. Serie temporale della conduttanza di superficie.

4.2. Surface conductance of sunn hemp

As Dirks and Hensen (1999) reported, the surface conductance plays an essential role regarding energy and mass exchanges between the environment and plant. It is also important for designation of LE and CO_2 assimilation. In this study, it has been calculated by rearranging the Penman-Monteith equation. In order to calculate surface conductance, first, the actual evapotranspiration was calculated by BREB method. b, LE and H were calculated by using Eqs. (8), (9) and (10), respectively. Secondly, g_a was calculated by Eq. (4). Then, raw flux data were checked by using Ohmura (1982) criterion and some unacceptable data were rejected in order to avoid the errors in the estimation of fluxes of sunn hemp. Finally, g_s was calculated by using Eq. (3).

Daily total evapotranspiration was lower as expected at the early phenological stages in August than the values at the flowering and maturity stages in September and October. In the last part of the measurements, the heavy rain caused high soil moisture. Besides, evapotranspiration (ET) was increased with crop growth. The total amount of actual ET for whole growing season was around 350 mm. Eventually, it can be mentioned that the highest ET during the growing season can be attributed to the highest soil moisture and precipitation amount. Daytime average global solar radiation was about 334 W m^{-2} and varied from 50 to 636 W m^{-2}. Additionally, the daytime average R_n was about 231 W m^{-2} with a maximum value of 405 and a minimum of 32 W m^{-2} over the period. It can be said that R_g showed a decreasing trend from the beginning to the end of the measurement period. Furthermore, the daytime average soil heat flux was about 28 W m^{-2}.

The results showed that most part of the available energy was used by ET of the sunn hemp. Temporal variation of the calculated surface conductance is presented in Fig. 4. The daytime averaged aerodynamic and surface conductance were about 31 mm s^{-1} and 16.7 mm s^{-1}, respectively. g_s value was lower in August than in September and October. These can be explained with the development of crop and increasing of the transpiration in the second half of the period as reported by Takagi *et al.*, (2009).

4.3. Training and testing of ANN and MLR models

In this study, the MATHLAB was used to create an ANN model for predicting the daily average surface conductance of sunn hemp crop. In order to test the ANN and MLR models, total data were split into training and testing data. The ANN model was trained by randomly selected 70% of the whole data. Remaining portion (30%) of the total data were used in order to test the ANN model. A total of 45 daily averaged data, which are calculated from 30-min measured data (totally 2577 data for 64 days) were used for training the model and remained part of data were applied for testing the model. Input and output variables were normalized within the range of 0.1 and 0.9 by using following equation and then normalized data were trained and tested by ANN and MLR.

$$x_i = \left[0.1 + 0.8 \frac{(x - x_{min})}{(x_{max} - x_{\mathrm{min}})} \right] \quad (12)$$

In training and testing of the ANN model, the number of epochs, the learning rate and hidden layers used in the optimization were 100, 0.30 and 2, respectively.

In the study, the back-propagation algorithm in ANN approach was used for training several multi-layer neural networks to estimate the daily average values of g_s. In the first step, the surface conductance of sunn hemp was modeled by ANN, MLR and Jarvis (1976) approaches as a function of global solar radiation, soil water content, vapor pressure and temperature; and then leaf area index was added to this combination. Finally, all variables such as the daily average air temperature, relative humidity, wind speed, vapor pressure deficit, soil water content at 0-30 cm depth; daily total precipitation and irrigation; daytime net radiation and daily leaf area index data had been used as inputs in ANN and MLR to train and test the data set. In order to find a relationship between g_s and input data, the network consisted of eight inputs, five neurons in two hidden layers and one neuron in the output layer. The training procedure was continued until the error function approached to a minimum value in ANN. After finishing the training, the developed model was tested. The output was the surface conductance calculated by ANN (g_{sANN}), MLR (g_{sMLR}) and Jarvis approaches (g_{sJRV}). After the training and testing, performance of the developed model by ANN (g_{sANN}) was compared with the developed model by g_{sMLR}, g_{sJRV} and surface conductance in the Penman-Monteith equation, which was calculated by Eq. (3). The performance of ANN, MLR and Jarvis type models was examined by looking at the average absolute relative error (AARE), root mean square error (RMSE) and determination coefficient (r^2). AARE of g_s was calculated using relative error (RE) given in Eq. 13 and 14.

$$RE = \frac{(g_s - g_{smodel})100}{g_s} \quad (13)$$

$$AARE = \frac{1}{n} \sum_{i=1}^{n} |RE| \quad (14)$$

The surface conductance was estimated in Takagi *et al.* (2009) earlier. It was found that daytime hourly average g_s was highly related to R_n by ANN and MLR approach, when daytime hourly data were used as input and output. However, in this study, daytime averaged energy fluxes, daytime surface conductance data, daily averaged meteorological variables, daily total precipitation and irrigation were used. Additionally, in this study, input variables including LAI and R_g (instead of R_n) for modeling of g_s were twice more than the input variables used in Takagi *et al.* (2009) study.

The relationships between each of the variables with g_s were examined separately. Fig. 5 represents the response of g_s to variables (u, RH, P+I, LAI, T, SWC, VPD, R_g, ET). The lines (dotted line for linear and straight line for nonlinear fittings) show the fittings of the functions for the data. As seen in Fig. 5, the variability of the g_s of sunn hemp depends highly on VPD, RH and u. The g_s increased when VPD, u decreased and RH increased; as expected. The g_s was high when T was low and LAI was high. The g_s value increased, while P+I increased. The response of g_s to the variability of T was similar to as reported by Kimura *et al.* (2006). The effects of R_g and SWC were weak on the g_s of sunn hemp during the measurement period. Despite of high SWC, g_s and ET values during the measurement period, a quite low relationship could be obtained between SWC and g_s.

By using this data set, it has been found that the highest determination coefficient (r^2=0.35) was estimated by MLR method for g_s in the training period when VPD and RH used together as inputs. In the test period, the MLR method estimated slightly higher r^2 (0.68). Similarly, the MLR for combination of VPD, RH and u gave better relationships (r^2=0.45) in the training period (Tab. 1). The MLR for combination of R_g, VPD, SWC and T, which are also meteorological input parameters in Jarvis type of model, showed a determination coefficient of (r^2) 0.40 with a high RMSE in training period, whereas r^2 was 0.82 in test period. Adding LAI into the combination of R_g, VPD, SWC and T caused to increase the relationship (r^2=0.49) in the training period. The MLR model had the highest r^2 with a value of 0.57 when all meteorological factors (VPD, RH, u, R_g, T, SWC, LAI, P+I) were considered as inputs. It increased between the training and test periods of the model (Tab. 1).

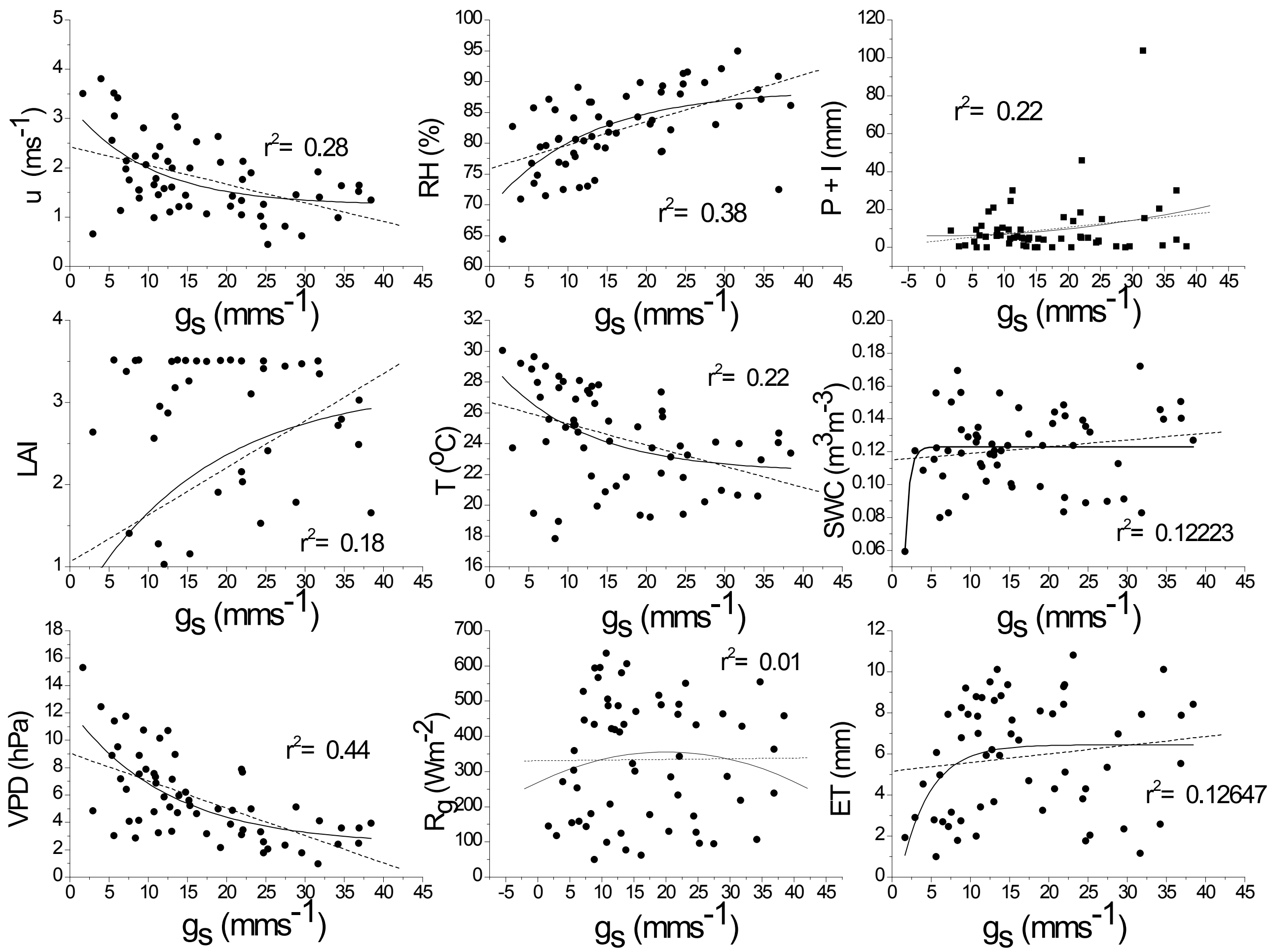

Fig. 5. Response of gs to the variables.
Fig. 5. Risposta delle conduttanza a diverse variabili ambientali.

Tab. 1. Performance criteria of the MLR model in the train and test periods.
Tab. 1. Criteri di rendimento del modello MLR e nei periodi di allenamento e test.

	Train data r^2	RMSE	Test data r^2	RMSE
g_s-VPD, RH	0.35	7.77	0.68	6.14
g_s-VPD, RH, u	0.45	7.16	0.43	8.68
g_s-VPD, T, SWC, R_g	0.40	8.43	0.82	3.81
g_s-VPD, T, SWC, R_g, LAI	0.49	6.73	0.59	8.49
g_s-VPD,T,RH,u,R_g,LAI,P+I,SWC	0.57	7.13	0.72	6.85

RMSE = Root mean square error - Errore quadratico medio.

Tab. 2. Performance criteria of the ANN model in the train and test periods.
Tab. 2. Criteri di rendimento del modello MLR e nei periodi di allenamento e test.

	Train data r^2	RMSE	Test data r^2	RMSE
g_s-VPD,RH	0.37	2.75	0.48	2.75
g_s-VPD,RH,u	0.50	2.36	0.26	3.05
g_s-VPD,T,SWC,R_g	0.87	1.95	0.63	2.34
g_s-VPD, T, SWC, R_g, LAI	0.81	1.97	0.79	2.27
g_s-VPD,T,RH,u,R_g,T,LAI,P+I,SWC	0.91	3.02	0.30	7.76

The performance criteria of the ANN model for the train and test periods were given in Tab. 2. The highest determination coefficient (r^2=0.37) in training period was estimated by ANN approach for g_s when VPD and RH were inputs. If we considered u as the combination of VPD and RH, resulting correlation sharply increased.

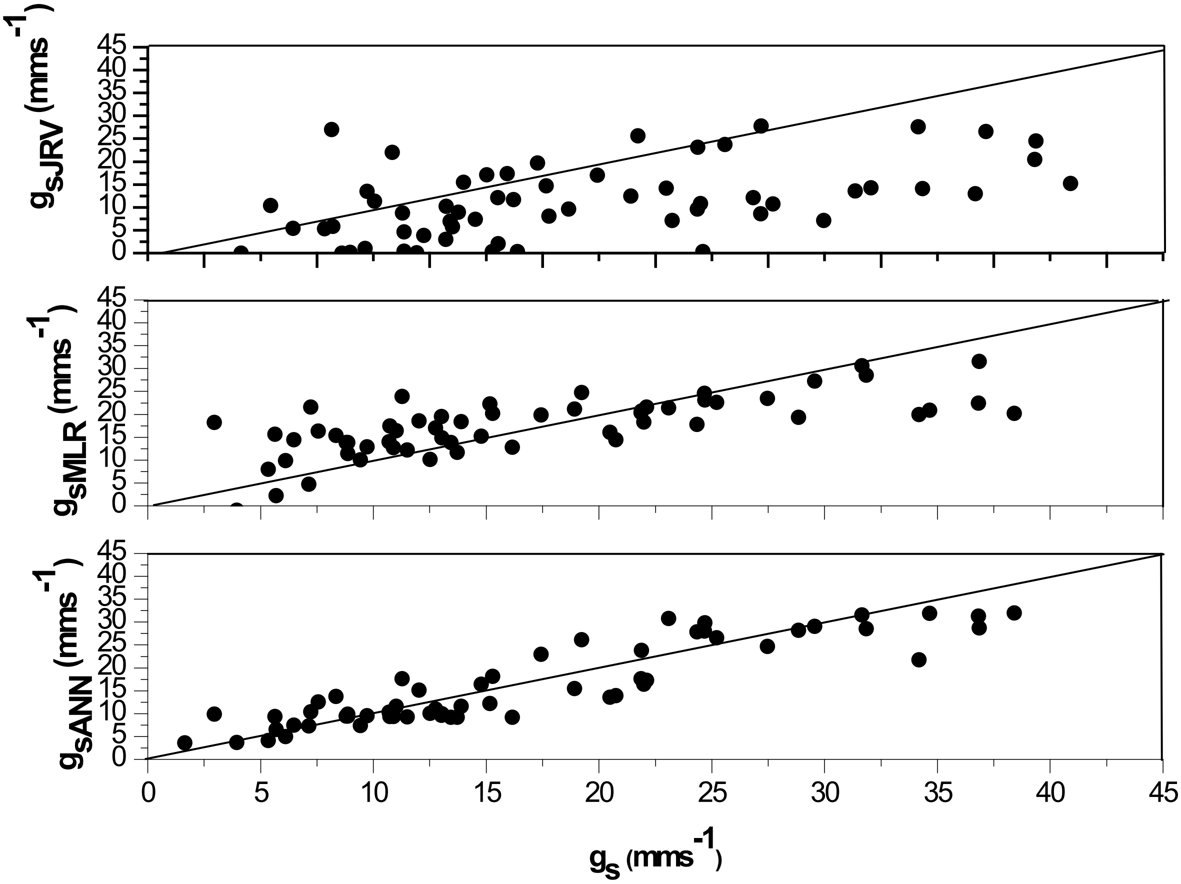

Fig. 6. The model g_s by ANN, MLR and JRV.
Fig. 6. Il modello della conduttanza su base ANN, MLR e JVR.

Similarly, adding R_g into the input list of VPD, T and SWC gave significant increase in the ANN model performance for train (r^2=0.87) and test (r^2=0.63) periods. Considering LAI with the input combinations of VPD, SWC, T and R_g showed a slight decrease in the performance of the ANN model in the training period and an increase in the test period. As seen in Tab. 2, adding P+I, RH, and u to the input combination of VPD, LAI, SWC, R_g, T resulted in an rise of ANN model performance for train period. In this case, it had the highest r^2 with a value of 0.91. When using VPD, T, SWC, R_g and LAI in test period, the highest relationship (r^2=0.79) was obtained, compared to MLR model (Tab. 2).

The actual g_s values calculated from Eq. 3 were compared to the performance of the Jarvis model. In addition, the g_s modeled using only variables considered in the Jarvis model (VPD, T, SWC, Rg, LAI) by ANN and MLR were compared with the actual g_s. The performance of the model g_s by ANN (g_{sANN}) was compared to the model g_s by multiple regressions (g_{sMLR}), Jarvis type (g_{sJVR}) and the g_s in Eq. (3) (Fig. 6). As seen in Fig. 6, the MLR model overestimated the g_s slightly, when g_s was lower than about 20 mm s^{-1} and underestimated when g_s was higher than about 20 mm s^{-1}. The relationship between actual g_s and g_{sMLR} was represented with a determination coefficient of 0.53. The Jarvis model underestimated the actual g_s and the relationship between g_s and g_{sJRV} was weak (r^2=0.26). In contrast, application of ANN approach on g_s gave very close relationship with the g_s (r^2=0.80) with a value of 26.54 % AARE during the period. It has been found that ANN has higher accuracy compared to classical method MLR and Jarvis type model (Fig. 6). Finally, it has been estimated that the Jarvis type of model gave the lowest relationship with the actual g_s.

After using the MLR between the meteorological and crop variables, which are independent variables, and surface conductance as dependent variable, it had been found that g_s increased when LAI, T, RH increased and VPD, u decreased.

5. DISCUSSION

In this study; ANN, MLR and Jarvis approaches have been applied for conductance during the measurement period of sunn hemp crop. ANN approach was compared to MLR, which is the traditional statistical technique and to Jarvis model as one of the commonly used approaches in the modeling of surface conductance. For training of the input data, eight variables were used in order to model the surface conductance. By using hourly daytime data calculated from 10-min averaged data, the surface conductance was modeled by ANN in Takagi *et al.* (2009). In that case, it was found that hourly averaged g_s was highly related to the hourly averaged R_n, whereas weak relationship was found between g_s and VPD, G, T. In our study, however, the daily averaged meteorological data, R_g and LAI were also used as inputs for the modeling of daytime averaged surface conductance of sunn hemp. The results showed that the daytime averaged surface conductance was mainly influenced by the variation of VPD, RH and u. A low determination coefficient (0.53) between g_s and all input variables had been found by using MLR analysis as a better relationship between daytime average g_s and all input variables was estimated by the ANN approach. Furthermore, the g_s seems to be affected slightly by SWC. This might be resulted from the high SWC, which is generally related to precipitation and irrigation. Using the same methodology in our study, Alves and Pereira (2000) also applied the Jarvis model and calculated the r_s by relating it with major meteorological parameters that affect the energy and mass transfers between the surface and atmosphere in the Penman-Monteith equation. The authors obtained satisfactory relationships between r_s, R_n and VPD which were represented with determination coefficients higher than 0.9. The finding of Shen *et al.* (2007) is also consistent with the results of this study.

Consequently, the ANN approach simulated the g_s better than MLR and Jarvis approaches, when the same meteorological variables were used for modeling as in Jarvis model. Adding LAI to this input combination like in Eq. (11), ANN gave high correlation with g_s for all cases. Finally, the ANN approach showed a better improvement against traditional statistical technique, when the same variables in the Jarvis model was considered for modeling. For this reason, it can be said that the ANN approach produced more accurate prediction for surface conductance than the Jarvis and MLR approaches. These results indicate that the ANN approach can be used for the estimation of non-linear time series and dynamic conditions.

ACKNOWLEDGEMENTS

The authors would like to thank all of the technicians working for the ALRC of Tottori University, for their help during the measurements. We also thank Prof. Dr. Zerefşan Kaymaz and Dr. Ahmet Öztopal for their comments.

REFERENCES

Allen, R.G., Pereira, L.S., Raes, D., Smith, M., 1998. Crop evapotranspiration: Guidelines for computing crop water requirements. FAO Irrig. and Drain. Paper 56, FAO, Rome, Italy.

Alves, I., Pereira, L.S., 2000. Modelling surface resistance from climatic variables? Agric. Water Manage. 42, 371-385.

Benali, L., Notton, G., Fouilloy, A., Voyant, C., Dizene, R., 2019. Application to normal beam, horizontal diffuse and global components. Renew. Energ. 132, 871-884.

Bolte, J.P., 1989. Application of neural networks in agriculture. ASAE Paper No. 89-7591. American Soc. of Agric. Eng., St. Joseph, MI.

Bowen, I.S., 1926. The ratio of heat losses by conduction and by evaporation from any water surface. Phys. Rev. 27, 779-787.

Dehghanisanij, H., Yamamoto, T., Inoue, M, 2004. Practical aspects of TDR for simultaneous measurements of water and solute in a dune sand field. J. of the Japan. Soc. of Soil Phys. 98, 21-30.

Dickinson, R.E., 1984. Modeling evapotranspiration for three dimensional global climate models. Climate Processes and Climate Sensitivity, Geophys. Mono. 29, 58-72.

Dirks, B.O.M., Hensen, A., 1999. Surface conductance and energy exchange in an intensively managed peat pasture. Clim. Res. 12, 29-37.

Doğan, E., 2008. Reference evapotranspiration estimation using adaptive neuro-fuzzy inference systems. J. Irrig. and Drain. 58, 617-628.

Hamidi, N., Kayaalp, N., 2008. Estimation of the amount of suspended sediment in the Tigres river using Artificial Neural Networks. Clean - Soil, Air, Water 36 (4), 380-386.

Hammerstrom, D., 1993. Working with neural network. IEEE Spectrum 30 (7), 46–53.

Haykin, S., 1994. Neural Networks: A comprehensive foundation. MacMillan College, New York.

Huntingford, C., Cox P.M., 1997. Use of statistical and neural network techniques to detect how stomatal conductance responds to changes in the local environment. Ecol. Model. 97, 217-246.

Jarvis, P.G., 1976. The interpretation of the variations in leaf water potential and stomatal conductance found in canopies in the field. Philosophical Transactions of the Royal Society Lond. B 273, 593-610.

Jensen, M.E., Burman, R.D., Allen, R.G., 1990. Evapotranspiration and irrigation water requirements. ASCE-Manuals and Reports on Engineering Practice, 70.

Kaul, L., Hill, R.L., Walthall, C., 2005. Artifical neural networks for corn and soybean yield prediction. Agric. Syst. 85, 1-18.

Khaledi, C.K.A., 2019. Projection of harvestable water from air humidity using artificial neural network (Case study: Chabahar Port). Italian J. of Agrometeorol. 24 (1), 3-11.

Kimura, R., Fan, J., Zhang, X., Takayama, N., Kamichika, M., Matsuoka, N., 2006. Evapotranspiration over the grassland field in the Liudaogou basin of the Loess plateau, China. Acta Oecologica. 29, 45-53.

Kişi, Ö., 2007. Evapotranspiration modeling from climate data using a neural computing technique. Hydro. Proc. 21, 1925-1934.

Kohonen, T., 1984. Self-organization and Associative Memory. Springer, Berlin.

Kumar, M., Raghuwanshi, N.S., Singh, R., Wallender, W.W., Pruitt, W.O., 2002. Estimating evapotranspiration using artificial neural network. J. Irrig. and Drain. Eng. 129, 224-233.

Lin, C.H., Chao, C., Chen, W.F., 2007. Estimation of regional evapotranspiration by adaptive network-based fuzzy inference system for dan-shui basin in Taiwan. J. Chin. Instit. Eng. 30 (6), 1091-1096.

Lopez, G., Rubio, M.A., Martinez, M., Batlles, F.J., 2001. Estimation of hourly global photosynthetically active radiation using artificial neural network models. Agric. For. Meteorol.107, 279–291.

Mohandes, M., Rehman, S., Halawani, T.O., 1998. Estimation of Global Solar Radiation Using Artificial Neural Networks. Ren. Ener. 14, 179-184.

Monteith, J.L., Unsworth, M.H., 1990. Principles of Environmental Physics. Edward Arnold, London.

Muttiah, R.S., Engel, B.A., 1991. Neural network methodology in agriculture and natural resources. ASAE Paper No. 917018. ASAE, St. Joseph, MI.

Niedbala, G., 2019. Simple model based on artificial neural network for early prediction and simulation winter rapeseed yield. J. Integr. Agricul. 18 (1), 54-61.

Niyogi, D.S., Raman, S., 1997. Comparison of four different stomatal resistance schemes using FIFE observations. J. Appl. Meteorol. 36 (7), 903-917.

Noilhan, J., Planton, S., 1989. A simple parametrization of land surface processes for meteorological models. Monthly Weather Review 117 (3), 536-549.

Ohmura, A., 1982. Objective criteria for rejecting data for Bowen ratio flux calculations. J. Appl. Meteorol. 21, 595–598.

Öztopal, A., 2006. Artificial neural network approach to spatial estimation of wind velocity data. Ener. Conv. Manage. 47 (4), 395-406.

Pachepsky, Y.A., Timlin, D., Varallyay, G., 1996. Artificial neural networks to estimate soil water retention from easily measurable data. Soil Science Society of American Journal 60, 727–733.

Ribeiro A., Russo, A., Gouveia, C., Pascoa, P., 2018. Modelling drought impacts over agricultural areas in Iberia using hydro-meteorological and satellite-based drought indices. Geophysical Research Abstracts Vol. 20, EGU2018-187-1.

Sahoo, G.B., Ray, C., Wade, H.F., 2005. Pesticide prediction in ground water in North Carolina domestic wells using artificial neural Networks. Ecol. Model. 183, 29–46.

Sellers, P.J., Bounoua, G.J., Collatz, D.A., Randall, D.A., Dazlich, S.O., Los, J.A., Berrry, I., Fung, C.J., Tucker, C.B., Jensen, T.G., 1996. Comparison of radiative and physiological effects of doubled atmospheric CO_2 on climate. Science 271, 1402–1406.

Shen, Y., Kondoh, A., Tang, C., Zhang, Y., Chen, J., Li, W., Sakura, Y., Liu, C., Tanaka, T., Shimada, J., 2002. Measurement and analysis of evapotranspiration and surface conductance of a wheat canopy. Hydrol Pro. 16 (11), 2173-2187.

Stewart, J.B., 1988. Modelling surface conductance of pine forest. Agric. For. Meteorol. 43, 19-35.

Şaylan, L., Bernhofer, C., 1993. Using the Penman-Monteith approach to extrapolate soybean evapotranspiration. Theor. Appl. Climatol. 46, 241-246.

Şaylan, L., Kimura, R., Çaldağ, B., Akataş, N., 2017. Modeling of soil water content for vegetated surface by artificial neural network and adaptive neuro-fuzzy inference system. Italian J. of Agrometeorol. 22 (3), 37-44.

Şen, Z., Altunkaynak, A., Alp, K., 2009. Contour diagram fuzzy model for maximum surface ozone prediction. Expert Syst. with App. 36, 6389-6402.

Takagi, K., 2005. Estimation of evapotranspiration using the ratio of actual evapotranspiration to the potential evaporation. Master's Thesis. Tottori University, p. 67.

Takagi, K., Kimura, R., Şaylan, L., 2009. Variability of surface characteristics and energy flux Patterns of sunn hemp (Crotalaria juncea L.) under well-watered conditions Theor. Appl. Climatol. 96, 261-273.

Terzi, O., Keskin, M., 2005. Modeling of daily pan evaporation. J. App. Sci. 5 (2), 368-372.

Thai, C.N., Shewfelt, R.L., 1991. Modeling sensory color quality of tomato and peach: neural networks and statistical regression. Trans. ASAE. American Soc. Agricul. Eng. 34, 950–955.

Van Wijk, M.T., Bouten, W., 1999. Water and carbon fluxes above European coniferous forests modeled with artificial neural networks. Ecolog. Model. 120, 181–197.

Woodward, F.I., Smith, T.M., 1994. Global photosynthesis and stomatal conductance: modeling the controls by soil and climate. Advances in Botanical Res. 20, 1–41.

Yang, S., Feng., Q., Liang., T., Liu, B., Zhang, W., Xie, H., 2018. Modeling grassland above-ground biomass based on artificial neural network and remote sensing in the Three-River Headwaters Region. Remote Sens. Env. 204, 448-455.

Zhang, Y., Kadota, T., Ohata, T., Oyunbaatar, D., 2007. Environmental controls on Evapotranspiration from sparse grassland in Mongolia. Hydrolog. Proc. 21 (15), 2016- 2027.

Zhuang, X., Engel, B.A., 1990. Neural networks for applications in agriculture. ASAE Paper No. 90-7024. American Soc. of Agric. Eng., St. Joseph, MI.

Finito di stampare da
Logo s.r.l. – Borgoricco (PD) – Italia

RIGOROUS PEER REVIEW

Each submission to IJAm is subject to a rigorous quality control and peer-review evaluation process before receiving a decision. The initial in-house quality control check deals with issues such as competing interests; ethical requirements for studies involving human participants or animals; financial disclosures; full compliance with IJAm's data availability policy, etc.

Submissions may be returned to authors for queries, and will not be seen by our Editorial Board or peer reviewers until they pass this quality control check.

Each paper is subjected to critical evaluation and review by Field Editors with specific expertise in the different areas of interest and by the members of the international Editorial Board.

OPEN ACCESS POLICY

The Italian Journal of Agrometeorology provides immediate open access to its content. Our publisher, Firenze University Press at the University of Florence, complies with the Budapest Open Access Initiative definition of Open Access: By "open access", we mean the free availability on the public internet, the permission for all users to read, download, copy, distribute, print, search, or link to the full text of the articles, crawl them for indexing, pass them as data to software, or use them for any other lawful purpose, without financial, legal, or technical barriers other than those inseparable from gaining access to the internet itself. The only constraint on reproduction and distribution, and the only role for copyright in this domain is to guarantee the original authors with control over the integrity of their work and the right to be properly acknowledged and cited. We support a greater global exchange of knowledge by making the research published in our journal open to the public and reusable under the terms of a Creative Commons Attribution 4.0 International Public License (CC-BY-4.0). Furthermore, we encourage authors to post their pre-publication manuscript in institutional repositories or on their websites prior to and during the submission process and to post the Publisher's final formatted PDF version after publication without embargo. These practices benefit authors with productive exchanges as well as earlier and greater citation of published work.

COPYRIGHT NOTICE

Authors who publish with IJAm agree to the following terms:

Authors retain the copyright and grant the journal right of first publication with the work simultaneously licensed under a Creative Commons Attribution 4.0 International Public License (CC-BY-4.0) that allows others to share the work with an acknowledgment of the work's authorship and initial publication in IJAm.

Authors are able to enter into separate, additional contractual arrangements for the non-exclusive distribution of the journal's published version of the work (e.g., post it to an institutional repository or publish it in a book), with an acknowledgment of its initial publication in this journal.

Authors are allowed and encouraged to post their work online (e.g., in institutional repositories or on their website) prior to and during the submission process, as it can lead to productive exchanges, as well as earlier and greater citation of published work (See The Effect of Open Access).

PUBLICATION FEES

Unlike many open-access journals, the Italian Journal of Agrometeorology does not charge any publication fee.

WAIVER INFORMATION

Fee waivers do not apply at Firenze University Press because our funding does not rely on author charges.

PUBLICATION ETHICS

Responsibilities of IJAm's editors, reviewers, and authors concerning publication ethics and publication malpractice are described in IJAm's Guidelines on Publication Ethics.

CORRECTIONS AND RETRACTIONS

In accordance with the generally accepted standards of scholarly publishing, IJAm does not alter articles after publication: "Articles that have been published should remain extant, exact and unaltered to the maximum extent possible". In cases of serious errors or (suspected) misconduct IJAm publishes corrections and retractions (expressions of concern).

Corrections

In cases of serious errors that affect or significantly impair the reader's understanding or evaluation of the article, IJAm publishes a correction note that is linked to the published article. The published article will be left unchanged.

Retractions

In accordance with the "Retraction Guidelines" by the Committee on Publication Ethics (COPE) IJAm will retract a published article if:

- there is clear evidence that the findings are unreliable, either as a result of misconduct (e.g. data fabrication) or honest error (e.g. miscalculation)
- the findings have previously been published elsewhere without proper crossreferencing, permission or justification (i.e. cases of redundant publication)
- it turns out to be an act of plagiarism
- it reports unethical research.
- An article is retracted by publishing a retraction notice that is linked to or replaces the retracted article. IJAm will make any effort to clearly identify a retracted article as such.

If an investigation is underway that might result in the retraction of an article IJAm may choose to alert readers by publishing an expression of concern.

ARCHIVING

IJAm and Firenze University Press are experimenting a National legal deposition and long-term digital preservation service.

SUBMITTING TO IJAm

Submissions to IJAm are made using FUP website. Registration and access are available at: https://riviste.fupress.net/index.php/IJAm/submission

For more information about the journal and guidance on how to submit, please see https://riviste.fupress.net/index.php/IJAm/index

Principal Contact
Simone Orlandini, University of Florence
simone.orlandini@unifi.it

Support Contact
Alessandro Pierno, Firenze University Press
alessandro.pierno@unifi.it

GUIDE FOR AUTHORS

1. Manuscript should refer to original researches, not yet published except in strictly preliminary form.
2. Articles of original researches findings are published in Italian Journal of Agrometeorology (IJAm), subsequent to critical review and approval by the Editorial Board. External referees could be engaged for particular topics.
3. Three types of paper can be submitted: original paper, review, technical note. Manuscript must be written in English, with the exception of technical note that can be both in English or in Italian. All pages and lines of the manuscript should be numbered.
4. First Name, Last Name, position, affiliation, mail address, telephone and fax number of all the Co-Authors are required. Corresponding Authors should be clearly identified.
5. The abstract should be no longer than 12 typed lines and should be written in both English and Italian.

Keywords and title should be written in both English and Italian.

6. Full stop, not comma, must be used as decimal mark (e.g. 4.33 and not 4,33).
7. Figures, tables, graphs, photos and relative captions should be attached in separate files. All images must be vector or at least 300 effective ppi/dpi to ensure quality reproduction.
8. Captions should be written both in English and Italian and should be written as: Fig.x – Caption title, Tab.x – Caption title. Images should be referred to in the text as (Fig.x), (Tab.x). The translation must be written in italic: Fig.x – Caption title, Tab.x – Caption title.
9. For foreign authors, all requested translations into Italian will be made by AIAM.
10. Proof of the paper (formatted according to the Journal style) will be sent to the Corresponding Author for proof reading just one time. Corrections can be made only to typographical errors.
11. All the references in the text must be reported in the "References" section and vice-versa. In the text, only the Author(s) last name must be present, without the name or the first letter of the name (e.g. "Rossi, 2003" and not "Federico Rossi, 2003" or "F. Rossi, 2003"). If two authors are present, refer to them as: "Bianchi and Rossi, 2003" in the text (do not use "&" between the surnames). If more than two Authors are present, refer to them as: "Bianchi et al., 2003" in the text.

For journals, references must be in the following form:

Bianchi R., Colombo B., Ferretti N., 2003. Title. Journal name, number: pages.

For books:

Bianchi R., Colombo B., Ferretti N., 2003. Book title. Publisher, publishing location, total number of pages pp.

Manuscripts "in press" can be cited.

BECOME A REVIEWER

Peer review is an integral part of the scholarly publishing process. By registering as a reviewer, you are supporting the academic community by providing constructive feedback on new research, helping to ensure both the quality and integrity of published work in your field. Once registered, you may be asked to undertake reviews of scholarly articles that match your research interests. Reviewers always have the option to decline an invitation to review and we take care not to overburden our reviewers with excessive requests.

You must login before you can become a reviewer.

If you don't want to be a reviewer anymore, you can change your roles by editing your profile.

COMPETING INTERESTS

You should not accept a review assignment if you have a potential competing interest, including the following:

- Prior or current collaborations with the author(s)
- You are a direct competitor
- You may have a known history of antipathy with the author(s)
- You might profit financially from the work

Please inform the editors or journal staff and recuse yourself if you feel that you are unable to offer an impartial review.

When submitting your review, you must indicate whether or not you have any competing interests.

Italian Journal of Agrometeorology

Rivista Italiana di Agrometeorologia

n. 3 – 2019

Table of contents